# Cutin, wax and stomatal mutants of *Arabidopsis thaliana*: chemical and physiological analysis of the leaf barrier properties

Dissertation
zur
Erlangung des Doktorgrades (Dr. rer. nat.)
der
Mathematisch-Naturwissenschaftlichen Fakultät
der
Rheinischen Friedrich-Wilhelms-Universität Bonn

vorgelegt von

Charlotte Petruschke

aus

Münster

Bonn, 2019

Angefertigt mit Genehmigung der Mathematisch-Naturwissenschaftlichen Fakultät der Rheinischen Friedrich-Wilhelms-Universität Bonn.

1. Gutachter: Prof. Dr. Lukas Schreiber

2. Gutachter: Prof. Dr. Kerstin Koch

Tag der Promotion: 20.09.2019

Erscheinungsjahr: 2019

# Table of contents

# Affirmation

I herewith declare that I have written this thesis independently and myself. I have used no other sources than those listed. I have indicated all places where the exact words or analogous text were taken from sources. I assure that this thesis has not been submitted for examination elsewhere.

Bonn, date

Charlotte Petruschke

# List of abbreviations

| | |
|---|---|
| A | Area |
| ABA | Abscisic acid |
| *att1* | Aberrant induction of type three 1 mutant |
| AM | Arithmetic mean |
| ANOVA | Analysis of variance |
| BSTFA | Bis(trimethylsilyl)trifluoroacetamide |
| C | Concentration |
| °C | Degree Celcius |
| Col-0 | Columbia-0 ecotype |
| CM | Cuticular membrane |
| cm | Centimeter |
| $cm^2$ | Square centimeter |
| demin | Demineralized |
| EMS | Ethyl methanesulfonate |
| FE-SEM | Field-emission scanning electron microscope |
| g | Gram |
| *flp* | Four lips mutant |
| FID | Flame ionization detector |
| GC | Gas chromatograph |
| h | Hours |
| $K_2CO_3$ | Potassium carbonate |
| KOH | Potassium hydroxide |
| kv | Kilovolt |
| l | Liter |
| LD | Leaf discs |
| m | Meter |
| mm | Millimeter |
| $mm^2$ | Square millimeter |
| $m^3$ | Cubic meter |

| | |
|---|---|
| ml | Milliliter |
| min | Minutes |
| mMol | Millimol |
| MS | Mass spectrometer |
| n | Number of replicates |
| p | Probability value |
| P | Permeances |
| PAM | Pulse Amplitude Modulation |
| PTFE | Polytetrafluoroethylene |
| PS | Photosystem |
| $r^2$ | Coefficient of determination |
| RWL | Relative water loss |
| s | Seconds |
| SD | Standard deviation |
| SEM | Scanning electron microscope |
| *shn3* | Shine 3 mutant |
| *st-RNAi* | Stomagen RNA interference mutant |
| *st-ox* | Stomagen overexpression mutant |
| t | Time |
| TEM | Transmission electron microscopy |
| *tmm* | Too many mouth mutant |
| µl | Microliter |
| µg | Microgram |
| µmol | Micromol |
| w/v | Weight per volume |
| v/v | Volume per volume |
| Ws | Wassilewskija ecotype |
| WT | Wild type |
| WUE | Water use efficiency |

# 1 Introduction

During plant evolution, two major indispensable characteristics evolved in the process of land colonization, which took place around 450- 470 million years ago (Graham, 1993). For one, terrestrial plants are covered by a thin continuous layer, the cuticular membrane (CM). This plant–atmosphere interface evolved to protect plants from desiccation in their transition from an exclusively aquatic to a terrestrial lifestyle (Edwards et al., 1982). Simultaneously stomatal pores evolved, more than 410 million years ago, disrupting the CM on the plants' surface (Edwards et al., 1998). Stomata are not only crucial for $CO_2$ uptake during photosynthesis but also essential in the control of water loss. The plant faces the trade-off between opening the stomata for the already mentioned necessary uptake of $CO_2$ and the loss of transpired water at the same time. When environmental conditions are unfavorable, for instance during water stress, and hence stomata close, the plant's prevention from desiccation only relies on the cuticular membrane as the limiting barrier to water loss. To establish this efficient barrier the outer epidermal cell walls of upper and lower plant parts are equipped with the aliphatic biopolymers; cutin, suberin and their associated waxes. Cutin, along with its associated waxes, forms the cuticle, the already mentioned lipid and wax rich layer covering all aerial parts of plants in their primary developmental stage (Schönherr, 1982). Suberin exerts the same function and can be found in secondary shoots and roots of the plant. The cuticle, in general, is of high importance for protecting plants against biotic and abiotic stresses such as wind, rain and high UV radiation (Percy and Baker, 1990; Krauss et al., 1997). Additionally, it plays a fundamental role as a barrier against herbivores and pathogens attacks, as well as viruses, bacteria, and fungi (Mendgen, 1996; Bird and Gray, 2003).

## 1.1 The cuticle: chemistry and structure

The general structure of the cuticle can be divided into three different parts (Figure 1). Starting from the physiological outer side of the cuticle, the cuticle proper (CP), with superimposed epicuticular and embedded intracuticular waxes, covers the outermost part of the cuticle. It is a pectin and cellulose free and often lamella-like structure. Underlying is the cuticular layer (CL), which is traversed with microfibrils and additionally contains intracuticular waxes as well. Finally, the pectin-rich, pectinaceous layer (PC) binds the cuticular layer to the epidermal cell walls (CW).

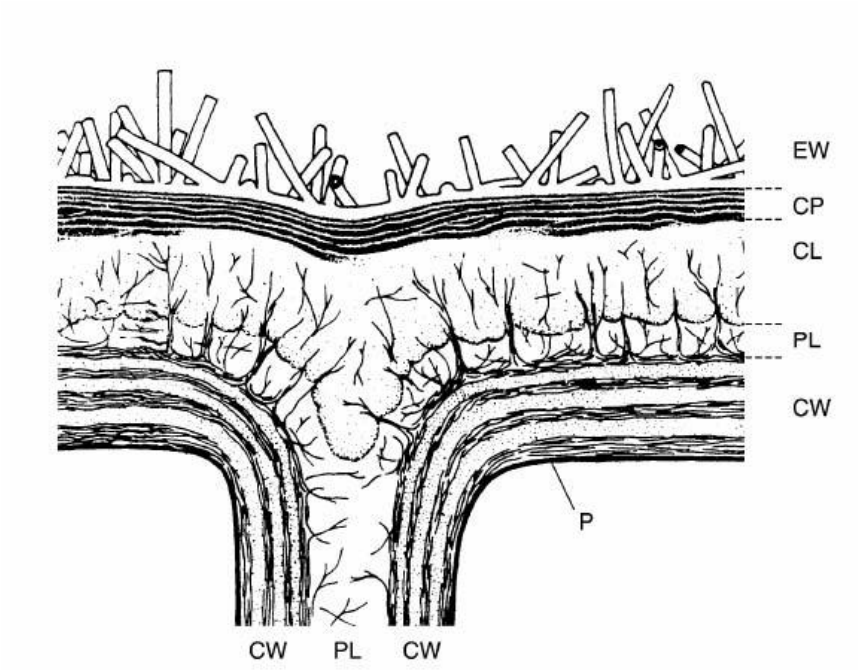


Figure 1: Schematic drawing of the outer parts of the plant epidermis cells (modified after Jeffree, 1986)

EW: Epicuticular wax, CP: Cuticle proper with lamellate structure, CL: Cuticular layer, PL: Pectinaceous layer and middle lamella, CW: Cell wall, P: Plasmalemma

On the molecular level, the cuticle is mainly characterized by its' two major components: Soluble waxes and the biopolymer cutin. Cutin is constructed of esterified hydroxy fatty acids with chain lengths of $C_{16}$ and $C_{18}$. It provides a mechanically stable matrix (Espelie et al., 1980; Kolattukudy, 1984; Nawrath, 2006), which is needed for the overall stability of the plant. Soluble waxes of the cuticular membrane constitute of aliphatic lipids and cyclic lipophilic constituents (Kunst and Samuels, 2003). They are not only embedded within the cutin polymer

(intracuticular waxes) but also on its surface (epicuticular waxes) (Baker, 1982; Holloway, 1982). Depending on the analyzed species the cuticle thickness can vary between approximately 30 nm in *Arabidopsis thaliana* (*A. thaliana*) leaves (Bonaventure et al., 2004) or 30 µm as it has been reported for the fruit of *Malus domestica* (Schreiber and Schönherr, 2009).

The chemical composition of cuticular waxes is rather complex. Wax components have been intensively studied in the past and compromise a variety of long chained, aliphatic substance classes such as primary fatty acids, alkanes, aldehydes, and alcohols as well as secondary alcohols and alkyl esters. Also, cyclic triterpenoids have been analyzed for many plant species (Kunst and Samuels, 2003; Jeffree, 2006; Jetter et al., 2006). The wax composition can vary within different species or even between different organs in one species and during organ ontogeny (Holloway, 1971; Kolattukudy and Walton, 1972; Jeffree, 2006; Jetter et al., 2006). This variety of different wax components and their composition lead to diverse three-dimensional surface structures. Responsible for particular structures are mainly the epicuticular waxes, superimposed on the cuticle (Koch and Barthlott, 2009). These waxes are crystalline (Schreiber et al., 1997) and of various shapes of different sizes ranging from 0.2 µm to 100 µm (Koch and Barthlott, 2009). In the plant family of *Pinaceae*, for instance, nonacosane 10- ol, a secondary alcohol in the epicuticular wax, was identified to be responsible for the shape and morphology of wax aggregates and crystals in the form of tubules as three- dimensional wax structure on the cuticle surface (Matas et al., 2003). However, one of the most intensively studied surface structures of leaves is the leaf of the sacred lotus plant (*Nelumbo nucifera*) (Barthlott and Neinhuis, 1997). Its surface is considered to be superhydrophobic which results in a self-cleaning effect of the leaf. To classify the wettability of leaf surfaces contact angle measurements are used. The surfaces of leaves on which an applied water droplet tends to spread have a low contact angle and are hence better wettable and vice versa. In the particular case of the lotus leaf, the measured contact angle is high (162°) and the leaf therefore not wettable. As stated before the structure of the epicuticular wax on the lotus leaf surface is

suggested to be the main reason for its' water repellent behavior (Koch and Barthlott, 2009). Here the superimposed waxes are randomly distributed as small hydrophobic wax tubules on convex cell papillae (Barthlott and Neinhuis, 1997). This results in a reduced contact area and adhesion of applied water droplets which then immediately roll off the leaf's surface (Koch and Barthlott, 2009). The biopolymer cutin can also play a role in forming the surface structure of the cuticle. Folding or tubercular patterns, for instance, originate by the cuticle itself (Barthlott, 1980).

## 1.2 The cuticle as transport barrier

The importance of cuticular waxes for the water barrier properties of the cuticle is widely studied (Schreiber, 2010). Results on water barrier properties of wax-free polymer matrix membranes showed that the water permeability of the cuticle increased between 100- 1000 fold in average (Schreiber and Schönherr, 2009) and therefore underlines the immense role of cuticular waxes as a transport barrier. In even more detail, Zeisler-Diehl et al., (2018) could show that epicuticular waxes do not establish the transport barrier but instead intracuticular waxes. Additionally, neither is the thickness nor the wax coverage of the cuticle correlated to the cuticular water permeability and is therefore not responsible for the effectiveness of its barrier to water loss (Riederer and Schreiber, 2001). However, it is known that certain sites on the leaf, such as trichomes, stomata, and anticlinal cell walls, are more permeable to polar compounds than areas on the leaf where the cuticle only covers pavement cells (Schlegel et al., 2005; Schönherr, 2006). Water as a small, uncharged and polar molecule is reported to be transported through the cuticle via two parallel pathways: Either through the lipophilic pathway formed by the lipophilic cutin and wax domains or via a polar transport pathway formed by polar pores (Schreiber et al., 2001; Schreiber, 2005). The polar pores are suggested to be formed by carbohydrate fibrils, located within the lipophilic cuticular membrane. Small amounts can extend from the epidermal cell wall through the cutin till up to

the outer cuticle surface enabling the permeance of polar compounds (Schreiber and Schönherr, 2009). The transport through the cuticle and hence the water permeability of the cuticle is affected by abiotic factors such as humidity and temperature (Schreiber and Schönherr, 1990; Schreiber et al., 2001). With increasing air humidity also the water permeability of the cuticle increases. High temperatures also lead to an increase of transpiration (Schreiber and Schönherr, 1990). For instance, the increase of the temperature from 10 °C to 55 °C results in an increase of water permeability, depending on the species by a factor of 264 (*Hedera helix*) (Schreiber, 2001). Besides the mentioned abiotic factors also industrial surfactants or bacterial produced biosurfactants are known to have an enhancing effect on the cuticle permeability (Riederer and Schönherr, 1990; Burch et al., 2014).

## 1.3 Wax and cutin biosynthesis

A rather complex process is the biosynthesis of waxes. Multiple cell compartments (plastids, cytoplasm and the endoplasmatic reticulum) are involved in wax synthesis. $C_{16}$ and $C_{18}$ fatty acids are built by an enzyme complex (fatty acid synthase) localized in the plastids. The elongation is catalyzed by fatty acid elongases, which are bound to the endoplasmatic reticulum. Here the chain length of fatty acids is extended with two carbon atoms and functionalized through hydroxylation and oxygenation. A following series of chemical reactions lead to different functionalized substances. The acyl-reduction pathway leads to aldehydes, primary alcohols, and their respective esters. Over the decarboxylation pathway odd-numbered carbon alkanes, as well as ketones and secondary alcohols are synthesized. Besides long chain aliphates, triterpenoids are present in the wax as well and are synthesized via the triterpenoid pathway (Kunst and Samuels, 2003; Jetter et al., 2006; Bernard and Joubès, 2013; Yeats and Rose, 2013; Joubès and Domergue, 2018), (Figure 2).

The cutin monomer biosynthesis has been mainly investigated in the model plant *A. thaliana*: The *de novo* synthesis and the elongation of fatty acids are the same as in the wax biosynthesis. The path diverges in the ER where the synthetization of

acyl CoA intermediates, ω- hydroxylation and midchain hydroxylation, take place. The following enzymes that mainly convert the ω-hydroxy-fatty acids into the most abundant cutin monomer in Arabidopsis, dicarboxylic acid, remain unknown. Nevertheless, it is likely, that cytochrome P450 enzymes such as ABERRANT INDUCTION OF TYPE THREE 1 (ATT1) are responsible for the conversion. Following is the last step for the synthesis of the cutin monomers for the polymerization of the biopolyester, where glycerol 3-phosphate acyltransferase produces 2-monoacylglyceryl esters (Yeats and Rose, 2013; Joubès and Domergue, 2018), (Figure 2).

The transport of cuticular compounds from the cytoplasm through the plasma membrane, the cell wall and finally to the organ surface is not quite clear yet. In Arabidopsis, a series of studies suggest that through Golgi- and trans-Golgi network-mediated vesicle trafficking the hydrophobic molecules are transported through the hydrophilic cytoplasm to the plasma membrane (McFarlane et al., 2014; Lee and Suh, 2015). Once the plasma membrane is reached the export is carried out by ABC transporters (*ATP binding cassettes),* (Bird et al., 2007), (Figure 2).

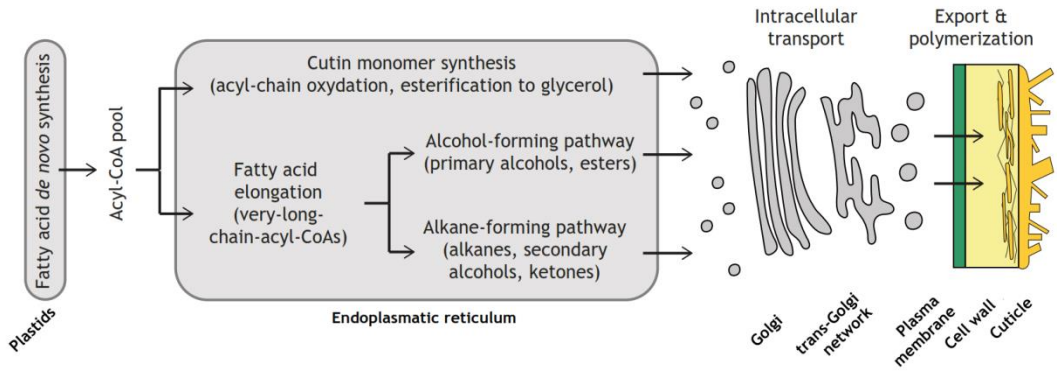


Figure 2: Cuticle biosynthetic pathway (according to: Joubès and Domergue, (2018))

Schematic drawing of the biosynthetic pathways of cutin and cuticular waxes. Starting from the plastids through the endoplasmatic reticulum. The intracellular transport leads to the plasma membrane (green), through the cell wall (yellow) to the cuticle (divided into: Cutin with embedded intracuticular waxes and superimposed epicuticular waxes).

### 1.3.1 Cuticular mutants

The gene At4g00630 which is involved in cutin biosynthesis codes for the protein ATT1, which functions as a catalyst for fatty acid elongation (Xiao et al., 2004). The gene is expressed in all plant tissues (Duan and Schuler, 2005). The mutant *att1* shows no visible phenotype under normal growth conditions, but plants have a reduced amount of cutin (Xiao et al., 2004). Other than for the cutin biosynthesis many genes have been identified, which play important roles in the wax biosynthesis. Some details have only been understood recently. The specific biosynthesis for alkanes was successfully reconstructed for yeast by Bernard et al., (2012). This study makes clear that the ECERIFERUM1 (CER1) and ECERIFERUM3/WAX2 (CER3/WAX2) protein is needed to produce alkanes. CER3/WAX2 acts as fatty acyl reductase to produce the alkane precursor fatty aldehydes or other intermediates which are currently not known (Bernard et al., 2012). Mutants (*wax2*- allele: *cer3-5*) with a defect in the *Cer3/Wax2* (At5g57800) gene show reduced wax amounts in Arabidopsis leaves and stems, especially due to a reduction in the alkane amount (Chen et al., 2003; Rowland et al., 2007). On the other hand, plants that overexpress the transcription factor SHN3, exhibit higher wax amounts in leaves. SHN3 was found to be a transcription factor involved in the regulation of the production of wax monomers (Aharoni et al., 2004). Phenotypically the mutant *shine3* (*shn3*) displays shiny, green leaf surfaces as well as leaf curling and a reduction in the trichome number.

## 1.4 Physiological and morphological aspects of stomata

Terrestrial plants are able to inhabit a range of different environments with fluctuating conditions. Key elements in the evolution of terrestrial life were stomatal pores and a cuticular membrane preventing non- stomatal water loss. Whereas the cuticle functions as a barrier to uncontrolled water loss (Schönherr, 1982) and is virtually impermeable to $CO_2$ (Lendzian and Kerstiens, 1991), gas exchange and controlled water loss between the photosynthetic tissues and the atmosphere is regulated through stomatal pores. They actively keep the balance between the $CO_2$

uptake for photosynthesis and the water lost through stomatal transpiration, which determines the water use efficiency (WUE), (Nobel, 1980). The stomatal transpiration depends on the opening and closing of the stomatal pores. Therefore when stomata are open water vapor simply follows its concentration gradient from the xylem inside the leaf, through the intercellular air space, across the substomatal cavity, through the stomata to the atmosphere, also known as transpiration stream (Biddulph et al., 1961). Stomatal opening and closing are managed over dynamic turgor changes in the guard cells (Gregory et al., 1950). In more detail, the fast response to open and close stomata on a physiological level is managed by ion channels in the guard cell membrane. Additionally, stomata can respond with closing under stress conditions. Here abscisic acid (ABA) for instance is the best-known phytohormone to induce closing of stomata as a response to abiotic stress (Daszkowska-Golec and Szarejko, 2013). Morphologically stomata consist of a pore, flanked by two sister guard cells. Stomatal density and morphology, as well as their distribution, are usually a result of long term adaptation processes (Haworth et al., 2011). They usually depend on the plants' habitat and fluctuating abiotic factors such as humidity, light intensity, and $CO_2$ concentration and are therefore different for each species (Mott and Michaelson, 1991; Hronková et al., 2015; Muir, 2015). The stomatal patterning, on the other hand, is in most cases determined by a spatial regularity: The one- cell spacing rule states that stomatal guard cells are not in direct contact with each other (Sachs, 1991), which is thought to improve the efficiency of gas exchange (Nadeau and Sack, 2002).

A commonly known method in science is to use mutants which all exhibit alterations in the property of interest and compare them to the corresponding wild type. For Arabidopsis, many stomatal mutants, which all exhibit diverse stomatal properties in their distribution, morphology or density, are known. Yang and Sack, (1995) identified the gene *TOO MANY MOUTHS (Tmm*) to be involved in the stomatal development. It regulates the production of stomata by controlling the formation of the stomatal precursor cell (meristemoid cell) and therefore ensures correct stomatal patterning. The *tmm* mutant, derived from EMS mutagenesis,

promotes stomatal initiation and therefore exhibits stomatal clustering, but is also expressed organ specific, contrary to the leaves, a mutated *Tmm* gen suppresses initiation of stomata in the inflorescence stem (Yang and Sack, 1995; Geisler et al., 1998). Simultaneously to the gene *Tmm* the *Four lips* (*Flp*) gene was identified, which is involved in stomatal development. Loss of function in *Flp* leads to additional divisions of guard mother cells, which suggests the involvement of *Flp* in the cell division competence of those cells. The EMS-induced mutant *flp* primarily affects the production of guard mother cells, which leads to many paired stomata and a small percentage of unpaired guard cells (Yang and Sack, 1995). In addition to the previously mentioned mutants, which mainly show irregularities in their stomatal patterning, Sugano et al., (2010) generated an overexpression line (*st-ox*) and a silenced line (*st-RNAi*) which express different stomatal densities. *St-ox* shows significantly higher and *st-RNAi* lower stomatal density, when compared to the wild type. Responsible for inducing stomata activity in a dose dependent manner is a cysteine rich peptide, which is generated from a 102-amino- acid precursor protein: STOMAGEN. Additionally to a higher stomatal density in the overexpression line also many clustered stomata are formed in matured leaves. Contrarily the silencing of the gene with artificial microRNA leads to RNA interference lines with reduced stomatal densities in various organs (Sugano et al., 2010).

## 1.5 Goals

The cuticle as the plant atmosphere interface is interrupted by stomata which actively regulate the gas exchange of the plant. However, if stomata are closed during water stress, the cuticle is the most important barrier to prevent and reduce uncontrolled, passive water loss. This obvious interplay between stomata and cuticular membrane leads to the question if the cuticular membrane as leaf barrier is altered in its wax or cutin amount, composition and structure under the circumstances of high or low numbers and different patterning of stomata. Or if vice versa alterations in wax and cutin amounts have an influence on the production and distribution of stomata. Therefore the aim of this work was to elucidate whether

there is a relationship between wax or cutin amounts and stomatal density. Further, the physiological impact in terms of transpiration, either through the cuticular membrane or the stomata, and their possible relation is a central question of this work.

In the past, many Arabidopsis mutants have led to the identification of different genes, which control stomatal development and likewise a lot is known about the cutin and wax synthesis pathways and involved genes. In this work, Arabidopsis stomatal mutants, which are all defective in the pathway of stomatal development as well as cuticular mutants which exhibit disruptions in their biosynthesis pathways should be investigated to answer the main questions of this work.

To address those questions, alterations, and relationships between (i) the stomatal distribution, (ii) cuticular wax and cutin amounts as well as compositions and (iii) the physiological role in terms of transpiration either through the cuticular membrane or the stomata will be investigated.

Phenotypical changes in the here investigated mutants compared to their wild types will be observed prior to all following experiments via FE-SEM. Potential alterations in wax and cutin amounts of Arabidopsis leaves and stems will be measured qualitatively and quantitatively by gas chromatography and mass spectrometry. Since Arabidopsis leaves show amphistomy, wax extraction will be precisely and separately investigated on the adaxial and abaxial leaf side. Consequently, stomata densities and indexes will be investigated for both leaf sides as well. Additionally to alterations in the stomatal distribution as well as cuticular wax and cutin amounts and compositions the physiological properties of the different mutants, such as transpiration, will be in the focus of this work. To further describe these alterations contact angles of water on the outer leaf surface will be measured. In the end, a possible relation between the stomatal densities, cutin and wax amounts and the cuticular transpiration will be discussed.

# 2 Material and Methods

## 2.1 Material

### 2.1.1 Plants

All experiments in this work were carried out with plants with either the genetic background of *Arabidopsis thaliana* ecotype Columbia (Col-0) or ecotype Wassilewskija (Ws). The Arabidopsis stomatal mutants were kindly provided by prof. Jiří Šantrůček from the Faculty of Science, University of South Bohemia.

Arabidopsis stomatal mutants:

- *tmm* (SALK_011958 carries a point mutation at gene At1g80080.1),(Yang and Sack, 1995; Geisler et al., 1998).
- *flp* (SALK_033970 carries a point mutation at gene At1g14350), (Yang and Sack, 1995; Geisler et al., 1998)
- *st-RNAi* (At4g12970 known as STOMAGEN, RNA interference silencing), (Sugano et al., 2010)
- *st-ox* (STOMAGEN overexpression; overexpression via vector with inserted promotor region and At4g12970), (Sugano et al., 2010)

Arabidopsis wax and cutin mutants:

- *att1* (knockout At4g00360), (Xiao et al., 2004)
- *shn3* (overexpression: At5g25390), (Aharoni et al., 2004)

- *wax2* (*knockout* At5g57800), (Chen et al., 2003; Kurata et al., 2003; Rowland et al., 2007)

## 2.2 Methods

### 2.2.1 Cultivation and growth conditions on soil

The soil (Einheitserde Typ 1.5, Sinntal- Altengronau, Germany) was sterilized before usage. For the process of sterilization, the soil was moistured with tap water, filled into a STERILO 1K (Harter Elektrotechnik, Schenkenzell, Germany) and heated up to 65 °C. for 2 h. For imbibition, Arabidopsis seeds were kept in tap water. They were stored at 4 °C., overnight and in the dark to break dormancy. Next, for germination, the seeds were distributed on soil in a scheme of five seeds per pot. The trays were covered with transparent lids to ensure high humidity for 5 to 6 days. For growth the pots were transferred to a growth chamber with long day conditions: 18/6 h day/night cycle at 23/20 °C., relative humidity of 50/65 % and light intensity of 150/0 µmol $m^{-2}s^{-1}$. Plants were watered with tap water twice per week.

The plants were kept under these conditions until further usage. All experiments in this work were conducted with 4 weeks old plants.

### 2.2.2 Field emission scanning electron microscopy (FE-SEM)

Investigations of the leaf and stem surface morphology were performed by FE-SEM (Gemini Supra 40VP, Zeiss, Oberkochen Germany) at the Faculty of Life Science, Rhine-Waal University.

#### 2.2.2.1 Sample preparation

Small cuttings of leaves (approx. 0.5 $cm^2$) were prepared with a glycerol liquid substitution (Ensikat and Barthlott, 1993) to avoid alterations in cell shape and wax structure. Therefore the specimens were placed on a wet paper towel into a tilted petri dish. Over a time period of 21 h glycerol (90 %) was added dropwise to the petri dish. During the process, the tissue is slowly infiltrated with the glycerol and

water gets substituted. Unlike the leaves, the stems were cut in approximately 1.25 $cm^2$ long pieces and air dried.

After preparation, the specimens were fixed on aluminum stubs (Plano, Wetzlar, Germany) with double-sided adhesive tape (Double-sided Tape Universal, Tesa, Hamburg, Germany). All cut edges were sealed with conductive carbon cement (Plano, Wetzlar, Germany). Specimens were sputter coated (108auto SE, Cressington, Watford, UK) with gold as conducting material. This inhibits the specimen from charging through the electron beam and vice versa increases electrical conduction. After 60 seconds sputtering at 30 mA and a pressure of 0.1 mbar, the specimen was covered with an 8 nm gold layer.

#### 2.2.2.2 Sample investigation

SEM micrographs of the leaves were taken with an In-lens detector and a secondary electron detector at 3 kV. The images of the stems were taken at 10 kV with the secondary electron detector only.

### 2.2.3 Measurement of wetting properties

To characterize the wettability of the leaf surfaces contact angle measurements were taken. Contact angle values vary not only with the surface properties (e.g. surface structure and chemistry) but also depend on the applied liquid (hydrophilicity or hydrophobicity). Here the contact angle of water (10 µl) on the leaf surface of the different Arabidopsis genotypes was measured. As a control contact angle measurements of 10µl water droplets were also performed on parafilm representing a homogenous, lipophilic surface, mainly consisting of $CH_2$ groups. All contact angle measurements were performed with a fully automatically drop shape analyzer DSA 25 (Krüss GmbH, Hamburg, Germany). Leaves and parafilm were carefully attached onto cleaned glass slides using again adhesive tape. Care has been taken that the surface was not touched or disturbed during fixation At least three independent measurements were taken for each biological sample and leaf side (ab-/adaxial) to determine the mean value and standard deviation.

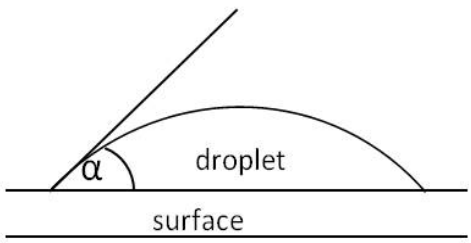


Figure 3: Schematic drawing of a contact angle (α) on a solid surface (Knoll, 1998)

Contact angle (α) of a water droplet on a solid surface (below 90 degrees); Surface: Either parafilm or Arabidopsis leaf.

### 2.2.4 Chlorophyll content analysis

The leaf chlorophyll content was measured using the Dualex Scientific+™ (Force A; Orsay, France; (Goulas et al., 2004)). Therefore a minimum of 6 rosette leaves from three plants for each genotype was measured. The measurements were taken on the adaxial leaf side, avoiding midribs.

### 2.2.5 Chemical analysis of plant waxes

For the analytical experiments glassware was cleaned with chloroform previously to all conducted experiments. This is necessary to prevent contamination of samples during the steps of sample preparation and extraction. To securely seal samples, lids were coated with polytetrafluoroethylene (PTFE) which is resistant to organic solvents.

#### 2.2.5.1 Sample preparation for total wax extraction

Whole leaves and stems of Arabidopsis were used for total wax extraction. Further wax was extracted from ad- and abaxial sides of the leaves. For total wax extraction leaves (n = 10) and stems (n = 4) were dipped in chloroform for 10 seconds. The dipped leaves/ stems were consequently scanned for area determination and directly immersed in chloroform:methanol (1:1, v/v) for cutin analysis (2.2.5.2). To extract wax only from one leaf side, a vial with rolled edges was used. For extraction chloroform (1.3 ml) was filled into the vial, which was then closely pressed onto the leaf surface. On top, the vial was closely sealed with a PTFE coated lid. The vial was carefully inverted for 10 seconds. Because low amounts of extracted wax were

expected at least 15-20 leaves per biological replicate for extraction of one leaf side were used. In addition, the amount of the internal standard was always adjusted to expected wax amounts. Therefore subsequently to extraction 5 µg of an internal standard, Tetracosane ($C_{24}$ alkane), was added to samples for ad- or abaxial leaf sides and 10 µg to samples for whole leaves or stem wax extractions. The wax containing chloroform volume was evaporated at 60 °C under a gentle nitrogen flow to a final volume of 200 µl.

#### 2.2.5.2 Sample preparation for cutin analysis

After wax extraction Arabidopsis leaves and stems were also analyzed for cutin amount and composition. Therefore they were incubated in chloroform:methanol (1:1; v/v) at room temperature under continuous shaking for 2 weeks. Additionally they were kept in the dark to keep diacids from reacting. Remaining lipids were excluded by exchanging chloroform:methanol at least 5 times. To further analyze the plant material leaves and stems were air dried under the fume hood and weighed afterward. After that samples were ready to be transesterified (2.2.5.3).

#### 2.2.5.3 Transesterification

For cutin analysis the biopolymer must be broken into its monomers. Therefore the samples need to be transesterified done by borontriflourid and methanol ($BF_3$-MeOH; 1:1, v/v). Thus the samples were incubated for 16 h at 70 °C. (Kolattukudy and Agrawal, 1974). Directly after incubation 10 µg of Dotriacontan ($C_{32}$- alkane) were added to the samples as an internal standard. The reaction was stopped by adding 2 ml of saturated sodium hydrogen carbonate and water ($NaHCO_3/H_2O$).

To successfully extract the lipid phase out of the samples, they were washed three times with 2 ml chloroform. After mixing thoroughly the lower phase of each analyte was collected carefully with a pipette. Subsequently, the samples were washed with $H_2O_{HPLC}$. They were then dried with water free sodium sulfate ($NaSO_4$). The remaining volume was evaporated at 60 °C under a gentle flow of nitrogen to a final volume of 200 µl.

#### 2.2.5.4 Derivatization

For chemical analysis, all samples needed to be derivatized to increase the volatility and mask polar functional groups being constituents in waxes and cutin. Accordingly 20 µl of bis(trimethylsilyl)trifluoroacetamide (BSTFA) and as a catalysator 20 µl of pyridine were added to each sample. BSTFA causes the polar functional groups to convert into their corresponding trimethylsilyl-esters (TMS,). After the addition of both substances, samples were mixed thoroughly and incubated at 70 °C for 45 minutes (Figure 4).

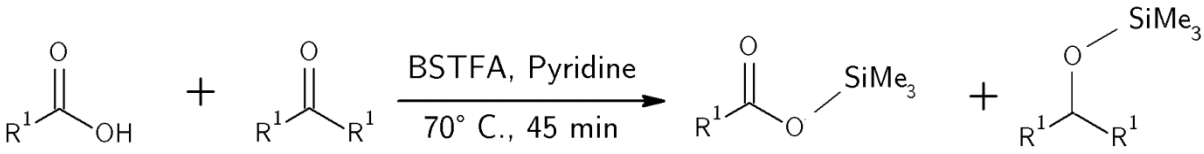


Figure 4: Reaction of derivatization

BSTFA and pyridine, as catalysator, convert the reactive groups into the corresponding trimethylsilyl-esters (created with ChemSketch; public domain, available at acdlabs.com)

#### 2.2.5.5 Gas chromatography

Following derivatization samples were arranged on to the gas chromatograph in random order. 1 µl of each sample was injected directly on the column. Here compounds of a sample were separated over a capillary column (stationary phase). Due to different size and polarity of individual components, separation takes place over time. For the analysis, a 6890N gas chromatograph (Agilent Technologies, Germany) with a capillary column (DB-1; 30 m x 0.32 mm, 0.1 µm (J&W, Agilent Technologies, Germany)) and $H_2$ as carrier gas (mobile phase, flow rate 2 ml x $min^{-1}$) was used. For the quantitative analysis compounds were detected with a flame ionization detector (FID). At the detector side, the separated compounds were oxidized. The produced electrons induced voltage which was recognized as a signal by a connected computer. The analyses in this work were performed according to the temperature programs shown in Table 1.

Table 1: Temperature programs for GC analyses

| wax analysis | cutin analysis | acid standard |
|---|---|---|
| Injection at 50 °C. | Injection at 50 °C. | Injection at 50 °C. |
| 2 min at 50 °C. | 2 min at 50 °C. | 1 min at 50 °C. |
| 40 °C/min up to 200 °C. | 10 °C/min up to 150 °C. | 40 °C/min up to 200 °C |
| 2 min at 200 °C. | 1 min at 150 °C. | 2 min at 200 °C. |
| 3 °C/min up to 310 °C. | 3 °C/min up to 310 °C. | 3 °C/min up to 310 °C. |
| 30 min at 310 °C. | 15 min at 310 °C. | 20 min at 310 °C. |

#### 2.2.5.6 Mass spectrometry

For the identification of the single compounds, a gas chromatograph coupled to a mass spectrometer was used. The compounds were separated over the length of the column. As they elute at different times they get ionized and separated according to their mass/charge ratio. Single compounds were fully identified by their typical ion fragmentation pattern. All analyses were carried out with a 5973 MS (Agilent Technologies, Germany). A DB-1-MS (30 m x 0.32 mm, 0.1 µm, (J&W Agilent Technologies, Germany)) column was used and Helium (He) served as the carrier gas.

#### 2.2.5.7 Maintenance of the column

The condition of the GC- FID and GC- MS column was tested and maintained before and after each analysis. Due to residues of not fully volatile compounds on the column the detector signal can decrease after each analysis. The quality of the capillary column was tested with an acid standard. A mixture of $C_{24}$ alkane and three monocarboxylic acids ($C_{29}$, $C_{30}$, $C_{31}$) in equal amounts were derivatized and injected on to the column following the temperature program shown in Table 1. To confirm efficient maintenance the ratio of the peak areas of the alkane and the $C_{31}$ monocarboxylic acid had to be better than 1.4.

If maintenance was necessary, the column was checked for irregularities on the inner coat. The areas exhibiting residues of prior run samples were cut off by using a

Teflon cutter. After cutting of the column, the system was heated up 310° C. and 140 kPa to fully eliminate contaminations. The temperature and pressure were held until the baseline stayed at a constant level around 10 pA. To determine the accuracy of the cleaned column an acid standard was run again.

#### 2.2.5.8 Evaluation of the chemical analysis

To evaluate the single chromatograms the GC-ChemStation (Hewlett Packard Corporation, U.S.A.) software was used. The different peaks received due to separation through GC-FID were integrated and the corresponding areas were assigned to the contained compounds in MS-Excel (Microsoft, U.S.A.). The compounds were identified by the fragmentation pattern of every single compound given through the analysis using mass spectrometry. The amount of the single compounds was calculated according to the known amount of the internal standard, which was added to each sample prior to all analytical steps (2.2.5.1, 2.2.5.3).

$$\textit{Substance amount } (\mu g) = \frac{\textit{Peak area x mass of internal standard } (\mu g)}{\textit{Peak area internal standard } (\mu g)}$$

Equation 1: Determination of the amount (µg) of the substances

Wax and cutin amounts were referred to the leaf and stem surface areas. Whereas the area for wax extraction of leaf's ad- and abaxial side was determined through the surface area of the opening of the vial (0.38 $cm^2$) they were extracted with. At least three biological replicates were analyzed in each experiment, therefore mean values and standard deviations were calculated in Excel (Microsoft, U.S.A.). All figures were created with OriginPro9 (OriginLab, U.S.A.).

### 2.2.6 Stomatal density

Stomatal density (SD) for ab- and adaxial leaf side or stem was determined with an axioplan universal microscope (Carl Zeiss, Jena, Germany). The imprints of the leaves and stems were prepared with nail polish (essence cosmetics, transparent, DM, Germany). Leaves and stems were applied onto double-sided tape mounted on

a piece of paper. The nail polish was gently brushed across the entire leaf/ stem surface and air dried for approximately 10 minutes. With adhesive tape the imprints were carefully transferred to a microscope slide. Stomata, as well as epidermal cells, were counted on leaves/ stems of three plants per mutant and wild type. In detail each side of the leaf/ stem was counted in ten fields of 0.09/0.37 $mm^2$ randomly distributed across the leaf/ stem. Images were taken with the Canon EOS Utility program (Krefeld, Germany) and evaluated with Image J (public domain, available at ImageJ.net). The results were displayed as counts of stomata or pavement cells per $mm^2$ of the projected leaf/ stem area. The stomatal index (SI) was calculated with SD and pavement cell density (PCD) in the following relation:

$$SI\,(\%) = \frac{SD}{SD + PCD} x\,100$$

Equation 2: Determination of the stomatal index, after (Salisbury E.J., 1927)

### 2.2.7 Stomatal conductance

To measure the stomatal conductance of the leaves a Porometer AP4 (Delta-T-Devices Ltd, Cambridge, Great Britain) was used. The principle of measurement relies on measuring the difference in humidity between the leaf interior and the inside of a sensor head. In more detail: The leaf is clipped in a sealed chamber where its evaporation of water vapor increases the humidity within the chamber (Figure 5). The rate of increase is mostly dependent on the stomata diffusion resistance. With the help of a previously accomplished calibration curve, the stomatal conductance is calculated.

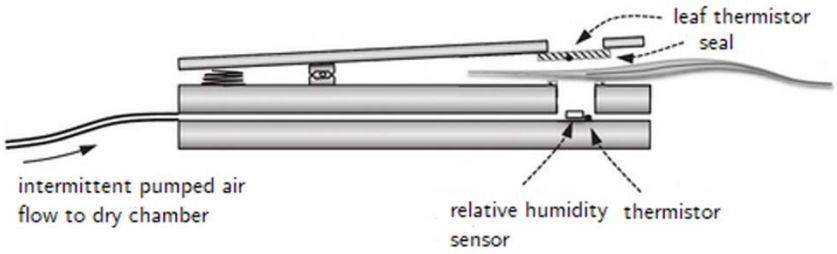


Figure 5: Schematic drawing of the used AP4 Porometer (modified after Jones, 2013)

Air is pumped in cycles into the measuring chamber to dry it out. Now the water vapor lost through the leaf is raising the humidity within the chamber again and is measured by the sensor. Additionally, two thermistors measure the accuracy of the temperature and resistance of leaf and chamber. Due to the obtained calibration curve the stomatal conductance is calculated.

Stomatal conductance was measured on ad- and abaxial sides for at least four rosette leaves of all Arabidopsis genotypes. Samples were not combined samples, as leaves of Arabidopsis are too fragile to measure them more than once with the porometer. Measurements took place at day time and in the climate chamber to ensure stable temperature, and light intensity conditions as well as open stomata. Before each measurement, the porometer was newly calibrated to achieve the most exact measuring results.

### 2.2.8 Chlorophyll-Fluorescence measurements

To provide information on the cuticular permeability of intact Arabidopsis leaves, an assay with a chlorophyll fluorometer (Junior- PAM, Walz, Effeltrich, Germany) was performed. The uptake of herbicides, which act as photosynthesis inhibitors, across the cuticle indirectly, measures the cuticular permeability via the decrease of the photosynthesis rate. The non-invasive measurements are an advantage of the PAM (Pulse Amplitude Modulation) technique. Therefore it is especially useful for measurements on small and fragile plants where cuticles are not easily isolated. The measurements can be taken in the climate chamber directly. Consequently, abiotic

factors such as light and temperature stayed constant during the measurements (2.2.1).

The PAM measures the fluorescence emitted by photosystem II (PS II) at two different time points. First, the constant emitted fluorescence yield ($F'$) is measured. This was done emitting a low energetic measuring light at 450 nm wavelength and 5 Hz to keep the reaction centers of PS II open. Secondly, a saturation pulse was emitted onto the leaf. Now all reaction centers in PS II are temporarily closed due to the strong light pulse. Due to the overcharge of the reaction centers maximal fluorescence ($F_M'$) can be measured. Alone with those two measurements the *Photosynthetic Yield* (*Y (II)*) can be calculated (Equation 3):

$$Y(II) = \frac{F_M' - F'}{F_M'}$$

Equation 3: Effective photochemical quantum yield of PS II (Genty et al., 1989)

For measurements leaves were monitored with the PAM for six minutes without any application of herbicide. This served as a control, whether the saturating pulses themselves had any influence on the photosynthetic yield. Thereafter either a 50 µl droplet of the herbicide metribuzine [4-amino-6-tert-butyl-3-(methylthio)-as-triazine-5(4H)-one], (100 µmolL$^{-1}$; Bayer, Leverkusen, Germany) or a 50 µl droplet of water (control) were applied onto the adaxial leaf surface. The intensity of the saturating pulse was set to 1 as well, which resembles 7000 µmol*m$^{-2}$*s$^{-1}$ PAR at a duration of 0.6 s.

Not only the decrease of the photosynthetic yield was evaluated but also the times of half and full inhibition were calculated and generated with the curves of each parallel measured and it's corresponding decreasing Y (II).

### 2.2.9 Measurement of the minimum conductance

The water permeability of stomatous leaves of the different Arabidopsis genotypes was measured gravimetrically. Three to four rosette leaves per genotype were cut off and stored over dry silica gel (Roth, Karlsruhe, Germany) at 25 °C in a sealed box.

These conditions set relative humidity to 0 %, and the driving force to a maximum, during the duration of the experiment. The amount of water lost over time (Figure 6) was measured with a balance which was precise to 0.01 mg (Sartorius, Göttingen, Germany). Detached leaves were weighed every 30 minutes over a total time of 6 hours. After the experiment leaves were stored in a 60 °C. heating cabinet overnight till a constant dry weight could be measured. To calculate the permeance P ($ms^{-1}$) for water across the leaf cuticle Equation 4 was used.

$$P = \frac{F}{A \times \Delta c}$$

Equation 4: Determination of permeance

P = Permeance; F = Flux, given by the slope of the regression line fitted through the gravimetric data ($g*min^{-1}$); A = surface area of the leaf; Δc = driving force; expressed as water concentration in the leaf

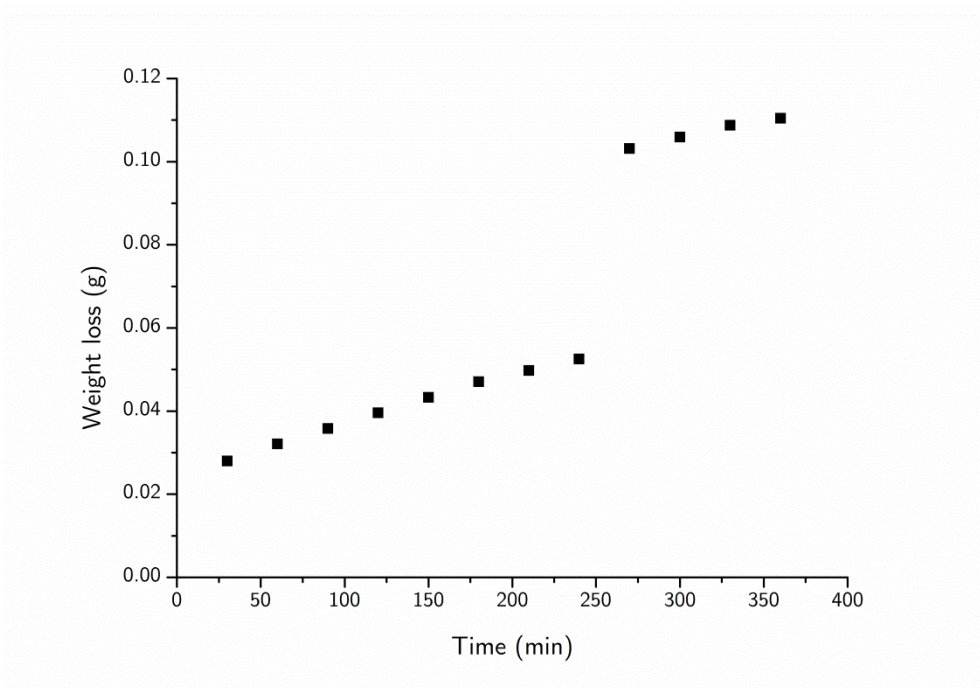


Figure 6: Representative leaf drying curve for Arabidopsis wild type (Col-0)

A representative result of a gravimetric measurement of water loss over time with a single leaf of Arabidopsis ecotype (Col-0).

In order to measure the permeability of the cuticular membrane water loss through present stomata needed to be considered. Thus the exact point of maximum

stomatal closure was determined. Therefore the relative water loss (RWL) was calculated at each time point measured. It is based on the relation of fresh weight and complete dry weight of the leaf. Likewise, minimal conductance (Equation 4) for each leaf and at each time point was calculated by the slope of the regression line fitted through the gravimetric data (Figure 6). The minimal conductance plotted against the RWL calculated for each time point and every leaf of each genotype determines the point at which transpiration through the cuticle occurred (Figure 7). Respective figures (Figure 6, Figure 7) are representative for one replicate. For at least four replicates of each drying curve, mean values and standard deviations were calculated.

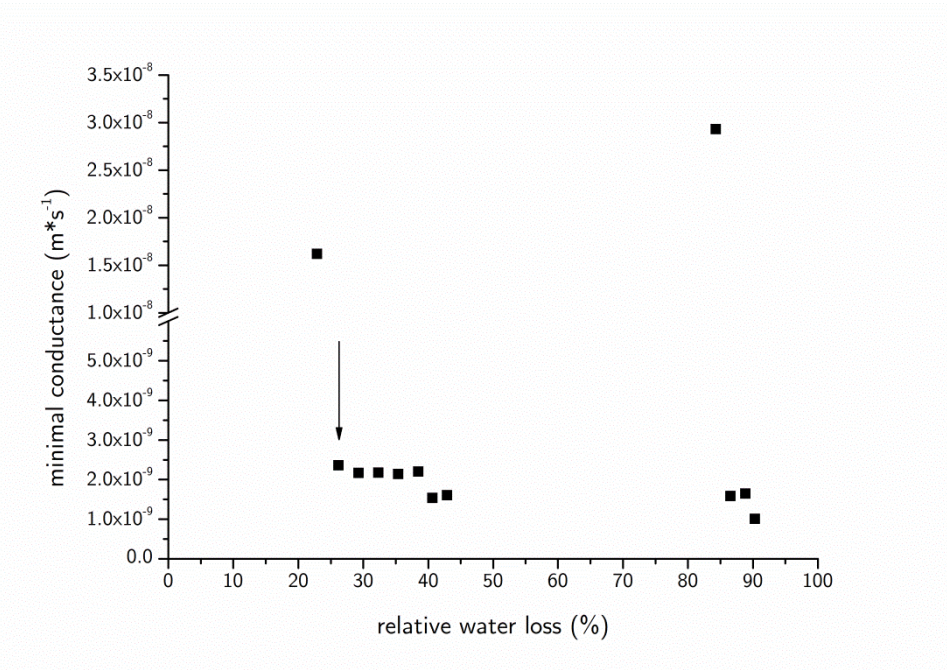


Figure 7: Representative leaf drying curve for Col-0 Arabidopsis wild type

The leaf minimal conductance was plotted against the relative water loss of the leaf. The initial minimal conductance is high with higher relative water loss it reaches a transition point (black arrow) from where on the conductance is constant. At this point, minimal conductance at total stomatal closure is reached

### 2.2.10 Statistical analysis

All data processing for this work was done with Microsoft Excel 2010 (Microsoft Corporation, Redmond, U.S.A.) and OriginPro9 (OriginLab, U.S.A.). Statistical tests for normal distribution of data were performed with the '*Shapiro Wilk*' test.

To test for significant differences between the means *'One way ANOVA'* with the *'Fisher LSD'* or student t-test was performed. The significance level for performed tests was set at $p < 0.05$.

# 3 Results

## 3.1 Leaf and stem surface characterization of different Arabidopsis genotypes and mutants

Field Emission scanning electron microscopy (FE-SEM) was used to study the leaf and stem surfaces of stomatal, wax and cutin mutants. With this approach described mutations in the literature of the here investigated Arabidopsis genotypes and mutants were observed. Mutants with prominent wax or stomatal appearance are shown. Cutin mutant *att1* did not exhibit prominent wax or stomatal structure either on stem or leaf (data in supplementals, 7.1).

### 3.1.1 Leaf surface morphology of wax and stomatal mutants

The surface of all Arabidopsis leaves was covered with a hardly visible thin wax film, and wax granules close to stomata (Figure 8). In the wild type, Col-0, stomata are single-spaced and follow the one spacing rule (circle), hence they are separated from each other by at least one pavement cell (Figure 8 A, B). In the stomatal mutant *tmm* and *flp,* stomata are clustered (Figure 8 C, D). In the *flp* mutant clusters are smaller than in *tmm* and stomata appear as units in adjacent pairs (Figure 8 E, F).

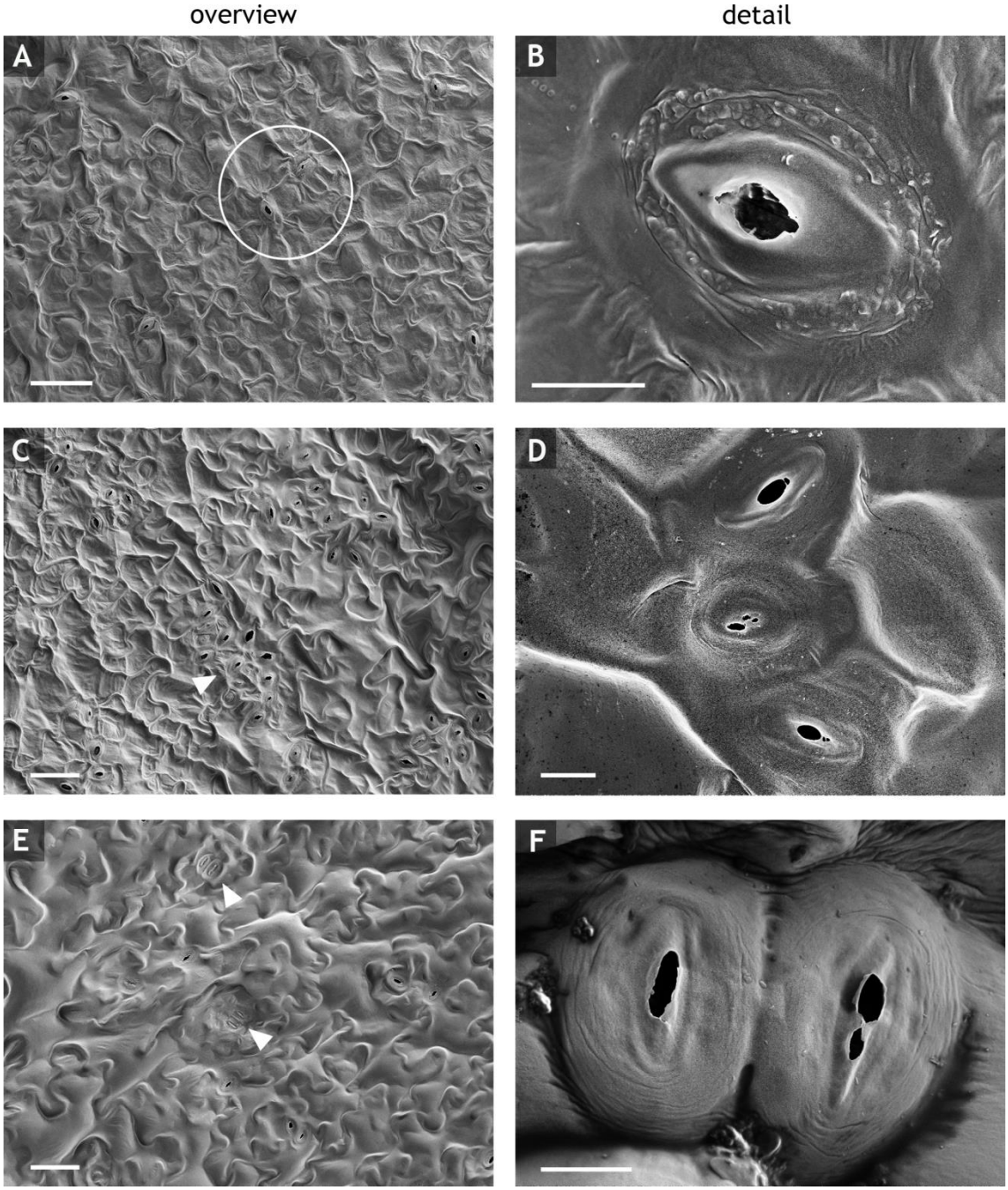


Figure 8: FE-SEM micrographs of the leaves' surface morphology

Overview (scale bars: 40 µm) and detail (scale bars: 5 µm) of Arabidopsis wild type and different stomatal mutants on the abaxial leaf side.

A, B: Col-0; C, D: *tmm*; E, F: *flp*. The circle emphasizes on the one spacing rule in stomatal patterning. Arrows indicate mutations in the formation of stomata.

Also different from the wild type Col-0 (Figure 8 A) the stomatal mutants *st-ox* and *st-RNAi* show high and low stomatal density respectively (Figure 9, A; E). Whereas the wax mutant *wax2* exhibits stomatal patterning not different from the wild type and therefore follows the one spacing rule (Figure 9 C). Unlike the wild type (Figure 8 B) where wax granules accumulate around stomata and on guard cells, those are not visible in *wax2* (Figure 9 D). Stomatal mutant *st-RNAi* does not show any abnormalities in stomatal appearance (Figure 9 F).

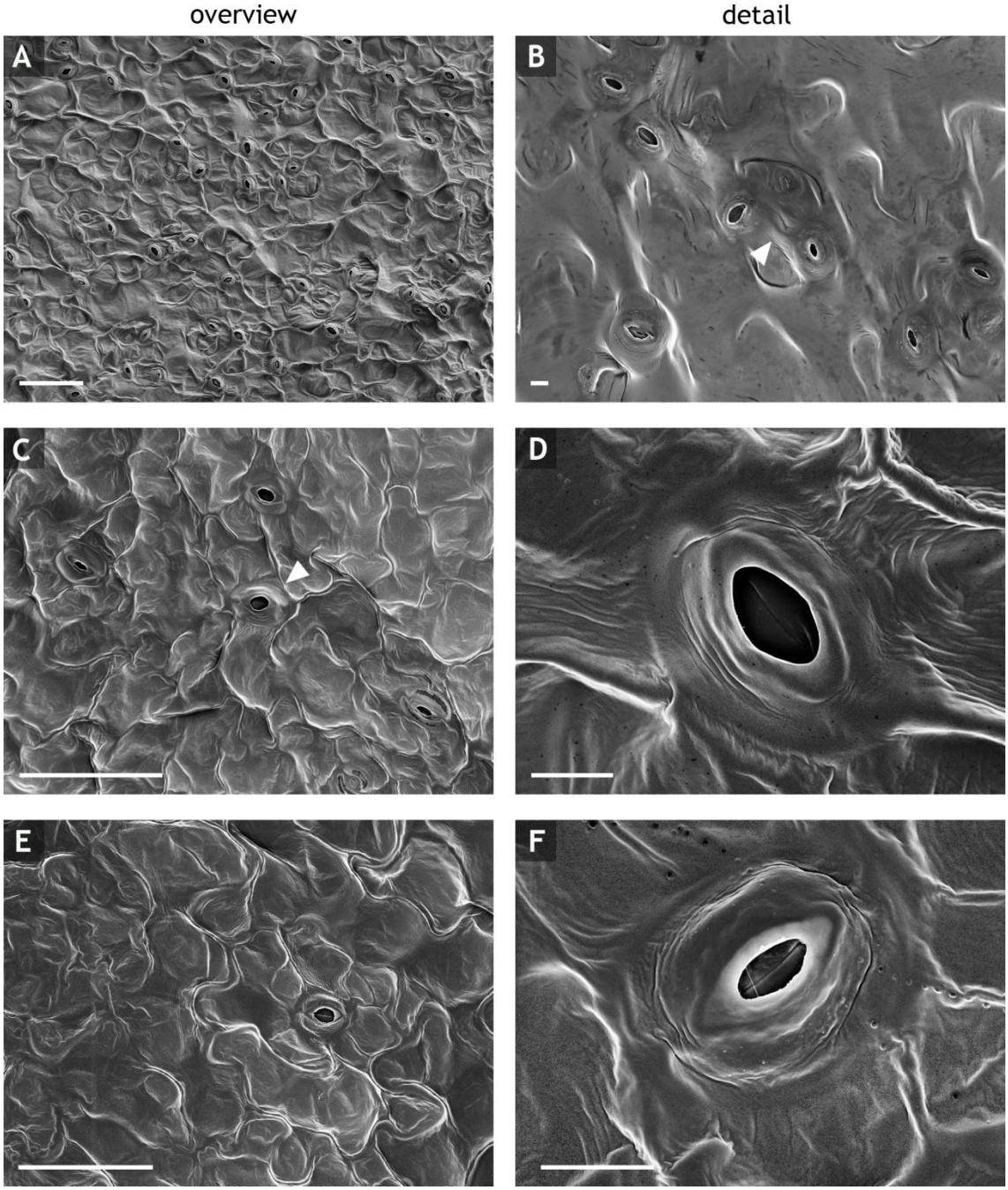


Figure 9: FE-SEM micrographs of the leaves' surface morphology

Overview (scale bars: 40 µm) and detail (scale bars: 5 µm) of Arabidopsis stomatal mutants and wax mutant on the abaxial leaf side.

A, B: *st-ox*; C, D: *wax2*; E. F: *st-RNAi*

### 3.1.2 Stem surface of wax and stomatal mutants

Epicuticular wax crystals can be found over the entire stem surface. The wild type Col-0 and the stomatal mutant *tmm* show polymorphism in their wax crystalloids: Tubules, as well as platelets and rodlets, are visible on the stem surface (Figure 10 B, D). *Flp*, on the other hand, shows rarely tubules and rodlets but exhibits mostly platelets (Figure 10 F). Additionally, there seem to be fewer wax crystals in this mutant overall (Figure 10 E), when compared to the wild type Col-0 (Figure 10 A). The stomatal mutation of the characteristic '*four lips*' is not found in the stem surface (Figure 10 E, F). *Tmm* is completely lacking stomata on the stem but otherwise exhibits the same structure of wax crystals as the wild type (Figure 10 C, D).

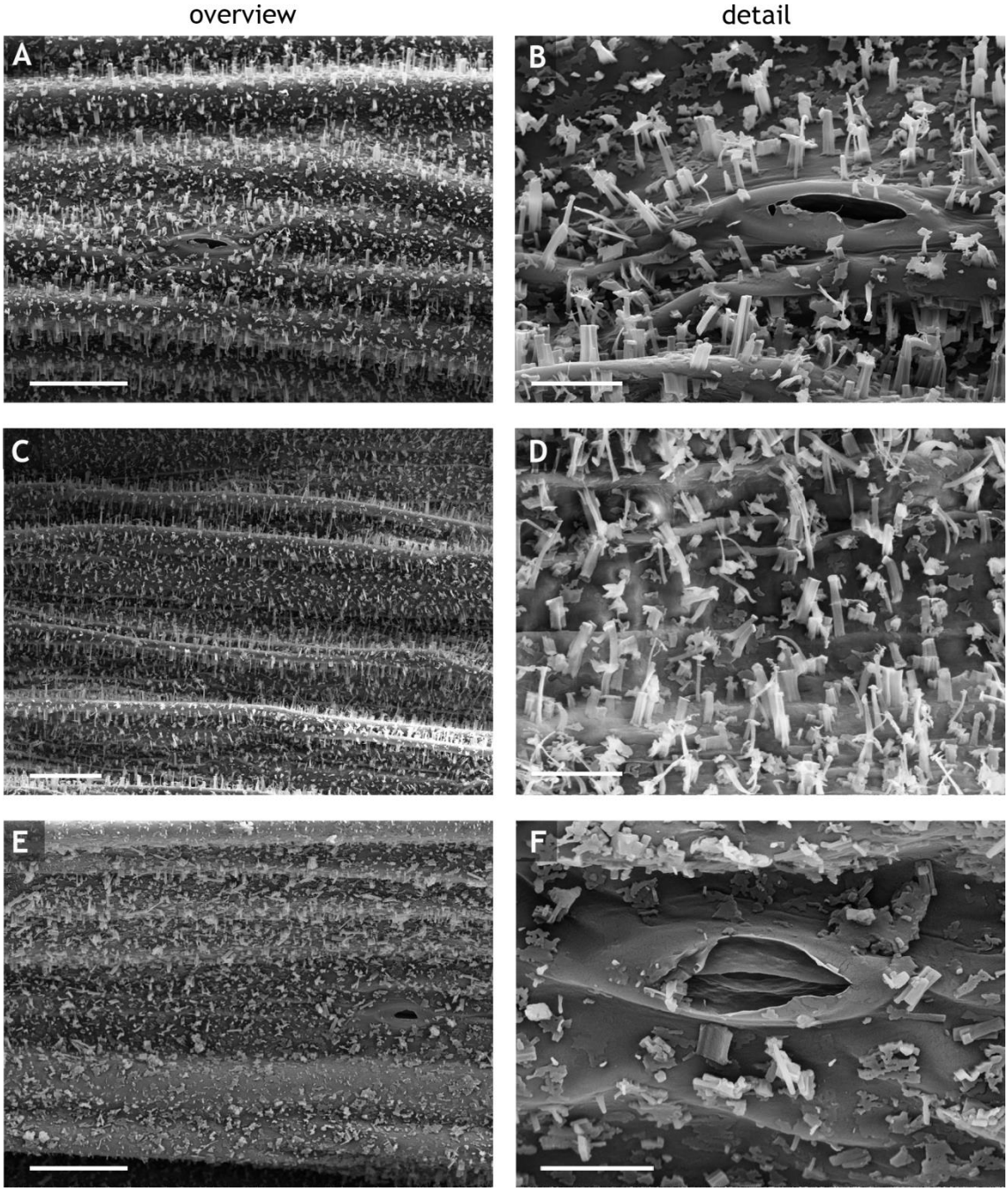


Figure 10: FE-SEM micrographs of the stems' surface morphology

Overview (scale bars: 20 µm) and detail (scale bars: 5 µm) of Arabidopsis wild type and different stomatal mutants.

A, B: Col-0; C, D: *tmm*; E, F: *flp*

The stomatal mutant *st-ox* (Figure 11 A) shows more stomata on the stem surface compared to the wild type (Figure 10 A). Also in its wax morphology, it is different from the wild type exhibiting only platelets (Figure 11 B). Stomatal mutant *st-RNAi* (Figure 11 F) does not show different wax morphology when compared to the wild type (Figure 10 B). The wax mutant *wax2* analogous to the leaf doesn't show any particular wax morphology and is instead covered with a thin wax film and few wax granules (Figure 11 C; D).

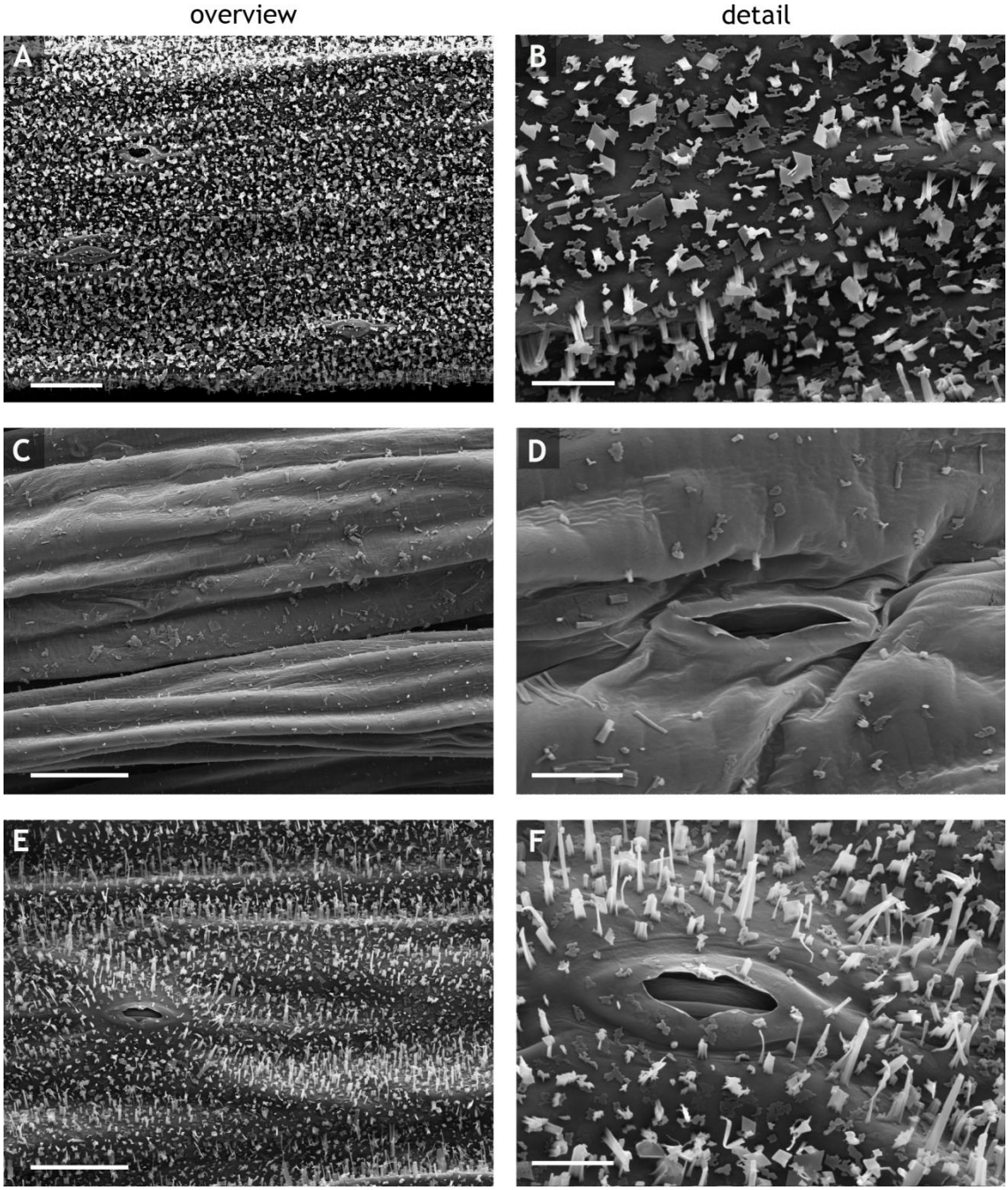


Figure 11: FE-SEM micrographs of the stems' surface morphology

Overview (scale bar: 20 µm) and detail (scale bar: 5 µm) of different Arabidopsis mutants. A, B: *st-ox*; C, D: *wax2*; E, F: *st-RNAi*

## 3.2 Measurement of wetting properties

Contact angles of 10 µl water droplets on the different leaf surfaces were measured to provide more information on the wetting properties and hence the surface structure of the leaves. The wettability of different Arabidopsis genotypes was measured on leaf's ad- and abaxial side. Water droplets on parafilm served as an additional control. There was a tendency that all measured values were higher for contact angles on the abaxial side than on the adaxial side. Arabidopsis ecotype Col-0 was the only exception with a higher contact angle on the adaxial leaf side than on the abaxial side. Further only the stomata mutants *st- RNAi* and *tmm* showed significant differences in the measured contact angle for both leaf sides compared to the wild type (Col-0) as did the cutin mutant *att*. Aside from those the other stomatal mutants only showed significant differences in the wettability of the abaxial leaf side, when compared to Col-0. The wax mutant *wax2* did not show any difference in the wetting properties for different leaf sides but instead on the adaxial leaf side when compared to the wild type (Table 2).

Table 2: Contact angle measurements on Arabidopsis genotypes, mutants and on parafilm

Taken contact angle measurements of the ad- and abaxial leaf sides and parafilm. Shown are means and standard deviation of at least three biological replicates. Asterisks indicate significant differences between means of mutants and corresponding wild type at a significance level of 0.05 in student's t-test.

| Genotype | contact angle (°) | |
|---|---|---|
| | adaxial | abaxial |
| *tmm* | 96.7 ± 4.1 * | 109.8 ± 5.4 * |
| *flp* | 115.8 ± 9.5 | 105.9 ± 9.1 * |
| *st-ox* | 108.6 ± 16.5 | 112.5 ± 2.5 * |
| *st-RNAi* | 104.9 ± 5.9 * | 118 ± 3.9 * |
| Col-0 | 114.7 ± 8.8 | 90.1 ± 3.2 |
| *wax2* | 89.42 ± 3.8 * | 89.7 ± 0.7 |
| *att1* | 96.7 ± 4.1 * | 116.4 ± 10.6* |
| Ws | 106.7 ± 8.5 | 104.8 ± 3.3 |
| *shn3* | 99.9 ± 1.7 | 106.9 ± 6.1 |
| parafilm | 106.2±1.5 | 110±1.3 |

## 3.3 Chemical analysis of plant waxes and cutin

To corroborate a possible relationship between stomatal density and wax or cutin amount in Arabidopsis leaves or stems, chemical analyzes were performed according to (2.2.5). With special interest, the wax and cutin amounts of the chosen set of Arabidopsis stomatal mutants were compared to the wild type.

Next to waxes of whole leaves also waxes of ab- and adaxial sides of the leaves of Arabidopsis were analyzed. Waxes were separately analyzed for both leaf sides, enabling for a subsequent comparison between stomatal density and wax content for both sides of the leaves. Additionally, stems of the chosen Arabidopsis mutants were chemically analyzed for wax and cutin amounts. Also, the biopolymer cutin was analyzed for both plant organs. The data for wax and cutin extraction is presented

in the following for at least 3 biological replicates with standard deviation for each Arabidopsis genotype.

### 3.3.1 Chemical analysis of waxes for whole Arabidopsis leaves

The total wax extraction for whole leaves was performed as described in 2.2.5.1. For the Arabidopsis ecotypes Col-0 and Ws the total wax amount was 0.76 (±0.09) µg*cm$^{-2}$ and 0.74 (±0.13) µg*cm$^{-2}$ respectively. The wax mutant *shn3*, as well as the cutin mutant *att1*, did not show any significant differences compared to the corresponding wild types. From leaves of the wax mutant *wax2,* a significant lower wax amount was extracted (0.33±0.09 µg*cm$^{-2}$). All stomatal mutants, except for *st-ox*, had significantly lower wax amounts extracted from whole leaves than the wild type. *St-RNAi* leaves had 46 % less wax compared to the control. The mutants *tmm* (0.44±0.1 µg*cm$^{-2}$) and *flp* (0.54±0.08 µg*cm$^{-2}$) mutants showed a 1.73 and 1.4 fold decrease in wax amount compared to Col-0 (Figure 12).

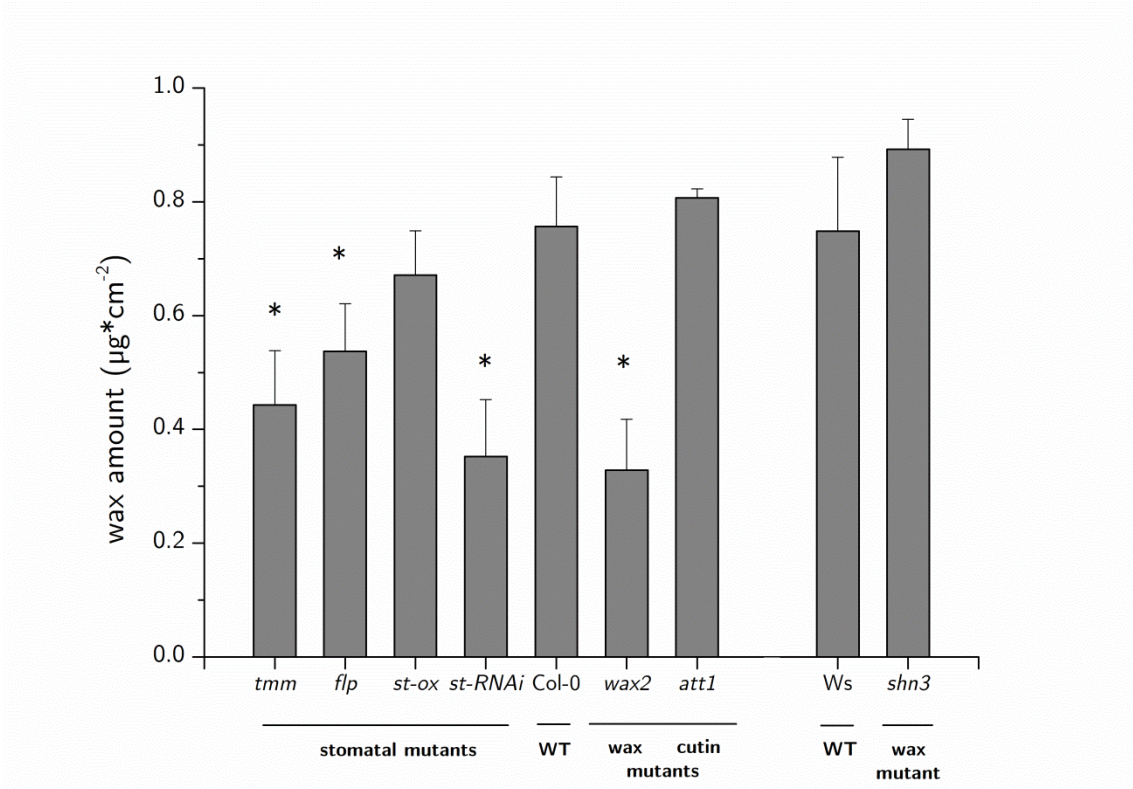


Figure 12: Total wax amount of whole Arabidopsis leaves

Amounts of total wax extracted from whole Arabidopsis leaves. Stomatal, wax and cutin mutants with Col-0 background are plotted together. Wax mutant *shn3* and corresponding wild type Ws are shown separately. Bars indicate mean values with standard deviation of at least three biological replicates. Asterisks indicate significant differences between means of mutants and corresponding wild type at a significance level of 0.05 in One-Way ANOVA (Fisher LSD).

### 3.3.2 Chemical analysis of waxes for ad- and abaxial Arabidopsis leaves

Wax extraction for ad and abaxial sides of Arabidopsis leaves was performed according to 2.2.5.1. Overall wax amounts on the adaxial leaf side were lower than on the abaxial side (Figure 13). However, significant differences could only be analyzed for waxes extracted from both the adaxial and abaxial leaf sides of stomatal mutant *st-RNAi* (0.57±0.04 / 0.5±0.13 µg*cm$^{-2}$) and wax mutant *wax2* (0.51±0.2 / 0.29±0.04 µg*cm$^{-2}$) when compared to the corresponding wild type Col-0 (0.75±0.04/ 0.8±0.07 µg*cm$^{-2}$), (Figure 13).

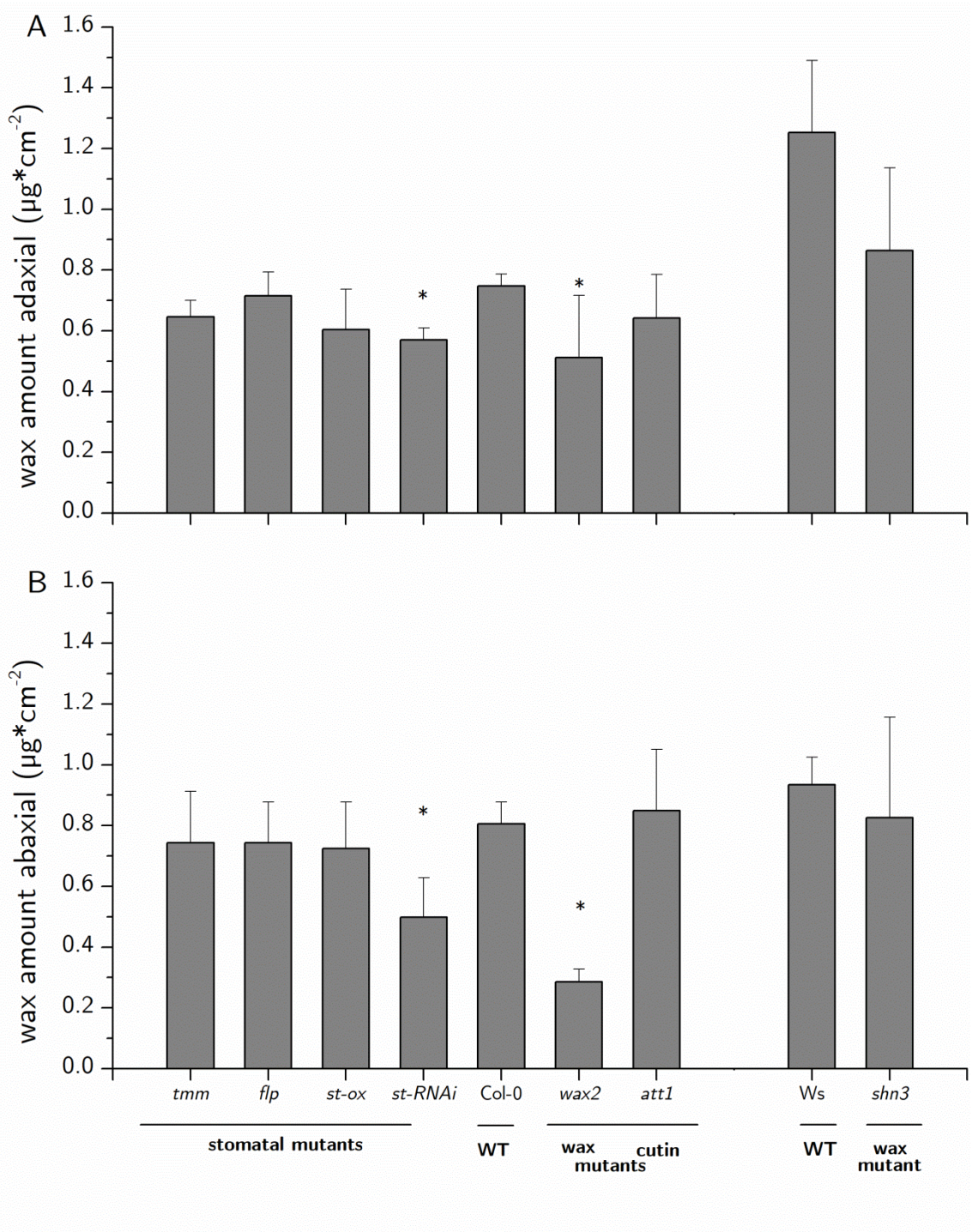


Figure 13: Wax amount of ad- and abaxial Arabidopsis leaves

Amounts of wax extracted from the ad- (A) and abaxial (B) leaf sides. Stomatal, wax and cutin mutant with Col-0 background are plotted together. Wax mutant *shn3* and corresponding wild type Ws are shown separately. Bars indicate mean values with standard deviation of at least three biological replicates. Asterisks indicate significant differences between means of mutants and corresponding wild type at a significance level of 0.05 in One-Way ANOVA (Fisher LSD).

To show the differences in the total wax amount of Arabidopsis leaf's ad- and abaxial sides for the stomatal mutant *st-RNAi* in more detail, amounts of cuticular wax substances were plotted (Figure 14). Even though total amounts for the ad- and abaxial leaf sides were consistent in itself for both the wild type and the mutant (Figure 13), significant differences were analyzed for the amount of wax monomers between wild type and mutant.

Within each substance class two to nine individual wax monomers could be identified. For the adaxial leaf side acids, aldehydes, primary and secondary alcohols were weakly affected. Acids ranging from chain lengths $C_{16}$ to $C_{34}$ made up 38.8 % (±5.05 %) of the total wax amount on the adaxial leaf side for the mutant *st-RNAi*. In the wild type Col-0, the substance class of acids was made up of 23.99 % (±6.37 %) wax and was, different from the mutant, not the most abundant substance class of the total wax. For the wild type alkanes were the most abundant substance class on the adaxial leaf surface (33.95±3.37 %). The main differences were found in the highest abundant monomer ($C_{31}$ alkane) analyzed in Arabidopsis wax for both ad- and abaxial leaf sides (Figure 14). The mutant showed significantly fewer amounts of the $C_{29}$- (0.03±0.004 $\mu g*cm^{-2}$) and $C_{31}$ alkane (0.06±0.01 $\mu g*cm^{-2}$) extracted from the epicuticular wax of the adaxial leaf side. Higher amounts of 0.08±0.001 $\mu g*cm^{-2}$ ($C_{29}$-) and 0.12±0.01 $\mu g*cm^{-2}$ ($C_{31}$ alkane) were analyzed for the wild type. Additionally 6.6- fold less amount was extracted of the $C_{29}$ secondary alcohol in the mutant (0.003±0.002 $\mu g*cm^{-2}$) when compared to the wild type (0.02±0.008 $\mu g*cm^{-2}$), (Figure 14 A).

On the other hand, wax extracted from the abaxial side of the leaf showed overall lower amounts of wax monomers in all substance classes in the mutant. In the substance class of alkanes, $C_{31}$ alkane with the highest abundance in wild type (0.12±0.02 $\mu g*cm^{-2}$), was significantly decreased in the mutant *st-RNAi* (0.05±0.02 $\mu g*cm^{-2}$). As on the adaxial leaf, side acids are the most abundant substance class in the mutant *st-RNAi* with and 39 % (±6.95 %). Acids in the wax of Col-0 made up 29.78 % (±9.2 %). A significant difference was analyzed for the $C_{16}$ and $C_{18}$ acid, which was not present in the wild type at all but detected in *st-RNAi*

(0.04±0.01 / 0.03±0.003 µg*$cm^{-2}$). When comparing ad- and abaxial leaf sides an increase in the amount of the single monomers of $C_{34}$ acid and $C_{32}$ alcohol are evident for the abaxial leaf side of the wild type wax (Figure 14 B).

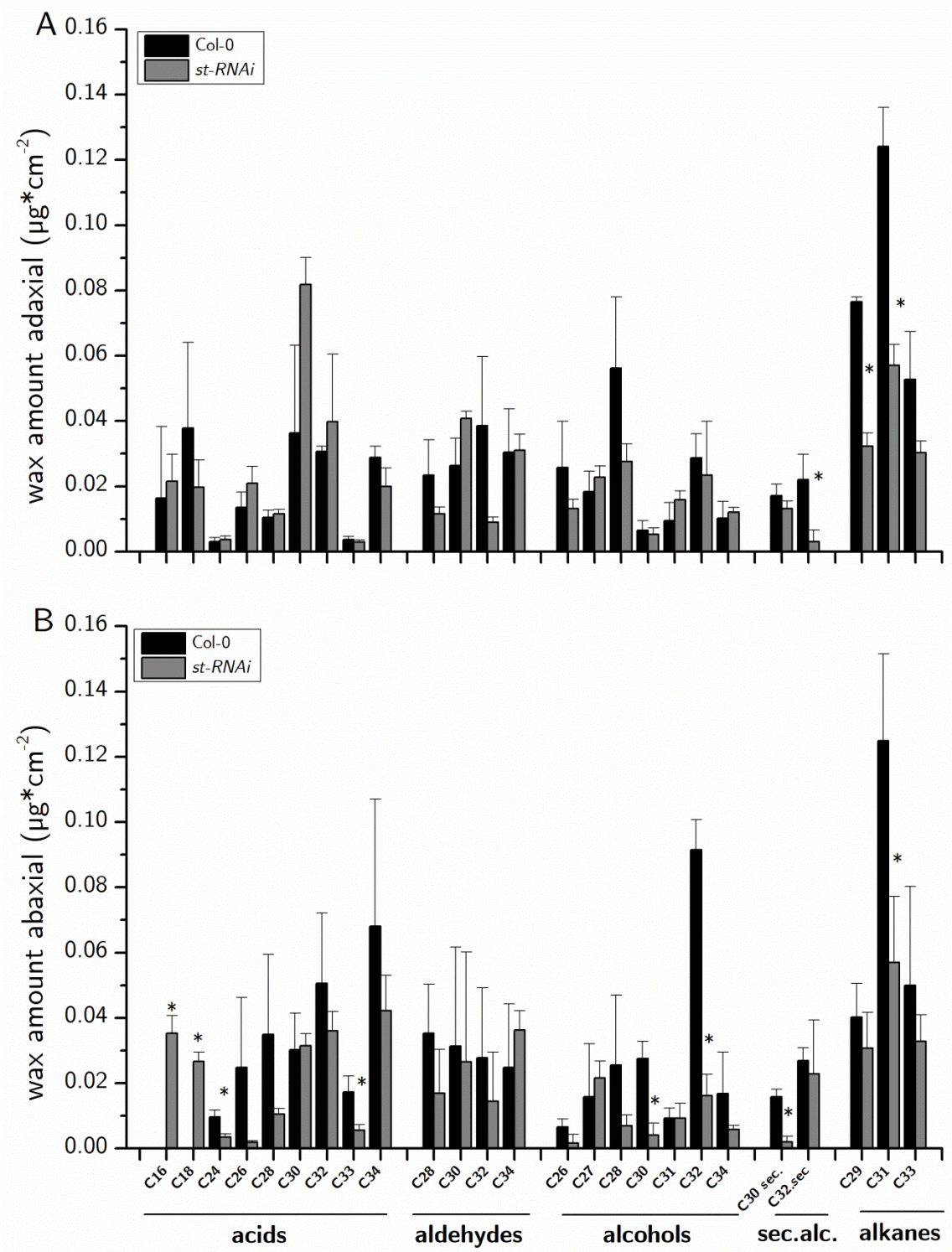


Figure 14: Amounts of wax monomers identified in Arabidopsis leaf sides

Wax amounts of stomatal mutant *st-RNAi* of ad- (A) and abaxial (B) leaf side in comparison to the corresponding wild type Col-0 are shown in means of at least three biological replicates with standard deviation. Within each substance class (acids: primary fatty acids; aldehydes: primary aldehydes; alcohols: primary alcohols; sec.alc.: secondary alcohols; alkanes: linear alkanes) wax constituents of different chain lengths were identified. Asterisks indicate significant differences between means of mutant and the wild type at a significance level of 0.05 in student t-test.

### 3.3.3 Chemical analysis of cutin for whole Arabidopsis leaves

In order to further elucidate the relationship between stomatal density and changes in cuticular chemistry, the biopolymer cutin was chemically analyzed for the different Arabidopsis mutants. Cutin extraction was performed as previously described in 2.2.5.2.

Overall all stomatal mutants showed lower amounts of cutin extracted from the Arabidopsis leaves. Especially the *flp* mutant showed a significant lower cutin amount (0.8±0.08 µg*cm$^{-2}$) compared to the wild type Col-0 (1.58±0.47 µg*cm$^{-2}$). Likewise, the cutin mutant *att1* showed a 46.2 % (0.81±0.05 µg*cm$^{-2}$) decrease in cutin amount when compared to the wild type. The cutin amounts of *shn3* (1.52±1.04 µg*cm$^{-2}$) were 1.46-fold higher than in the corresponding wild type (Figure 15).

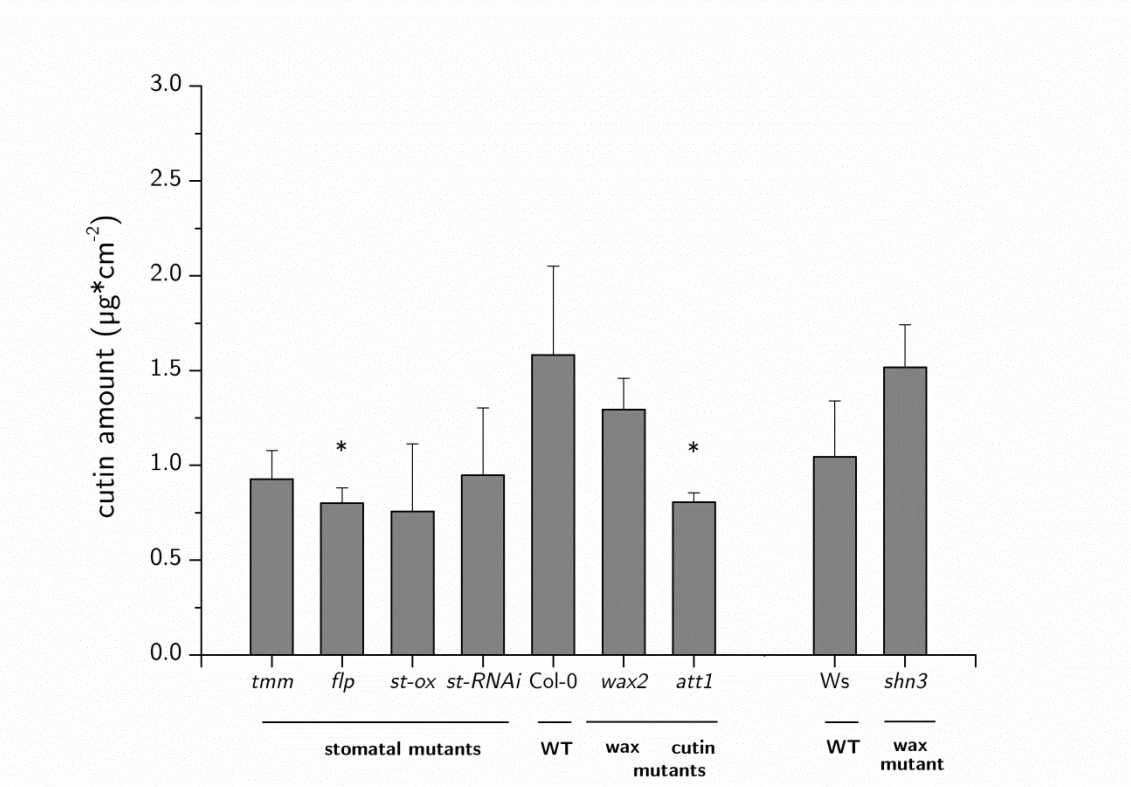


Figure 15: Cutin amount of Arabidopsis leaves

Amounts of cutin extracted from Arabidopsis leaves of different genotypes. Stomatal, wax and cutin mutants with Col-0 background are plotted together. Wax mutant *shn3* and corresponding wild type Ws are shown separately. Bars indicate mean values with standard deviation of at least three biological replicates. Asterisks indicate significant differences between means of mutants and corresponding wild type at a significance level of 0.05 in One-Way ANOVA (Fisher LSD).

### 3.3.4 Chemical analysis of waxes for Arabidopsis stems

Information about the possible impact of stomatal density on the wax amount in the stem of the plants was investigated (2.2.5). To compare the chosen set of Arabidopsis stomatal mutants the set of wax and cutin mutants was analyzed as well. All lines had significant higher wax amounts on the stems compared to the leaves (Figure 12, Figure 13, Figure 16). Further, all stomatal mutants showed significant differences compared to the wax amount of the wild type. Only the mutant *tmm* showed lesser wax amount (10.26±0.78 µg*cm$^{-2}$) than the wild type Col-0 (14.5±2.51 µg*cm$^{-2}$). For the *flp*, (22.99±5.3 µg*cm$^{-2}$), *st-ox* (21.47±2.18 µg*cm$^{-2}$) and *st-RNAi* (19.99±4.61 µg*cm$^{-2}$) mutants significantly higher amounts of wax were revealed. The wax mutant *wax2* had 3.02- fold less wax

extracted from the stem (4.84±0.7 µg*cm$^{-2}$) than the wild type Col-0. The other mutants and the corresponding wild type did not show any significant differences in their wax amount (Figure 16).

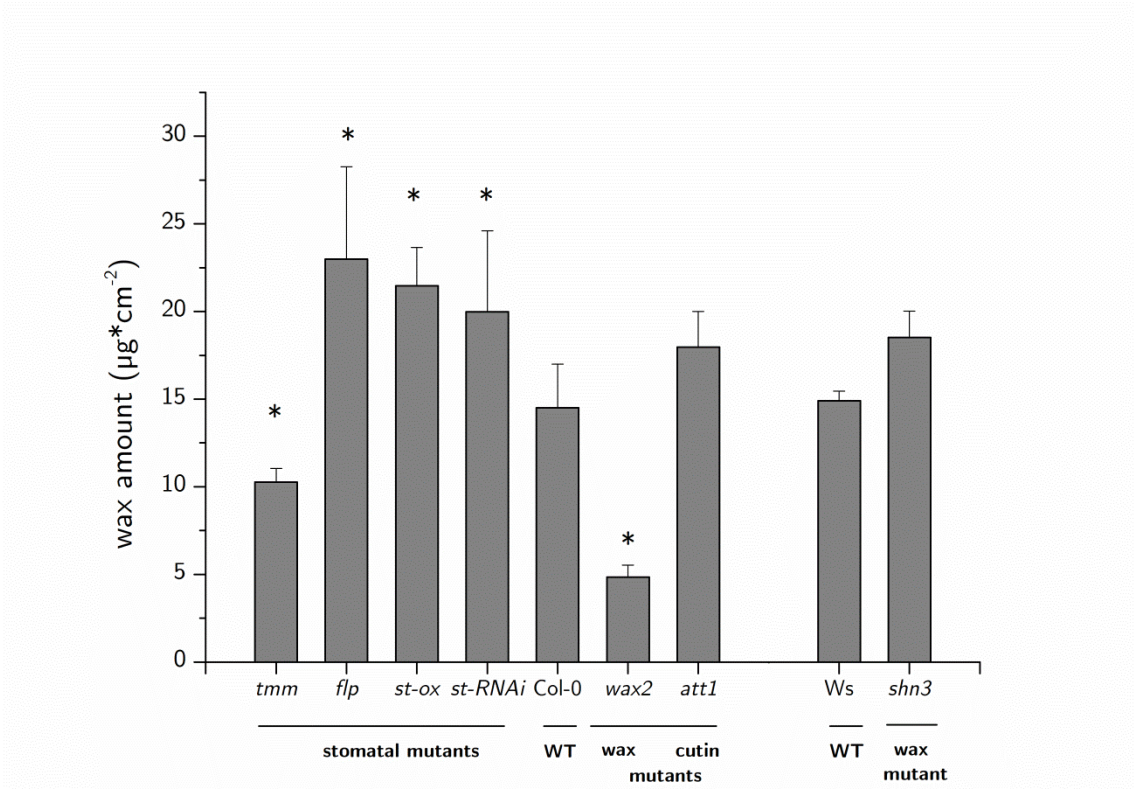


Figure 16: Wax amount of Arabidopsis stems

Amounts of wax extracted from Arabidopsis stems of different genotypes. Stomatal, wax and cutin mutants with Col-0 background are plotted together. Wax mutant *shn3* and corresponding wild type Ws are shown separately. Bars indicate mean values with standard deviation of at least three biological replicates. Asterisks indicate significant differences between means of mutants and corresponding wild type at a significance level of 0.05 in One-Way ANOVA (Fisher LSD).

### 3.3.5 Chemical analysis of cutin for Arabidopsis stems

Information about the possible impact of stomatal mutations on the deposition of cutin in the stem was of particular interest. Therefore cutin was also extracted from the stem of different Arabidopsis mutants. Similar to wax all the Arabidopsis lines showed significant higher cutin amounts on the stems compared to leaves (Figure 15). The stomatal mutants *flp* (6.69±1.04 µg*cm$^{-2}$) and *st-ox* (6.52±1.64 µg*cm$^{-2}$) had an increased amount of cutin extracted from the stems compared to the wild

type Col-0 (4.58 µg*cm$^{-2}$). Vice versa the mutant *tmm* (2.36±0.82 µg*cm$^{-2}$) showed a significantly lower amount of cutin. Additionally, the overall cutin coverage in the stem of the mutant *att1* (1.25±0.37 µg*cm$^{-2}$) was 27.3 % lesser than in Col-0 (Figure 17).

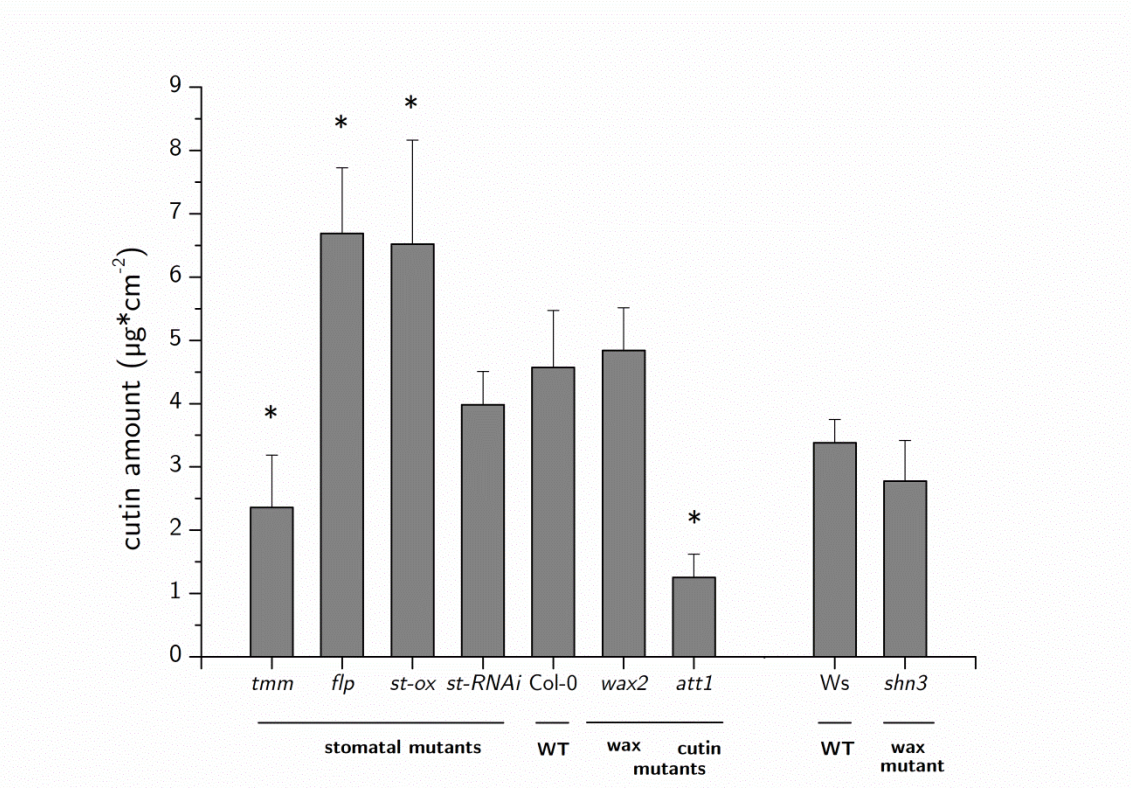


Figure 17: Cutin amount of Arabidopsis stems

Amounts of cutin extracted from Arabidopsis stems of different genotypes. Stomatal, wax and cutin mutants with Col-0 background are plotted together. Wax mutant *shn3* and corresponding wild type Ws are shown separately. Bars indicate mean values with standard deviation of at least three biological replicates. Asterisks indicate significant differences between means of mutants and corresponding wild type at a significance level of 0.05 in One-Way ANOVA (Fisher LSD).

## 3.4 Stomatal density of Arabidopsis leaves and stems

Stomatal density was determined to further investigate a possible correlation between the amounts of both leaves' and stems' wax and the stomatal density for both plant organs. Counting of stomata was conducted as described in 2.2.6.

### 3.4.1 Stomatal density of Arabidopsis leaves

The total amount of stomata counted for Arabidopsis leaves showed significant differences between the control (196±38 $mm^{-2}$) and all stomatal mutants except for *tmm* (210±24 $mm^{-2}$). *St-ox* was the only mutant that showed a significantly higher amount of stomata (403±26 $mm^{-2}$) than the wild type. The mutants *flp* (117±19 $mm^{-2}$) and *st-RNAi* (35±13 $mm^{-2}$) contrarily showed significantly lower stomatal density. Likewise, the wax mutant *wax2* (93±5°$mm^{-2}$), as well as the wax mutant *shn3* (79±6 $mm^{-2}$), had significantly lower amounts than the corresponding wild types Col-0 and Ws (166±8 $mm^{-2}$) respectively (Figure 18).

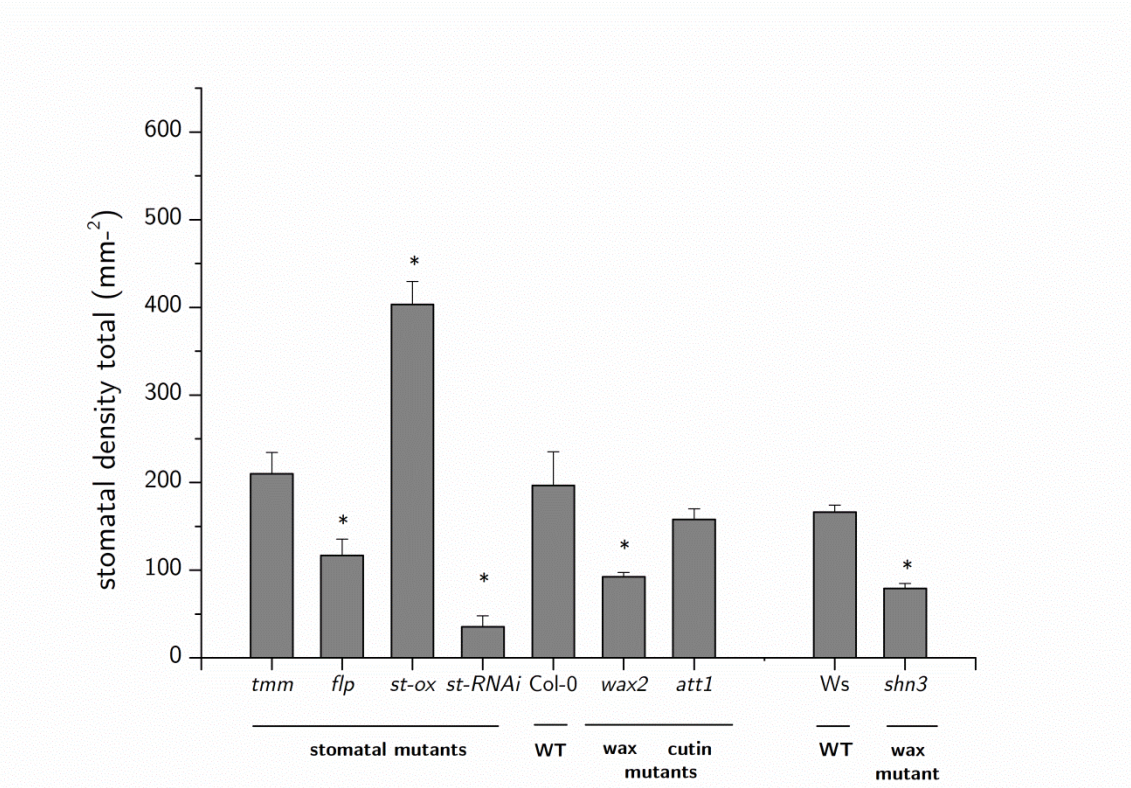


Figure 18: Density of stomata per $mm^2$ of Arabidopsis leaves

Stomatal density in Arabidopsis stomatal, wax and cutin mutants leaves. Stomatal, wax and cutin mutants with Col-0 background are plotted together. Wax mutant *shn3* and corresponding wild type Ws are shown separately. Presented is the sum of adaxial and abaxial single values divided by two. The bars indicate mean values with standard deviation of at least three biological replicates. Asterisks indicate significant differences between means of mutants and corresponding wild type at a significance level of 0.05 in One-Way ANOVA (Fisher LSD).

### 3.4.2 Stomatal density of ad- and abaxial leaf sides of Arabidopsis

To differentiate between the two leaf sides and to further compare the number of stomata with the wax amount per leaf side, stomata were additionally counted for ad- and abaxial leaf sides. Overall fewer stomata were counted for the leaf's adaxial side (Figure 19 A). *Tmm* was the only mutant showing a decrease in stomatal density (SD) on the adaxial (78±17 $mm^{-2}$) side and an increase on the abaxial (342±32 $mm^{-2}$) leaf side when compared to the wild type (169±43 / 235±86 $mm^{-2}$). The amount of the wild type Col-0 for ad- and abaxial side was only slightly different from each other. However, the wild type values for SD compared to the values in corresponding stomatal mutant *st-RNAi* (20±7 / 51±23 $mm^{-2}$) and wax mutant *wax2* (88±3 / 98±7 $mm^{-2}$) were significantly lower on both leaf sides for the mutants (Figure 19 A, B). Whereas the stomatal mutant *st-ox* only showed a significant increase in SD on the abaxial leaf side (577±43 $mm^{-2}$), (Figure 19 B). The stomatal mutant *flp* instead decreased in SD on the adaxial side (87±41 $mm^{-2}$). The wax mutant *shn3* also showed a decrease of SD (55±3 $mm^{-2}$) on the adaxial leaf side when compared to the control Ws (141±16 $mm^{-2}$).

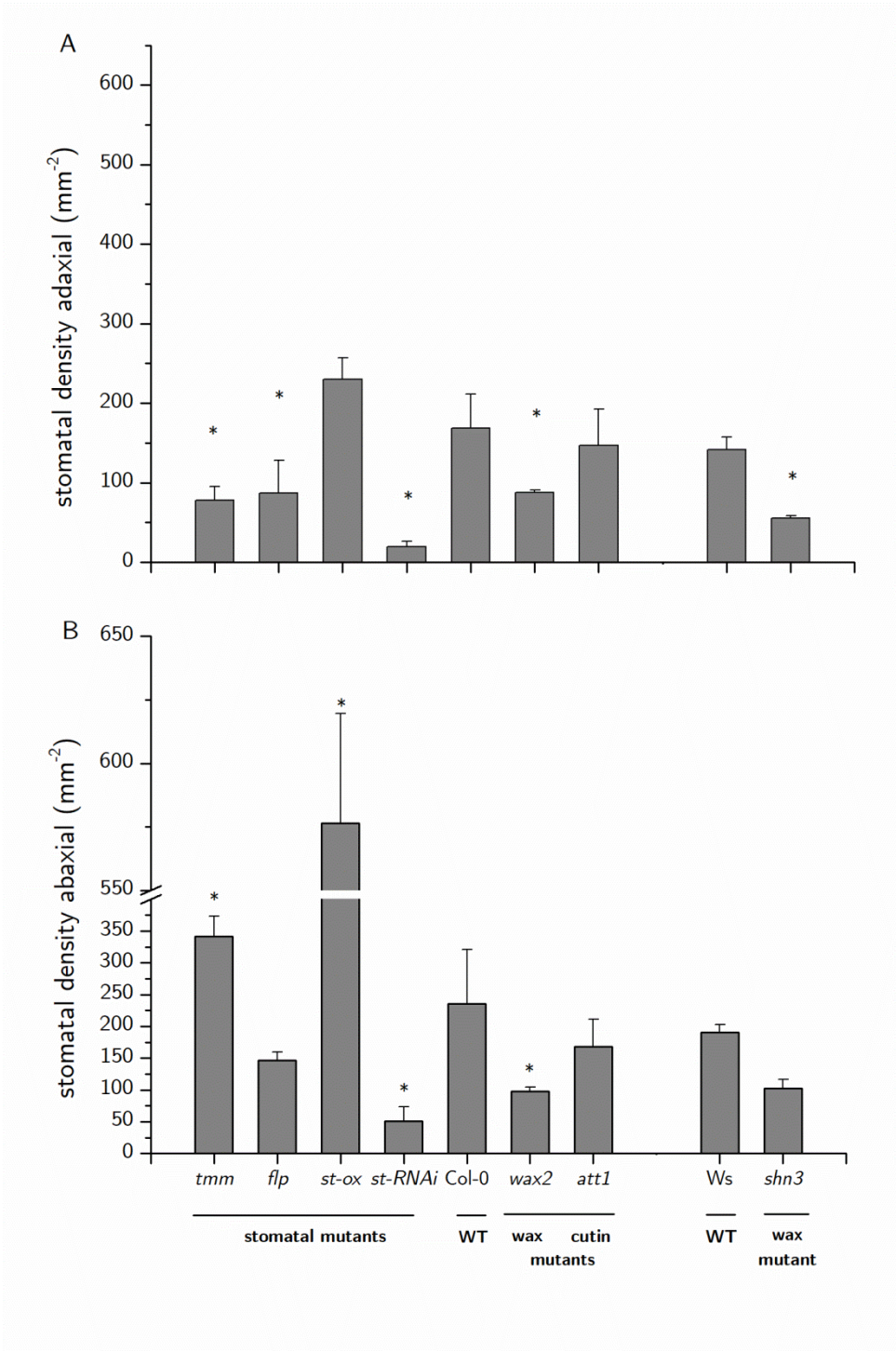


Figure 19: Density of stomata per $mm^2$ of Arabidopsis ad- and abaxial leaf sides

A: Stomatal density in Arabidopsis stomatal, wax and cutin mutants of the adaxial leaf side. B: Stomatal density in Arabidopsis stomatal, wax and cutin mutants of the abaxial leaf side. Stomatal, wax and cutin mutant with Col-0 background are plotted together. Wax mutant *shn3* and corresponding wild type Ws are shown separately. Bars indicate mean values with standard deviation of at least three biological replicates. Asterisks indicate significant differences between means of mutants and corresponding wild type at a significance level of 0.05 in One-Way ANOVA (Fisher LSD).

### 3.4.3 Stomatal index for ad- and abaxial leaf side

The stomatal index (SI) for different Arabidopsis mutants and their corresponding wild types were calculated as described in 2.2.6. The SI sets pavement cell density and stomatal density in relative relation. Therefore results for different sets of mutants and wild types were calculated for both leaf sides, additionally to the absolute number of stomata per $mm^{-2}$ (3.4.1).

Overall the SI did not differ between the leaf's ad- and abaxial sides for the single genotypes. The only exceptions were the stomatal mutants *tmm*, *st-RNAi* and *st-ox*. The mutant *tmm* did not show a significant difference in the SI on the adaxial leaf side (26.01±5.82 %) compared to the wild type (21.42±1.79 %), but instead a significantly higher number on the abaxial side (50.29±3.58 %) than Col-0 (19.71±5.82 %). A significant increase of SI could also be determined for *st-ox* but here on both leaf sides (38.21±1.29 / 54.5±2.31 %). The mutant *st- RNAi* had instead reduced amounts of the SI on both leaf sides, but only a significant reduction could be analyzed for the abaxial leaf side (12.95±2.2 %) when compared to the control.

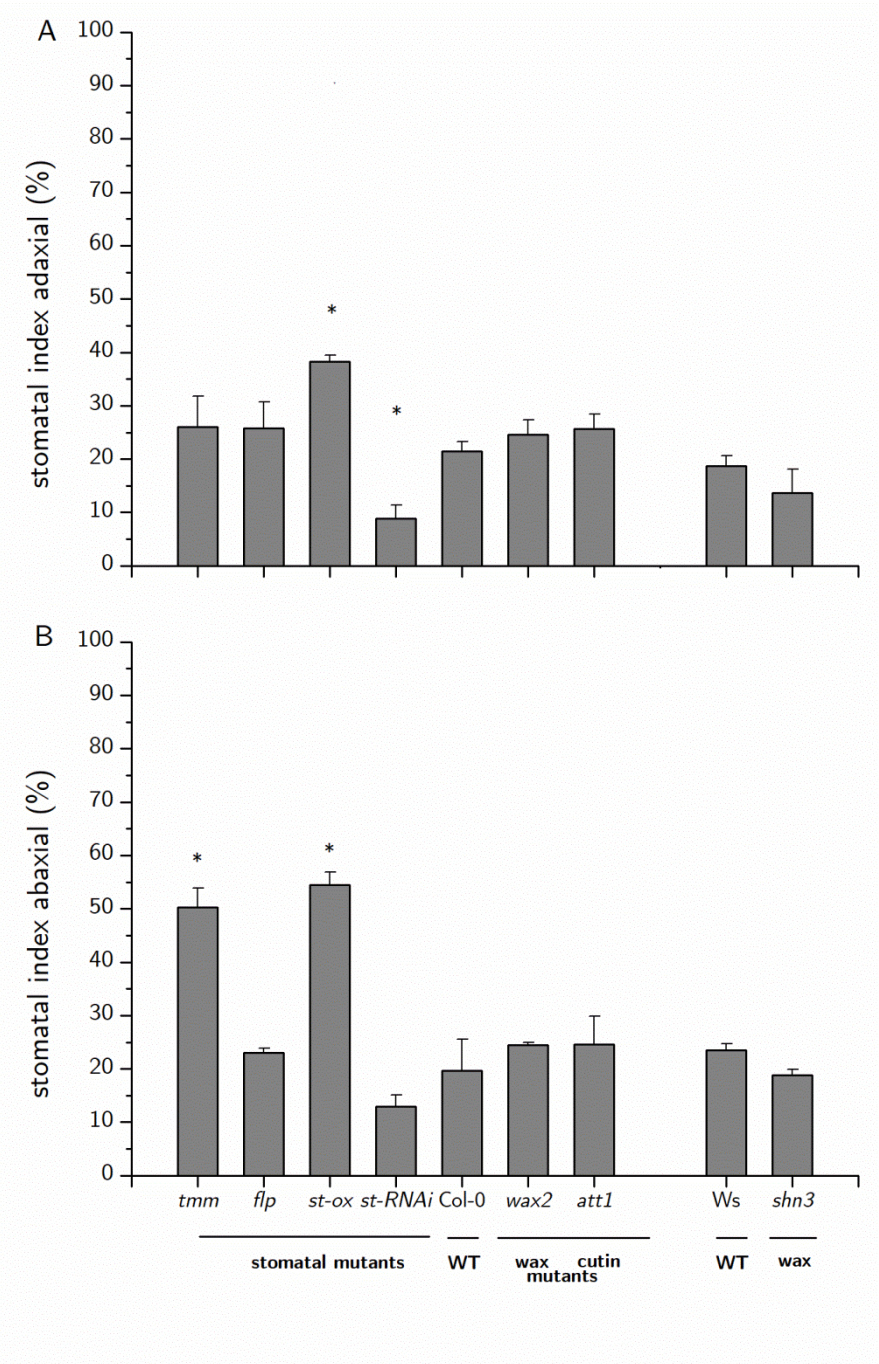


Figure 20: Stomatal index of ad- and abaxial Arabidopsis leaves

A: Stomatal index of Arabidopsis stomatal, wax and cutin mutants' adaxial leaf side. B: Stomatal index of Arabidopsis stomata, wax and cutin mutants' abaxial leaf side. Stomatal, wax and cutin mutants with Col-0 background are plotted together. Wax mutant *shn3* and corresponding wild type Ws are shown separately. Bars indicate mean values with standard deviation of at least three biological replicates. Asterisks indicate significant differences between means of mutants and corresponding wild type at a significance level of 0.05 in One-Way ANOVA (Fisher LSD).

### 3.4.4 Stomatal density of stems

The number of stomata counted for Arabidopsis stems showed significant differences between the Col-0 (135±39 $mm^{-2}$) and stomatal mutants *tmm* which did not exhibit stomata on the stem at all, *st-ox* (202±15 $mm^{-2}$) and *st-RNAi* (19±1 $mm^{-2}$). All cuticular mutants showed significantly lower numbers of stomata than their corresponding wild types. *Wax2* (76±8 $mm^{-2}$) and *att1* (72±10 $mm^{-2}$) showed 56 % and 53 % less stomata on the stem than Col-0. Likewise, the wax mutant *shn3* (48±14 $mm^{-2}$) exhibited significantly fewer stomata on the stem than its corresponding wild type Ws (110±13 $mm^{-2}$), (Figure 21).

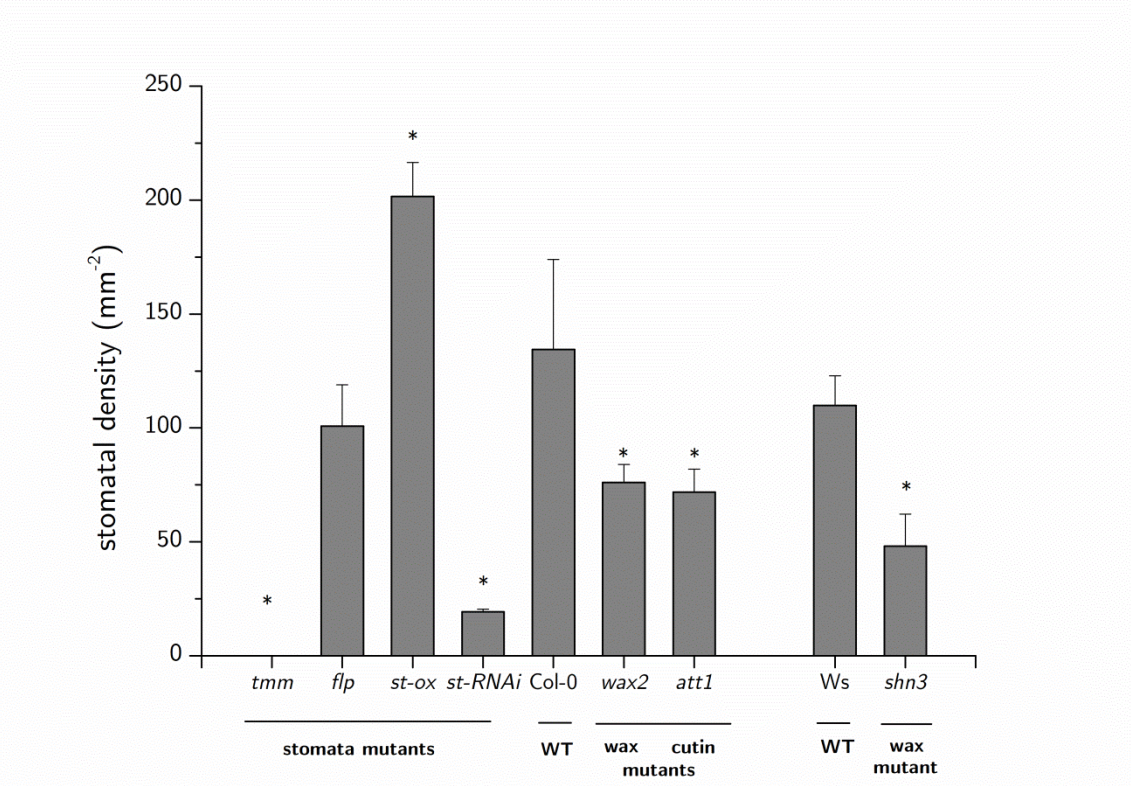


Figure 21: Density of stomata per $mm^2$ of Arabidopsis stems

Stomatal density of Arabidopsis stomatal and cuticular mutants stems. Stomatal, wax and cutin mutants with Col-0 background are plotted together. Wax mutant *shn3* and corresponding wild type Ws are shown separately. Bars indicate mean values with standard deviation of at least three biological replicates. Asterisks indicate significant differences between means of mutants and corresponding wild type at a significance level of 0.05 in One-Way ANOVA (Fisher LSD).

## 3.5 Correlation between stomatal density and wax coverage of Arabidopsis leaves and stems

To combine analyzes of wax coverage in plant organs (leaf and stem), (3.3.1, 3.3.4) and in more detail on leaves ad- and abaxial side (3.3.2) data for stomatal density (3.4) and the wax amount was correlated per area ($cm^{-2}$). When setting stomatal density and wax amount for whole leaves into relation no correlation of the amounts was determined ($r = 0.19$), (Figure 22 A). Likewise, the correlation between stomatal density and wax amount in Arabidopsis stems did not show a positive or negative correlation (Figure 22 B).

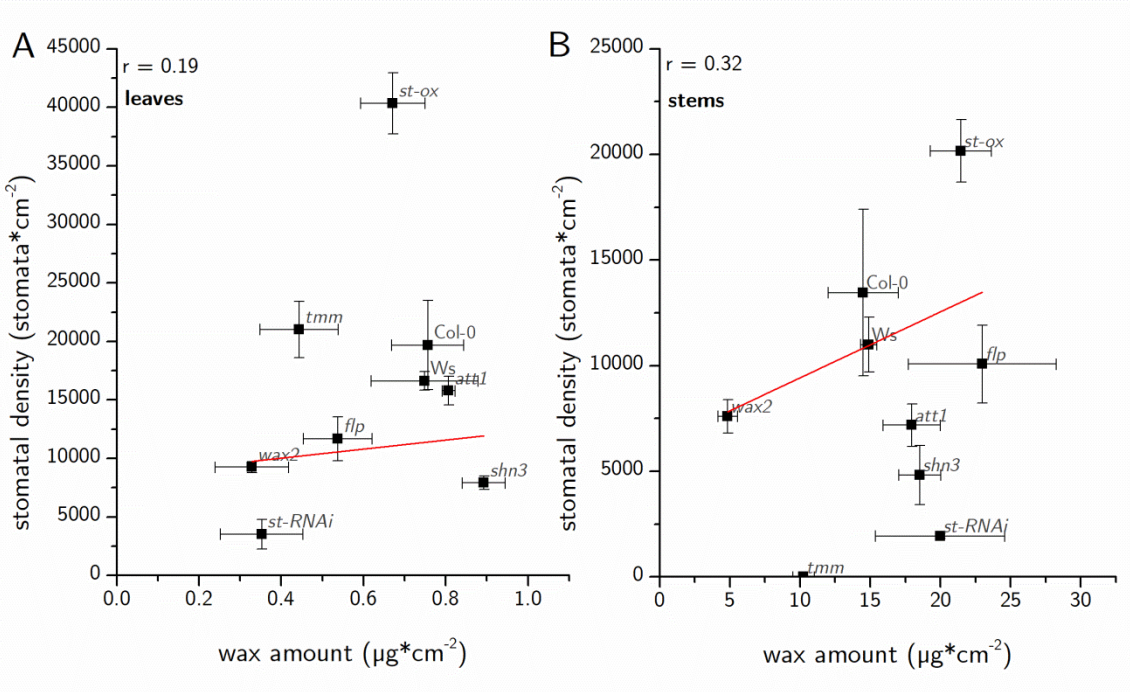


Figure 22: Correlation between stomatal density and the wax amount of different Arabidopsis genotypes

A: Correlation between stomatal density and wax amount of different Arabidopsis genotypes in the whole leaves projected to the leaf area in $cm^{-2}$. The stomatal density was the mean of ad- and abaxial leaf sides. B: Correlation between stomatal density and wax amount of different Arabidopsis genotypes in the stems projected to the leaf area in $cm^{-2}$.r shows the correlation coefficient for negative (-1) positive (+1) or no correlation (0). Squares represent the mean of stomatal density and wax amount with standard deviations for at least three biological replicates.

Since stomatal densities, as well as wax amount, differ on ad- and abaxial leaf sides correlation for the leaf sides with wax amount and stomatal density was performed (Figure 23). Neither numbers for stomatal density or wax amount on the adaxial (r = 0.26) nor on the abaxial leaf side (r = 0.5) correlated (Figure 23 A, B).

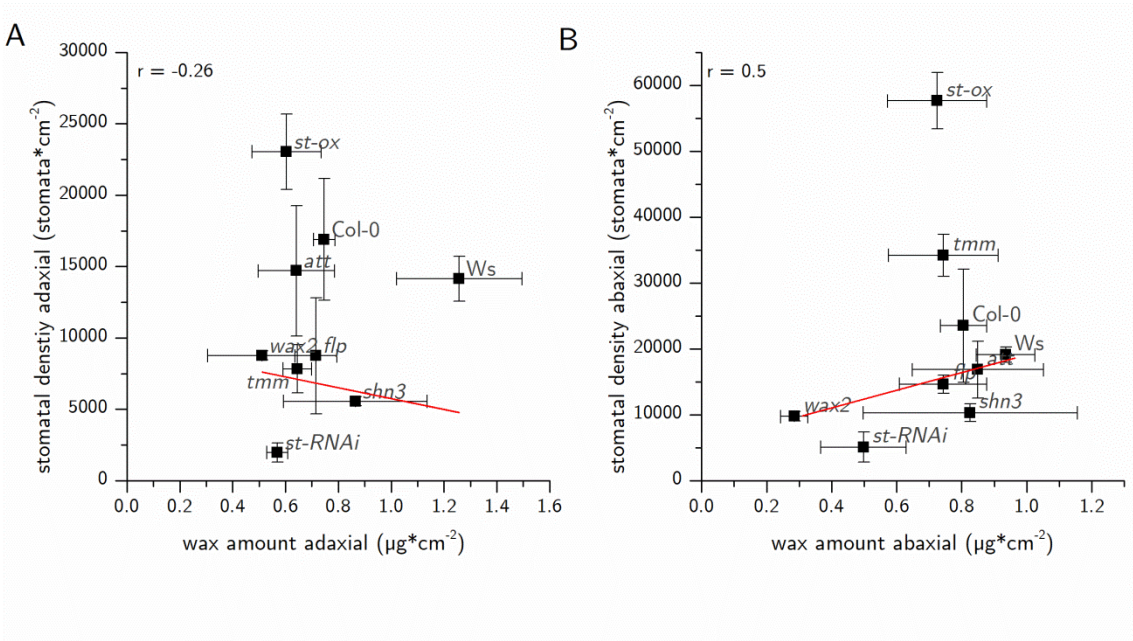


Figure 23: Correlation between stomatal density and the wax amount of different Arabidopsis genotypes

A: Correlation between stomatal density and wax amount of different Arabidopsis genotypes on the adaxial leaf side projected to the area in $cm^{-2}$. B: Correlation between stomatal density and wax amount of different Arabidopsis genotypes on the abaxial leaf side projected to the area in $cm^{-2}$. r shows the correlation coefficient for negative (-1) positive (+1) or no correlation (0). Squares represent the mean of stomatal density and wax amount with standard deviations for at least three biological replicates.

## 3.6 Stomatal conductance

For further information on the physiology of the chosen Arabidopsis stomatal and cuticular mutant sets stomatal conductance was measured with a leaf porometer (2.2.7). The stomatal conductance for all genotypes was always higher on adaxial leaf sides than on the abaxial side. However, when mutants are compared to the corresponding wild type Col-0 (52.23±27.61 / $mmol*m^{-2}*s^{-1}$) stomatal conductance for the stomatal mutant *st-ox* (134.25±37.01 / 297.25±151.8 $mmol*m^{-2}*s^{-1}$) as well as the cutin mutant *att1* (220.25±65.79 / 278.25±34.34 $mmol*m^{-2}*s^{-1}$) was significantly increased on both ad- and abaxial leaf sides. Additionally, stomatal mutants *tmm* (72.4±19.55 $mmol*m^{-2}*s^{-1}$) and *st-RNAi* (68.7±16 $mmol*m^{-2}*s^{-1}$) showed significantly decreased stomatal transpiration on the abaxial leaf side in comparison to Col-0.

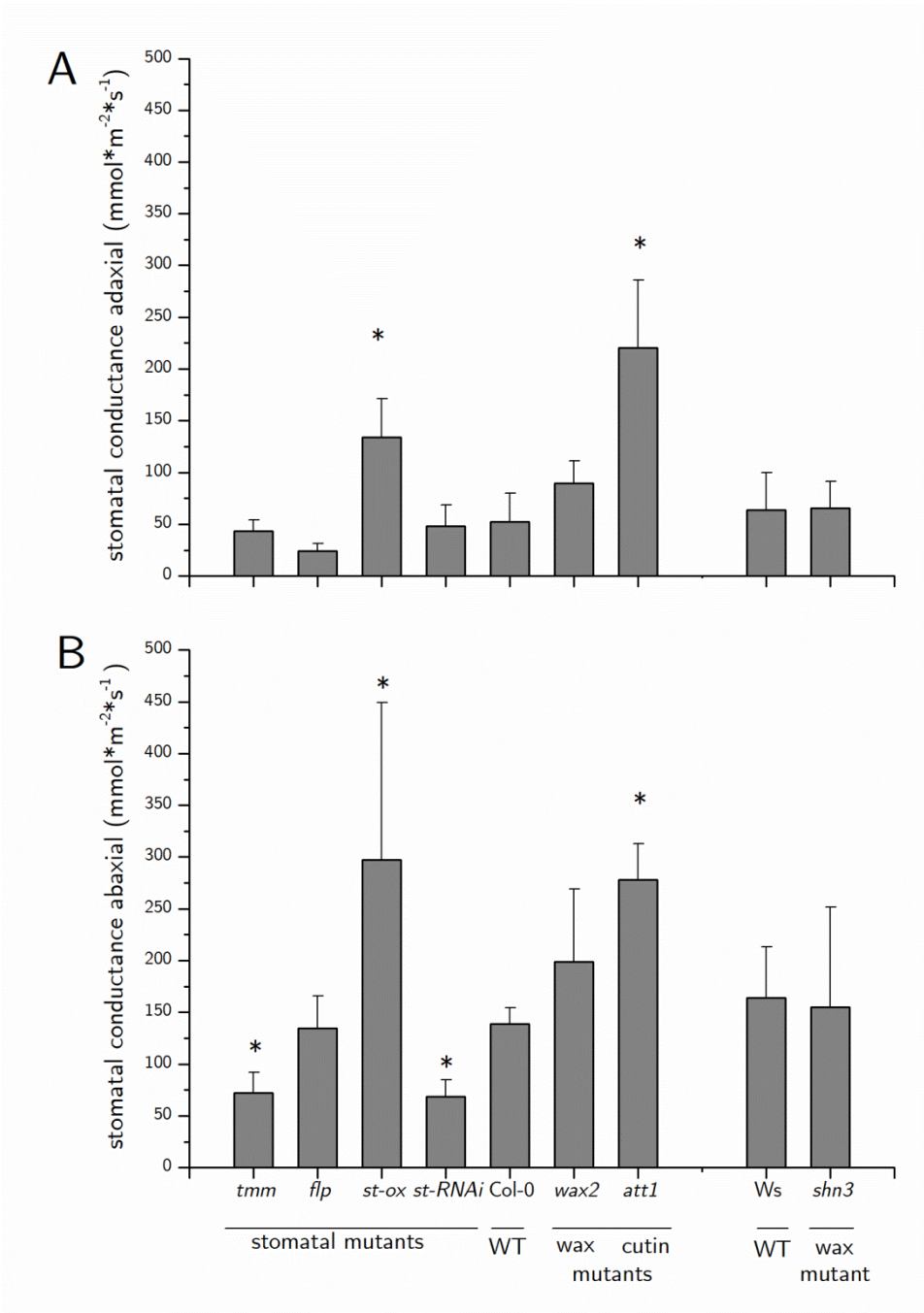


Figure 24: Stomatal conductance of Arabidopsis genotypes

A: Stomatal conductance of adaxial leaf side of Arabidopsis genotypes B: Stomatal conductance of the abaxial leaf side of Arabidopsis genotypes. Stomatal, wax and cutin mutants with Col-0 background are plotted together. Wax mutant *shn3* and corresponding wild type Ws are shown separately. Bars indicate mean values with standard deviation of at least four biological replicates. Asterisks indicate significant differences between means of mutants and corresponding wild type at a significance level of 0.05 in One-Way ANOVA (Fisher LSD).

## 3.7 Chlorophyll content analysis

Chlorophyll measurements were conducted as described in 2.2.4. The chlorophyll content for all genotypes did not differ significantly when compared to the corresponding wild types Col-0 or Ws respectively.

Table 3: Chlorophyll content of different *Arabidopsis thaliana* genotypes under normal ambient conditions

Chlorophyll contents of Arabidopsis wild types and corresponding stomatal, wax and cutin mutants. Plants were four weeks old and grown under long day conditions with a light intensity of 150 / 0 µmol $m^{-2}s^{-1}$.

| Genotype | Chlorophyll (µg*$cm^{-2}$) |
|---|---|
| *tmm* | 17.0 ± 1.04 |
| *flp* | 17.1 ± 1.3 |
| *st-ox* | 15.9 ± 0.06 |
| *st-RNAi* | 17.3 ± 0.6 |
| Col-0 | 16.1 ± 0.2 |
| *wax2* | 18.6 ± 2.9 |
| *att1* | 17.6 ± 1.70 |
| Ws | 18.6 ± 3.5 |
| *shn3* | 17.50 ± 0.9 |

## 3.8 Chlorophyll-Fluorescence measurements

Besides investigating the cuticular permeability of the Arabidopsis leaves via leaf desiccation (3.9) the herbicide metribuzine was used to further evaluate the cuticular barrier properties of the genotypes. For the indirect measurement of the cuticular permeability via pulse- amplitude modulation (PAM) the fluorometer monitored the photosynthetic yields (Y II) in the photosystem II as described in 2.2.8. Before all conducted measurements with the herbicide, water, as control, was applied onto the adaxial leaf side and photosynthetic yield was measured. All plants

used for the experiments did not show a decrease in the photosynthetic yield after water application (data in supplemental, 7.2).

The herbicide was applied on the adaxial leaf side after three consecutive measurements at which point all plants had a Y (II) between 0.7 and 0.79. In all investigated Arabidopsis ecotypes and mutants, the photosynthetic yield decreased non- linearly over time (Figure 25), (Figure 26). In all stomatal, wax and cutin mutants a complete inhibition of photosynthesis was obtained faster than in the wild type Col- 0, with the exception of the stomatal mutant *flp*, (Figure 25 b) which took longer for complete inhibition than Col-.0 (Figure 25). The decrease of the photosynthetic yield of *shn3* was also obtained faster than in its corresponding wild type Ws (Figure 26).

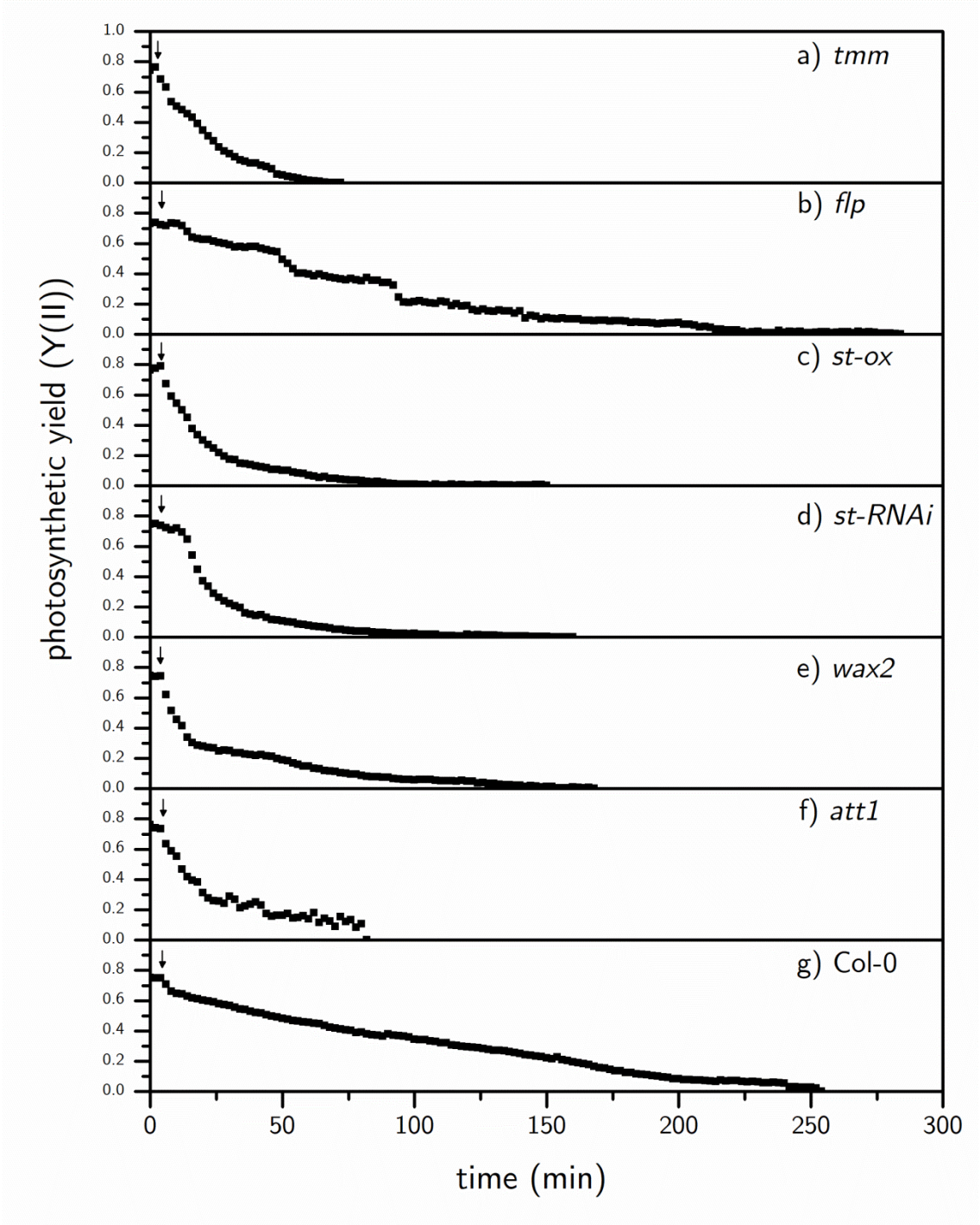


Figure 25: Decrease of the photosynthetic yield in Arabidopsis genotypes

Kinetics are shown for different Arabidopsis mutants (a) *tmm*, (b) *flp*, (c) *st-ox*, (d) *st-RNAi*, (e) *wax2*, (f) *att1*, in comparison to the corresponding wild type (g) Col-0. Arrows indicate the application of the herbicide on the adaxial leaf surface. Kinetics represent the means calculated from single values of individual leaves used (n= at least 3 biological replicates).

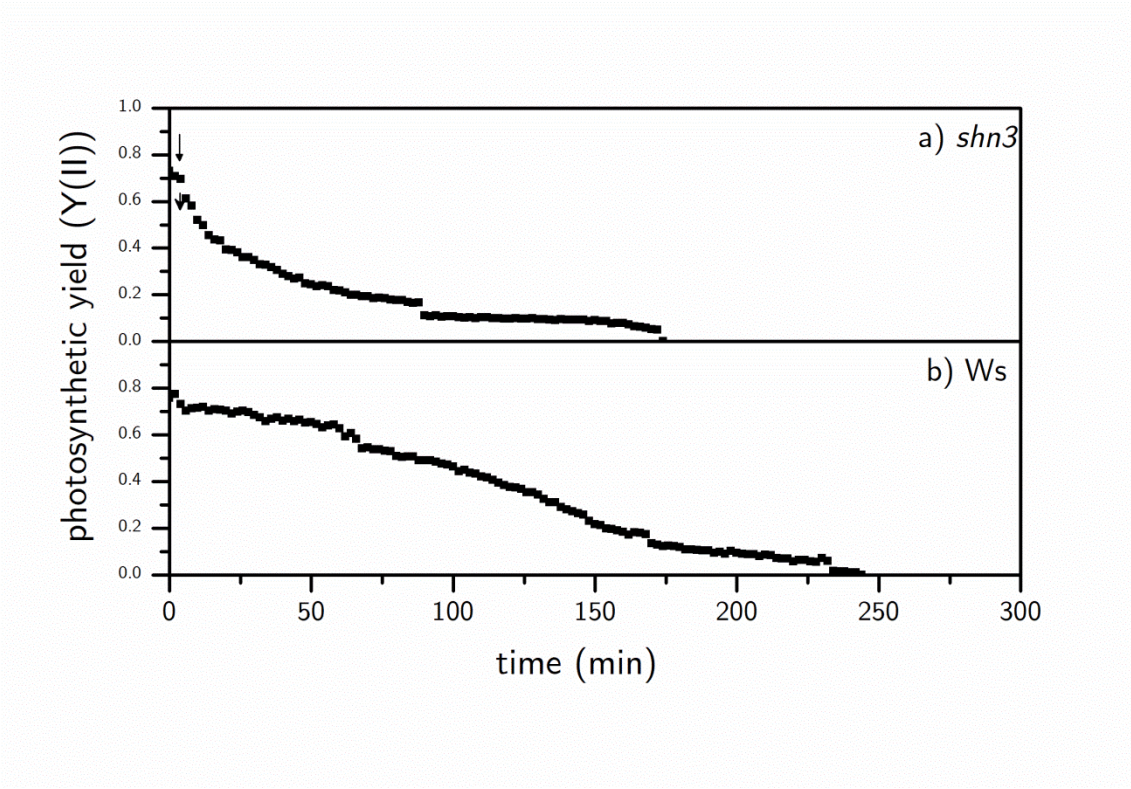


Figure 26: Decrease of the photosynthetic yield in Arabidopsis genotypes

Kinetics are shown for Arabidopsis mutant (a) *shn3* in comparison to the corresponding wild type (b) Ws. Arrows indicate the application of the herbicide on the adaxial leaf surface. Kinetics represent the means calculated from single values of individual leaves used (n= at least 3 biological replicates).

Half time and complete inhibition of photosynthesis were consecutively calculated for each replicate separately (2.2.8). The results are given in boxplots (Figure 27). The median for Col-0 for the time needed for 50 % inhibition of the photosynthesis was at 95 min. Except for the stomatal mutant *flp* (84 min.), half times for the other Arabidopsis mutants were shorter than for Col-0 or Ws (119 min.) respectively in the case of *shn3* (21 min.). All the other mutants revealed faster uptake of metribuzine according to the half times of inhibition: The median for *tmm* was 21 min. where the median for the cutin mutant *att1* was 15 min. The half time inhibition for *wax2* compared to Col-0 was the shortest with 12.5 min and *st-ox* also showed a faster uptake than Col-0 with 14 min. half time inhibition (Figure 27 A). Complete inhibitions of photosynthesis were obtained in shorter times for the mutants respectively when compared with the wild types Col-0 (230 min) and Ws (236 min.). *Shn3* with Ws background had a photosynthetic yield of zero after 21

min. In the stomatal mutants *tmm* (52 min.), *st-ox* (40 min.) and *st-RNAi* (40 min.) photosynthesis was faster inhibited than in the wild type, whereas the inhibition of the photosynthesis of *flp* took 144 min.

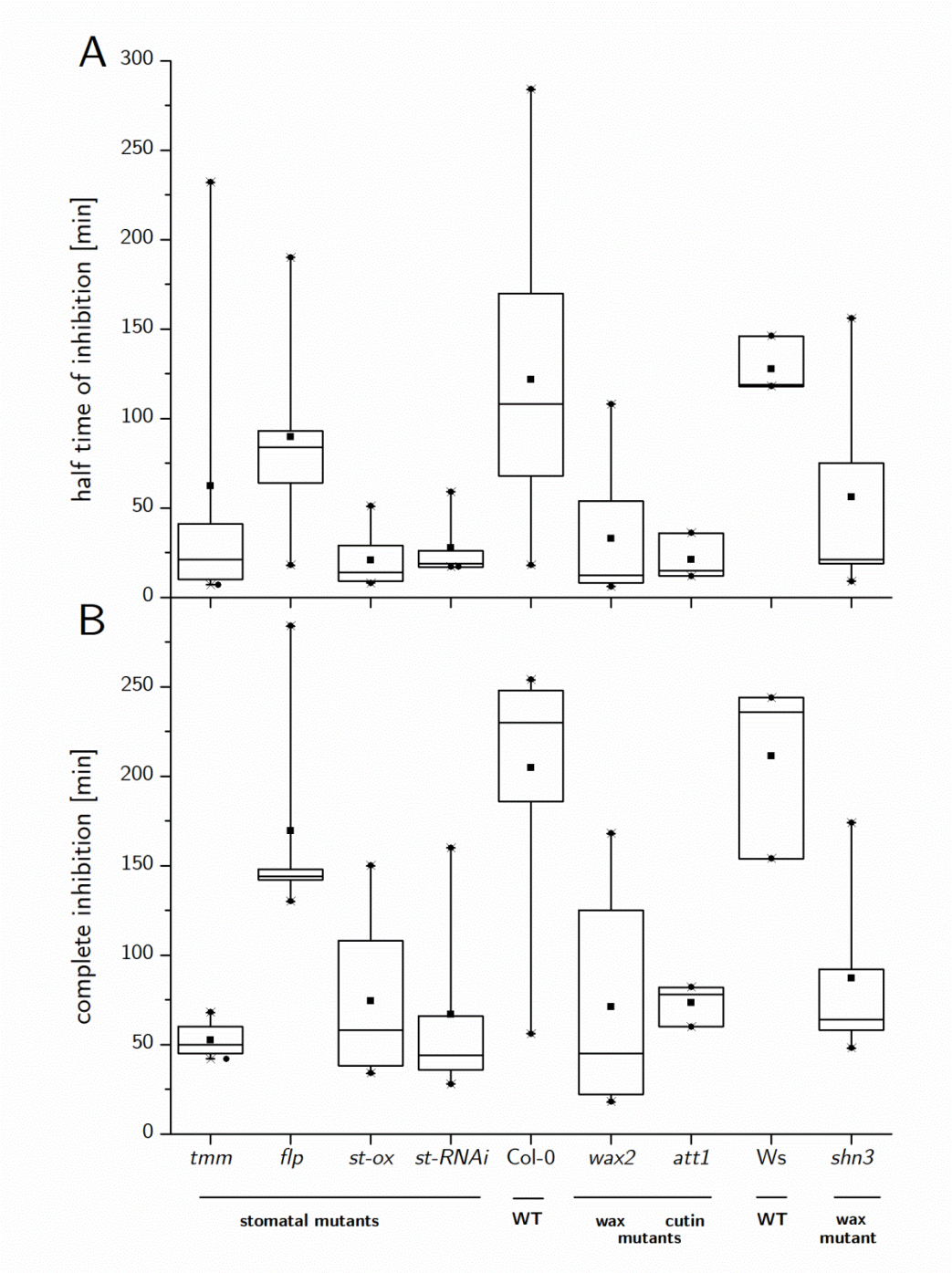


Figure 27: Half time and complete inhibition of photosynthetic yield in Arabidopsis leaves after the application of the herbicide metribuzine (100 µMol).

A: Half time inhibition shows the decrease in the photosynthetic yield at 50 % in min. B: Complete inhibition shows the decrease in the photosynthetic yield at 100 % in min. Stomatal, wax and cutin mutants with Col-0 background are plotted together. Wax mutant *shn3* and corresponding wild type Ws are shown separately. The boxes range from 25 to 75 percentiles. The black square in the box represents the mean value. Boxplots consist of at least 3 biological replicates. The whiskers range to the outliners.

## 3.9 Minimum conductance of Arabidopsis leaves

The leaf's minimum conductance for different Arabidopsis genotypes was based on leaf drying curves. As stomata occurred on both the ad- and abaxial leaf surfaces the minimum conductance was calculated at the point of maximum stomatal closure (2.2.9). The minimum conductance for all mutants was increased when compared to the corresponding wild types. However significant differences were found in minimum conductance of the leaves of the stomatal mutants *flp* ($4.88 \times 10^{-9} \pm 2.53 \times 10^{-9}$ $m*s^{-1}$), *st-ox* ($6.63 \times 10^{-9} \pm 2.29 \times 10^{-9}$ $m*s^{-1}$) and *st-RNAi* ($4.55 \times 10^{-9} \pm 9.68 \times 10^{-10}$ $m*s^{-1}$) when compared to the control, Col-0 ($2.1 \times 10^{-9} \pm 3.6 \times 10^{-10}$ $m*s^{-1}$). Additionally, wax mutant *wax2* ($4.32 \times 10^{-9} \pm 1.71 \times 10^{-10}$ $m*s^{-1}$) and cutin mutant *att* ($4.5 \times 10^{-9} \pm 8.16 \times 10^{-10}$ $m*s^{-1}$) also had a significantly increased stomatal conduction in comparison to the wild type (Figure 28).

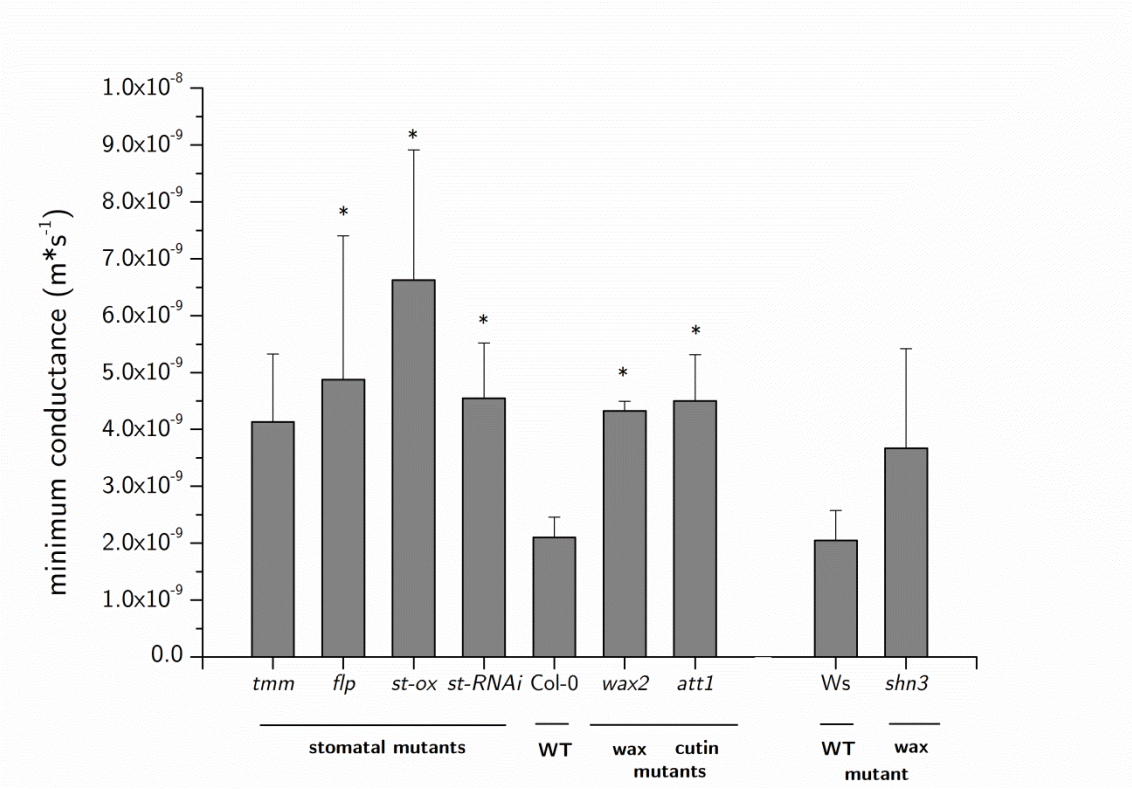


Figure 28: Minimum conductance of Arabidopsis leaves

Stomatal, wax and cutin mutants with Col-0 background are plotted together. Wax mutant *shn3* and corresponding wild type Ws are shown separately. Bars indicate mean values with standard deviation of at least four biological replicates. Asterisks indicate significant differences between means of mutants and corresponding wild type at a significance level of 0.05 in One-Way ANOVA (Fishers LSD).

# 4 Discussion

The cuticular membrane of plants mainly functions as a very effective barrier against uncontrolled water loss protecting the plant from desiccation (Schönherr, 1982). Stomata, which disrupt the cuticle, are on the other hand responsible for the gas exchange and at the same time the accompanying controlled water loss of the plant when stomata are open. However, if stomata are closed for instance during water stress, the quality of the cuticle as the main barrier to uncontrolled water loss becomes even more important. The understanding of the interplay between stomata and the cuticle has been rarely studied in the past. Therefore putative changes in barrier properties of the cuticle were investigated by the comparison of Arabidopsis wild types to corresponding mutants that are either altered in their wax or cutin biosynthesis and therefore exhibit changes in their wax/ cutin amount and chemical composition or vice versa stomatal mutants with alterations in their stomatal distribution.

## 4.1 Leaf and stem surface characterization of different Arabidopsis genotypes and mutants

In the FE-SEM micrographs of Arabidopsis leaf sides, all genotypes exhibit a thin, smooth film of epicuticular waxes (3.1.1.) as also described by Jenks et al., (1995). The leaf surfaces of Arabidopsis are equipped with a thin cuticle of 22°nm in the leaf blades (Franke et al., 2005). The epicuticular waxes only make up a small portion of this layer and are therefore hardly visible by FE- SEM. Small wax granules close to stomata are the visible evidence of the barely observable wax film (Figure 8, Figure 9). It is known that epicuticular waxes accumulate around stomata on the leaf surface (Barthlott and Neinhuis, 1997) here they should hinder water from entering the intracellular air spaces (Lemieux, 1996). The structure of epicuticular waxes can be highly diverse (Jenks et al., 2002). Surface waxes can differ in structure and chemistry as well as in their appearance (Lemieux, 1996). A

glaucousness appearance or so-called waxy bloom, for example, characterizes the stems of Arabidopsis. Arabidopsis leaves on the other hand usually appear non-glaucous or glossy because they lack reflective wax crystals and instead are covered by a smooth thin wax film (Jenks et al., 1995, 2002). An exception of this finding is the mutant *shn3*. Its leaves also appear shiny but not because of less wax covering the leaf. The opposite is the case; the wax amount is increased compared to the wild type (Figure 12). This is due to the structure of the epicuticular waxes. Interestingly the waxes, observed in the FE-SEM, are orientated in platelets which are able to reflect the light, different from other waxy cuticles with superimposed wax crystals, or as already mentioned the waxy film usually covering Arabidopsis leaves (Sugano et al., 2010). This emphasizes the importance of the orientation of the epicuticular waxes on the leaf surface. The here investigated stomatal mutants exhibit the same wax orientation as the corresponding wild type. Defined wax structures are not visible in the leaves which were instead also covered by a thin waxy film (Figure 8, Figure 9). The stomatal patterning in the investigated wax and cutin mutants is the same as in the wild type. They all follow the one spacing rule, which is defined to guarantee the functioning of single stomata (Figure 8, Figure 9). The stomata are consistently patterned so that they are never adjacent to one another (Sachs, 1991). The mutations in the cutin and wax biosynthesis, for the here investigated cuticular mutants, do not have a visible effect on the stomatal morphology or patterning. In the stomatal mutants, on the other hand, the mutations in stomatal patterning could be confirmed morphologically for all mutants. The mutant *tmm* showed barely clustered stomata on the adaxial leaf side (7.1, Figure 30) however more and bigger clusters were detected on the abaxial leaf side (Figure 8 C). These defects in clustering originate in the regulation of spacing divisions by *Tmm* (Geisler et al., 2000). The described defect in the patterning of the mutant *flp* could be recognized for the leaf's ad- and abaxial side (Figure 8 E). The stomata build units with paired guard cells or so-called twinned stomata (Yang and Sack, 1995), (Figure 8 F). The overexpression of STOMAGEN in the mutant *st-ox* led to many stomata which also formed clusters (Figure 9 A). Sugano et al., (2010) also stated that cotyledons of the same line showed adjacent meristemoid

cells to stomata. This could not be confirmed for specimens in this work, but since the adjacent meristemoid cells were only observed in cotyledons the loss of those cells in rosette leaves during organ ontogeny can be a possible explanation.

Completely different from the epicuticular waxes covering leaves of Arabidopsis the stems showed a variety of wax structures in the different mutants and the wild type (Figure 10, Figure 11). The cuticle of Arabidopsis stems (50 – 80 nm) is more than twice as thick as in the leaves (Nawrath, 2002). It therefore possibly consists also of a thicker layer of epicuticular waxes. Data however on the exact diameter of the epicuticular wax layer are missing in literature. Wax crystals on the stem usually appear as plates or tubules with approximately 0.3 to 3.9 µm in height and 0.2 to 0.5 µm in width as investigated for Arabidopsis ecotype Ws in Jenks et al., (1995).

The only mutant obvious in a lack of wax crystals was *wax2* (Figure 11, C, D). Its stem appears weakly glaucous as it only inhabits few wax crystals (Jenks et al., 2002). Besides the wax mutant *wax2,* the stomatal mutant *flp* showed fewer wax crystals in comparison to the wild type (Figure 10, E, and F). The appearance of the stem was also shinier compared to the wild type which could be due to the structure of the observed waxes: Fewer tubules but more platelets were observed (Figure 10 F), which again, as described before for *shn3* could be the reason for the shiny appearance of the stem. *Flp* also lacked its stomatal mutation of adjacent guard cells, which are only visible and typical for the leaf (Yang and Sack, 1995). Jenks et al., (2002) investigated the epicuticular waxes of stems of 11 Arabidopsis mutants. They all belonged to the mutant line of *eceriferum* family meaning 'without wax' however the wax crystals detected on the surface of the stems exhibited diverse appearance. Much as it is true for both stomatal and cuticular mutants in this study. For the investigated mutants *tmm*, *st-RNAi*, and *att1*, tubules were observed (Figure 10, Figure 11). But the already described mutants *flp* and *wax2* and also, the overexpression line *st-ox,* which expresses more stomata than the wild type, had a different wax structure than the wild type. Only platelets were found in *st-ox* which again led to a shinier appearance of the stem (Figure 11

B). The structure of the superimposed waxes can differ due to the chemical composition (Gülz, 1994) and change its appearance under the influence of environmental factors (Baker, 1974) as well as during ontogeny (Bringe et al., 2006). According to the here observed structures, they may also be organ dependent and exhibit different structures between leaves and stems.

Interestingly the stomatal mutants *flp* and *tmm* did not express the described mutations of the leaf in the stems, which indicates differences in the regulation of the patterning for the stems. Stomatal mutant *tmm* even completely lacked stomata in the stems (Figure 10 C). Yang and Sack, (1995) suggest that the *tmm*- contrary to *flp* mutation prevents the pathway of stomatal precursor cells in the stem, which ultimately leads to an absence of stomata. *St-ox* on the other hand also showed more stomata in the stem than the wild type, as it was observed in the leaves as well (Figure 11 A), which underlines the expression of Stomagen in both organs of the plant (Sugano et al., 2010).

The combination of chemical composition and structure of the waxes are known to play a role in the surface wettability of leaves (Holloway, 1970). In addition surface structures such as trichomes are responsible for the wettability of leaves (Koch and Barthlott, 2009). To further characterize the leaf surface the contact angle for both leaf sides was measured (3.2). A leaf/ surface is considered hydrophilic with a contact angle less than 90° and as hydrophobic when it is greater than 90° (Bhushan, 2003). Arabidopsis genotypes showed differences between the wettability of the different leaves sides as well as in between the mutant and the corresponding wild type (Table 2). However, all genotypes, except the wax mutant *wax2*, have contact angles greater than 90° and are therefore considered hydrophobic. Conspicuously contact angles for the adaxial leaf sides are for most of the genotypes lower than for the abaxial side. The structure of the epicuticular waxes does not differ in their appearance as they all have been detected as a smooth, thin film (3.1). Instead, other factors must be responsible. It is known that due to environmental factors the wettability is influenced on different leaf sides. Over time rain, wind or dust and dirt can influence the hydrophobicity of the more exposed

adaxial leaf surface and hence lower the wettability (Cape, 1983). Due to the erosion of the epicuticular waxes the contact angle would lower when droplets are applied. However, this finding can be excluded for the genotypes investigated in this study since they were all grown in a growth chamber. Instead, present trichomes can play a major role in the wettability of the surface of the leaf. Brewer et al., (1991) found, that in 38 tested plant species leaves that exhibited trichomes are more water repellent. They also state that the trichome density is a factor to be considered. Most of the Arabidopsis genotypes in the present study have trichomes on the ad- and abaxial leaf surface. The only exceptions are the stomatal mutants *tmm*, *flp,* and *st-ox*. In addition, *shn3* exhibits a reduction in trichome number (Aharoni et al., 2004). However, the lower contact angle when compared to the wild type, which exhibits trichomes, is not true for all measurements. By comparing the data the high standard deviations can be recognized. This high variation can be explained by the heterogeneity of the surface of the leaf. However the relatively low contact angle in *wax2*, even though it exhibits trichomes, which are reduced in size (Nawrath, 2006), might be explained through the defective *Cer3/Wax2* gene. CER3/WAX2 encode for enzymes in the alkane forming pathway (Chen et al., 2003). Hegebarth et al., (2016) found high concentrations of alkanes in the epicuticular waxes covering trichomes. Also, the gene regulation in trichomes for Cer3/Wax2 was upregulated. The here investigated mutant *wax2* is defective in those genes and completely lacks alkanes in its wax composition (data not shown). Hence a lower amount of not only the epicuticular waxes on the leaves but specifically on the trichomes is expected. This together with reduced trichome size results in better spreading of the water droplet, despite the present trichomes on the adaxial and abaxial leaf side and subsequently to a lower contact angle, when compared to the wild type.

## 4.2 Chemical analysis of the cuticular membrane and stomatal distribution

In the course of chemical analysis, the potential relationship between stomatal density and changes in cuticular waxes or the biopolymer cutin should be investigated. Vice versa stomatal density and indexes were determined. Variations of extracted wax amounts from whole leaves did not tightly correlate with the stomatal density of the different genotypes (Figure 22 A). Only in the stomatal mutant *st-RNAi* and *flp* as well as in the wax mutant *wax2* coherence could be determined. While stomatal densities compared to the wild type, in the mentioned mutants, were significantly lower, likewise, the wax amount was significantly lowered (Figure 12, Figure 18). For stomatal mutants, this work provides the first information on the amount and composition of the chemically analyzed cuticle. Hence the here analyzed data cannot be compared with other data in the literature. However much is known about the wax coverage in *wax2*. The decrease of 56.6 % in the total wax amount compared to the wild type is less than what has been analyzed before (Figure 12). In Chen et al., (2003) and Sadler et al., (2016) the total decrease of the total wax amount was around 80 %. In both studies, the corresponding wild type showed different absolute values than the wild type used in this work. When looking at the relative relations of substance classes to the total amount in the mutant *wax2* the reductions analyzed in this study are confirmed by literature. Reduction of acids (31.65 %), alcohols (70.95 %), secondary alcohols (97.4 %) and a complete reduction of aldehydes and alkanes (data not shown) was also reported in Chen et al., (2003) and Sadler et al., (2016). Compared to the wild type the total wax amount of the stomatal mutants *flp* and *st-RNAi* were reduced by 30 % and 56 % (Figure 12). Other mutants did not show any significant differences in their stomatal densities or wax amounts. All showed, as already described in the morphological appearance, the expected mutations in the data for stomatal density and wax amount respectively. The only exception was the mutant *shn3*, which according to literature shows a significant increase of the wax amount in absolute

number (Sadler et al., 2016), which was not the case in this study. However, if relative data is compared to the increase of wax amount in the cuticle of *shn3* it is reported to be 126 % when compared to the corresponding wild type (Sadler et al., 2016). In this study, the increase in the wax amount is 120 % and therefore within the range of the biological variability of the plants.

Since the leaves of Arabidopsis exhibit dorsal- ventral asymmetries (Bowman, 2000) and in that course stomata show amphistomy it was necessary to rather determine and compare the stomatal density and wax coverage separately for both leaf sides than for the whole leaf. Here the significant reduction in the wax amount for *st-RNAi* and *wax2* was confirmed. However, *flp* did no longer show the reduction in wax amounts when separately analyzed for both leaf sides (Figure 13). When correlating the data of extracted wax for the discrimination of the ad- and abaxial sides of the leaves with counted stomata for both sides, again both variables did not tightly correlate with each other (Figure 23). Compared with data in literature the densities and indexes in this work all show the expected increase or decrease. The most obvious increase was found in the mutant *st-ox* for both ad- and abaxial leaf sides. However, the increase on the abaxial side (2.5- fold) was more pronounced than on the adaxial leaf side (1.3- fold) which was also found in Tanaka et al., (2013) and Hronková et al., (2015). The same authors also investigated the decrease of the suppressed STOMAGEN expression by RNA interference in *st-RNAi* and counted significantly lower numbers for stomata per area as it was also determined for the present study (Figure 19). Chen et al., (2003) also determined the stomatal density and index for *wax2*. They also found a reduction in the stomatal number per leaf area but present an increase in the index when compared to the corresponding wild type. Again the index for the wild type is not comparable to the determined index in this work. However, the stomatal index for *wax2* alone (adaxial: 24.7± 2.2 %/ abaxial: 24.2 ± 1.5 %) is similar in this work (adaxial: 25.72±2.68 %/ abaxial: 24.46±0.52 %, Figure 20).

The mutant *tmm* interestingly shows differences in stomatal density and at the same time anomaly in the appearance of clusters on the ad- and abaxial leaf sides (Figure 19, Figure 8, Figure 30). With barely observed stomatal clusters and decreasing density (78±17 $mm^{-2}$) on the adaxial leaf side the density increases significantly (342±32 $mm^{-2}$) and clusters arise on the abaxial side. This was also confirmed by Vráblová et al., (2017). The difference in the density of stomata in *tmm* on the ad- and abaxial side was expressed in a ratio of 4.3 more stomata occurring on the abaxial side. In the present study, the ratio is 4.3 as well. Even though the growth conditions slightly differed from the ones chosen for this study the overall result is comparable. This becomes even clearer when looking at the stomatal index. The index is the ratio of the number of stomata to the total number of pavement cells in a given area of the epidermis and is independent of cell size (Salisbury E.J., 1927). In the work of Vráblová et al., (2017) the stomatal index for the adaxial leaf side is 26±5 % and on the abaxial side 48±6 %. Similar data was collected in this study (26.01±5.82 % / 50.29±3.58 %). However, this surprising leaf side heterogeneity, which made it interesting to study for possible changes in wax coverage, induced by the mutation of *Tmm* has no specific impact on the wax amount (Figure 13) or composition (data not shown) of the mutant's cuticle either on ad- or abaxial side. The already mentioned mutant *st-RNAi* showed significant differences in its wax amount and stomatal densities as well as the stomatal index (Figure 13, Figure 19, Figure 20). This is why the detailed wax composition of single constitutes was shown in this work (Figure 14). However, from the detailed study of the wax monomers and chain lengths, a conclusion on significant changes, apart from the overall lower amount in waxes, cannot be drawn. This is also the case for the other stomatal mutants studied in this work and data is therefore not shown. When compared to the already mentioned reduced substance classes and single monomers in *wax2*, which at the same time also shows a lower stomatal density, no lack of substance classes such as alkanes or aldehydes could be analyzed for *st-RNAi.* Instead, an overall reduction takes place for the monomers in all substance classes. Nonetheless, the amount of the $C_{31}$ alkane was significantly lowered for both leaf sides. Yang et al., (2011), studied the relation of accumulation

of epicuticular waxes upon drought stress. Therefore, the authors positively regulated the expression of the *Win1/Shn1* gene which led to an overall increase of waxes but mostly alkanes. As a side effect, they noticed, that stomatal density was decreased in those mutants. This effect is contrary to the finding in this study where alkanes are significantly reduced in *st-RNAi* and *wax2* with a simultaneous decrease in stomatal density. However, the effect of wax accumulation and at the same time a reduction in stomatal density could be confirmed in this study. The mutant *shn3* showed the same effect (Figure 13, Figure 19). The total wax amount was increased by 120 % compared to the wild type Ws and especially the alkanes accumulated in the mutant by 166 % (data not shown).

Since all aerial parts of plants in their primary developmental stage are covered with the cuticle (Schönherr, 1982) and are also equipped with stomata Arabidopsis stems were also investigated for wax amount and composition as well as cutin deposition and stomatal density. It is well known, that the frequencies of asymmetric cell division for stomatal development and hence stomatal density is environmental dependent and varies with organ type (Bergmann and Sack, 2007). The low frequencies are also responsible for fewer stomata in stems in general and therefore the need for patterning corrections as it is the case in leaves is lowered (Geisler et al., 2000; Bhave et al., 2009). In the terms of wax coverage in Arabidopsis stems it has been widely studied, that the wax amount is much higher than in the leaves (Jenks et al., 1995; Suh et al., 2005; Greer et al., 2007; Bourdenx et al., 2011) and therefore changes in wax amount or composition are more easily detected on the stem. In addition, the wax and cutin amount, as well as their composition, remain constant along the stem (Suh et al., 2005). Data collected for the cuticular components cutin and wax were correlated with stomatal densities. Again no correlation was determined. Instead when compared to the relation of stomatal densities and wax coverage in leaves the only mutant that showed the same behavior was the wax mutant *wax2* (Figure 16, Figure 21). Here again, the wax amount in the stems, as well as the stomatal density in the stems, significantly decreased. Contrarily the stomatal mutant *st-RNAi* did not show decreased wax

amount in the stems upon low stomatal density but instead showed significantly increased wax amount in comparison to the wild type (Figure 16, Figure 21). Hence the conclusion that was drawn for leaves cannot be applied in stems for this specific mutant but is similar for the finding in the wax mutant *shn3* in the leaves, where also wax amount increased and stomatal density was lowered. This arrangement could also be confirmed in the stems, where the wax amount was higher than in the wild type and stomatal density decreased. As it was also hypothesized by Yang et al., (2011). This effect only vice versa was also reported by Gray et al., (2000). Here investigated *eceriferum* mutant lines, which have decreased wax amounts and often compositional differences when compared to wild types, showed greatly increased stomatal indexes (proportion of epidermal cells that are stomata). However, this could not be observed in any of the investigated genotypes of this study. The only mutant constantly showing increased stomatal density was the *Stomagen* overexpression line *st-ox.* While wax in the leaves did not show any significant differences compared to the wild type in the stems on the other hand stomatal density increased as well as the wax amount. This is contrary to the above-described findings of Gray et al., (2000). An opposite effect showed the stomatal mutant *tmm,* which completely lacked stomata in the stems (Figure 21). Bhave et al., (2009) investigated this phenomenon and found regulatory reasons in the stomatal development that resulted in a lack of stomata in the stems of *tmm*. However, an increase of wax amount while stomata are missing is not the case. The wax even decreases when compared to the wild type Col-0 (Figure 16). Apart from waxes, the cuticle as an efficient barrier to mainly water loss of plants also consists of the biopolymer cutin (Schönherr, 1982; Kolattukudy, 1984). The function of cutin is mainly to provide a stable matrix but can also play a role as a physical and chemical barrier in plant-pathogen interaction (Wang et al., 2000; Nawrath, 2002). Therefore the potential impact of changes in the stomatal densities on the biopolymer cutin or an opposite effect of alteration in cutin on stomata was investigated in this study. Likewise as with waxes cutin amounts and compositions were investigated for leaves and stems. Collected data revealed no consistent pattern or relationship between the cutin amount in leaves and the counted

stomatal densities or indexes (Figure 15, Figure 18). Tendencies however in the trend, that mutants with fewer cutin amounts also exhibit less stomatal densities could be found for the stomatal mutants *flp* and *st-RNAi*. The cuticular mutants with the here analyzed increase in the cutin amount for the wax mutant *shn3* is reported in the literature (Sadler et al., 2016). The cutin mutant *att1* showed the expected reduction in the cutin amount when compared to the wild type. However, no correlation with the stomatal density was observed. Other than in *shn3* the again tendency to an increase in the cuticular amount in means of cutin shows a significant decrease in stomatal density, analogically to the observation made in the leaves and stems for wax amounts. This trend could however not be observed for cutin amounts in the stems, where the amount was similar to the corresponding wild type Ws (Figure 17). Other mutants rather showed a consistent pattern in the cutin of the analyzed stem and the determined number of stomata. When the cutin amount was significantly lower compared to the wild type, likewise the stomatal density was significantly increased. This was observed for stomatal mutants *tmm*, and *st- RNAi* as well as for the cutin mutant *att1*.

However, general conclusions from the comparison of stomatal densities and chemical analyzed cuticular substances (wax/cutin) in different genotypes and in different plant organs are difficult to obtain. No consequent patterns in either up- or down- regulated wax/ cutin amounts or compositions in response to higher or lower stomatal densities, or vice versa could be determined. However, tendencies are recognizable. Especially in a pattern where significantly or at least tending increased wax or cutin amounts in leaves, on the other hand, show decreased stomatal densities as it was shown for *shn3*. In addition wax mutant *shn3* and stomatal mutant *st-RNAi* showed a consistent pattern in both organs when the wax amount was lower also stomatal density was decreased.

## 4.3 Physiological properties of the leaf barrier

To draw a conclusion on the possible impacts of alterations in stomatal distributions and on the other hand wax and cutin amounts or compositions physiological

experiments were conducted and the results taken into account. Transpiration through stomata and the cuticle were investigated for all genotypes (3.6, 3.8, 3.9). The stomatal conductance in the leaves of plants is predominantly determined by stomatal size and density. When stomatal pores are at their widest apertures, the maximum leaf diffusive conductance or stomatal conductance to $CO_2$ and water vapor is reached (Franks et al., 2009). The values for stomatal conductances show a great variety throughout the entire kingdom of vascular plants and can vary over two orders of magnitude. Within one plant family, however, they are rather constant and remain in one range (Hetherington and Woodward, 2003). The stomatal conductances measured for Arabidopsis genotypes in this study, basically correlated with the stomatal density determined for ad- and abaxial leaf sides (Figure 19, Figure 24). Stomatal conductance was, in general, higher on the abaxial leaf sides where at the same time stomatal densities were increased. On the other hand, with decreasing stomatal density on the adaxial leaf side the conductance decreased likewise. An exception was the stomatal conductance for the stomatal mutant *tmm*. Stomatal density on the abaxial leaf side was significantly higher whereas stomatal conductance was significantly lower than in the wild type. The *tmm* mutant shows a higher number of stomatal clusters on the abaxial leaf side than on the adaxial side, where only very few small clusters can be detected (Figure 8, Figure 30; (Yang and Sack, 1995)). The changes in the stomatal patterning may affect the functioning of an individual stoma and therefore the stomatal conductance. In Dow et al., (2014) the authors state that the mutant *tmm* is impaired from completely opening their stomatal pores, due to the formed clusters and results in a lower stomatal conductance. Apart from the stomatal mutant *tmm* also the cutin mutant *att1* shows a disruption in the correlation of stomatal density and conductance. While stomatal densities were consistent for both leaf sides and not different from the wild type the stomatal conductance significantly increased on ad- and abaxial leaf side. This cannot easily be explained by the FE-SEM micrographs (Figure 30) or the determination of stomatal densities (Figure 19), which both did not show any abnormalities in the patterning or density of stomata in *att1*. The increase of the stomatal conductance in the overexpression mutant *st-*

*ox*, however, is clearly correlated with the high stomatal density of the mutant. Vráblová et al., (2017) made similar observations in another stomatal mutant. The *sdd1-1* mutant is phenotypically not different from the wild type (C24) but exhibits a difference in stomatal density and distribution. The stomatal density shows a 2.5 fold increase when compared to the wild type and at the same time the stomatal conductance was significantly increased. Nonetheless, comparisons of results need to be taken carefully since the authors measured stomatal conductance by taking the area and depth of stomata into account. This was not possible in this work. However, results, shown here, are further underlined by investigations of Tanaka et al., (2013), which also confirmed the correlation of increase in stomatal density and likewise an increase in stomatal conductance for *st-ox*.

Since a central question of this work was to investigate possible relations between the prevention of additional water loss through the cuticle when stomata are closed the effectiveness of the cuticular barrier was investigated. Therefore indirect measurements of the cuticular permeability were conducted (3.8) and minimum leaf conductances (3.9) were determined. To determine the cuticular permeability of leaves, it is common, to isolate astomatous cuticular membranes for appropriate transport experiments (Riederer and Schreiber, 2001). However, since Arabidopsis exhibits amphistomy and a thin cuticular membrane with many trichomes, the isolation of intact cuticular membranes is almost not possible. Different approaches, such as chlorophyll leaching (Lolle et al., 1997; Sieber et al., 2000; Schnurr et al., 2002; Seo et al., 2011) or staining with toluidine blue (Tanaka et al., 2004) have been used to provide information on the permeability of Arabidopsis leaves. However, especially staining with toluidine blue rather serves as a screen for Arabidopsis leaves with a defect in the cuticular membrane. The hydrophilic dye binds to polysaccharides, in this case, the pectin of the cell walls of the leaves and therefore indicates a defect in the cuticular membrane (Tanaka et al., 2004; Mitra and Loqué, 2014). Ballmann et al., (2011) introduced a new method to provide more precise and foremost quantitative information on the permeability of Arabidopsis leaves. The author's approach was to measure cuticular permeability

with a radioactive transport assay using $^{14}C$ labeled epoxyconazole as a tracer. Alternatively, chlorophyll fluorescence measurements can be performed (Sadler et al., 2016). The obtained rates of photosynthesis inhibitions correlated with the $^{14}C$ epoxyconazole uptake through cuticles. Therefore the indirect measurement of cuticular permeability of Arabidopsis leaves via chlorophyll fluorescence measurements is an easy, rapid and non- invasive technique to provide information on the cuticular barrier properties of Arabidopsis leaves and was hence used in this study (2.2.8, 3.8). The inhibition of photosynthesis was investigated by applying metribuzine as a photosynthesis- inhibitor onto the leaf surface of the different Arabidopsis genotypes. Metribuzine is broadly used in agriculture, as an herbicide, which binds to the D1- protein in PS II and hence inhibits the electron transport. As a consequence the measured fluorescence increases and at the same time the photosynthetic yield decreases (Draber et al., 1991). The plant cuticle is the limiting barrier for the uptake of foliar applied solutes, therefore the measurement of the decrease in the photosynthetic yield is possible and provides information on the cuticular permeability (Schönherr and Riederer, 1989; Sadler et al., 2016). The uptake of metribuzine was faster in most of the mutants (*tmm*, *st-RNAi*, *st-ox*, *wax2*, *att1*, *shn3*) compared to the corresponding wild types (Col-0, Ws), (Figure 25, Figure 26). Therefore it can be concluded, that the permeability in those mutants was higher than in the wild types. Which also corresponds to the here performed measurements for minimal leaf conductances, where the obtained results for the cuticular transpiration of the leaves, of the previously mentioned mutants was also increased compared to the wild types (Figure 28). The only mutant which did not take up the herbicide faster than the corresponding wild type Col-0 was the stomatal mutant *flp*. Since the uptake is accomplished strictly over the cuticle, the stomatal mutation cannot directly influence the uptake. In general, the infiltration of stomata is not possible since the metribuzine solution is aqueous and has a surface tension around 73.05 $mN*m^{-1}$. Since the leaf is hydrophobic it must be lowered to at least 30 $mN*m^{-1}$ to infiltrate stomata (Schönherr and Bukovac, 1972; Zeiger et al., 1987). The wax amount and composition on the adaxial leaf side is not affected either (Figure 13). This also has been postulated by Sadler et al.,

(2016) the authors tested several mutants, that were altered in their wax or cutin biosynthesis and therefore exhibited more or less wax/ cutin loads and compositions. They were analyzed with the above mentioned radioactive transport assay, which revealed, no recognizable correlation between wax/ cutin amounts and the cuticular permeability as it was also suggested before by (Becker et al., 1986; Schreiber and Riederer, 1996; Riederer and Schreiber, 2001). In this study, the authors further suggest that the ultrastructure of the cuticle could be the reason for different permeability values in mutants compared to the wild type. Transmission electron microscopy (TEM) can provide insights on the layered structure of the cuticle. Therefore a thick but less reticulated cuticle could be the reason for a higher permeability as it was postulated for *wax2*, for example. For *att1* the loose ultrastructure of the cuticular membrane was also identified with TEM and showed a less electron dense membrane when compared to the wild type (Xiao et al., 2004) and therefore underlines the here measured increased permeability of the cuticle. Other studies from Kim et al., (2017) also found differences in the cuticle structure via TEM when compared to the wild type. Arabidopsis plants were exposed to hypoxic stress treatments and tested for their permeability, wax composition and amount as well as further for their cuticular structure with TEM. They found changes in the cuticular proper and layer. The plants exposed to stress showed a more permeable cuticle with a thinner electron- translucent cuticle proper and an electron-dense cuticular layer. The control on the other side was less permeable and possessed a distinct electron translucent cuticle proper and a more electron dense cuticular layer. However, the wax amount was likewise lowered in the stress-exposed Arabidopsis plants. Nevertheless, the conclusion, that the cuticular ultrastructure is altered in response to different wax amounts and composition was proven. This might also be the case for changed wax amounts and compositions as well as changes in cutin in this study. Further, this can be the reason for different outcomes of the penetration of the herbicide and a resulting more or less permeable cuticle. As it was measured for *flp* in a less permeable membrane even though no decrease in wax amount was recognizable in the GC analysis or on the other hand all other

mutants (*tmm, st-RNAi, st-ox, wax2, att1, and shn3*) where the permeability was severely increased when compared to the wild type, but wax amount or composition was not significantly altered. Another question is, whether the stomatal density has an influence on the cuticular permeability, independent from wax load or composition. If data of the chlorophyll fluorescence measurements are related to the stomatal density of the adaxial leaf side, no specific correlation is recognizable. The mutant *shn3*, for instance, shows a low stomatal density and at the same time an increased permeability. This result can also be observed for the mutants *st-RNAi* and *wax2*. However, a less permeable cuticle when stomata density was significantly increased could not be measured. In the case of the stomatal mutant *st-ox*, for example, the permeability of the cuticle is increased whereas the stomatal density is also significantly increased.

To investigate the question, whether mutations affecting the stomatal distribution, in turn affect the cuticular permeability in any way, not only chlorophyll fluorescence studies were performed, but also the minimum conductance for the Arabidopsis leaves was investigated. This was also the quantitative approach to determine leaf cuticular transpiration (3.9). In the measurements for minimum leaf conductance, a significant leap in the graph is striking (Figure 6, Figure 7). This is best explained by looking at the amount of water lost over time. In the exemplary graph, the leap appears after 240 min. After that, the amount of water lost is close to 100 %. It is suggested that, when epidermal cells die stomata are locked open, unable to close again, as observed by (Prats et al., 2006) after pathogen inoculation of barley leaves. In the results presented herein, stomata close after abscission, to prevent water loss. With increasing dehydration of the leaf at the point of cell death they lock open and therefore release the residual amount of water at once. Hence a

significant leap in the data appears (Figure 29).

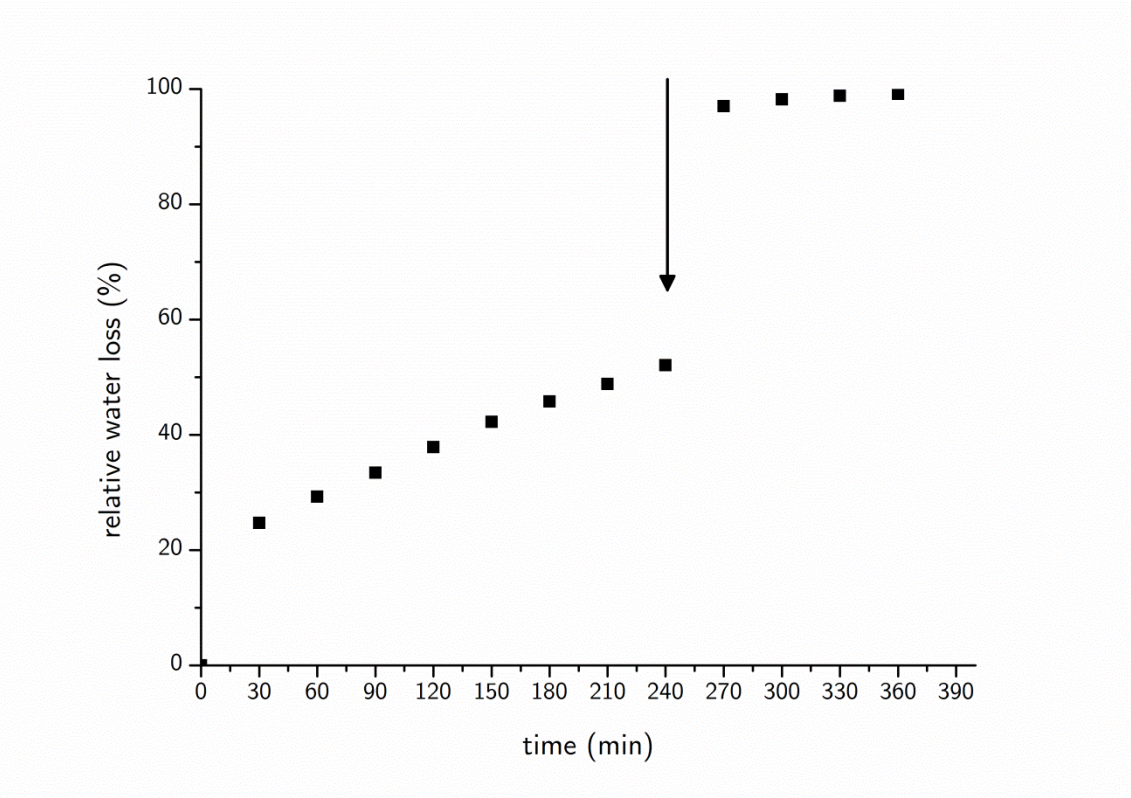


Figure 29: Representative leaf drying curve for Arabidopsis wild type (Col-0)

A representative result of a gravimetric measurement of water loss over time with a single leaf of Arabidopsis ecotype (Col-0). Arrow indicates the point of cracked open stomata.

Due to the already mentioned amphistomy of Arabidopsis leaves the water loss through the cuticle was measured under conditions of maximum stomatal closure (2.2.9). As mentioned before the results mainly mirror the indirect approach to measure cuticular permeability with the chlorophyll fluorescence method: Permeances of the mutants *flp*, *st-ox*, *st-RNAi*, *wax2*, and *att1* were significantly increased when compared to the wild type. The mutants *shn3* and *tmm* also showed tendencies to higher permeabilites than the corresponding wild type (Figure 28). Permeances measured were one order of magnitude lower when compared to the suggested transpiration value of Ballmann et al., (2011). This could be due to the completely different approaches to determine the cuticular transpiration of the Arabidopsis leaves. As explained above Ballmann et al., (2011) estimated the transpiration through radioactive transport measurements. The measurements of co-

permeability experiments ($^{14}C$-epoxyconazole/ $^{3}H_2O$) revealed a high correlation between the permeability of the two substances through the cuticular membrane. Due to this correlation, the water permeance for Arabidopsis could be estimated as $4.55 \times 10^{-8} ms^{-1}$ for the wild type.

# 5 Summary

Stomatal pores and the cuticular membrane are the two major key elements to regulate the gas exchange and water balance of plants. The hydrophobic cuticle covers all aerial parts of plants in their primary developmental stage (Schönherr, 1982). It forms an effective barrier against uncontrolled water loss and thus prevents plants from desiccation (Edwards et al., 1982). Stomata perforate the cuticular membrane and are indispensable for the uptake of $CO_2$ and the release of $O_2$ to maintain photosynthesis. This gas exchange is accompanied by the controlled release of water vapor. If the plant is exposed to drought, stomata close. Under these conditions, the plant's survival depends on the amount of water lost through the cuticle. To further understand this important interplay between stomatal regulation and the permeability of the cuticular membrane a multifaceted approach investigating stomatal and cuticular mutants for (i) their stomatal distribution, (ii) cuticular wax and cutin amounts as well as compositions and (iii) the physiological role in terms of transpiration either through the cuticular membrane or the stomata has been accomplished. Chemical analyses for wax/ cutin amounts and compositions revealed no significant correlation with determined stomatal densities or indexes. Even though in a few mutants, such as *st-RNAi* and *wax2* which showed lower stomatal densities and at the same time lower wax amounts, no clear pattern of such regularities could be observed for all the mutants. Inconsistencies, for instance, were underlined by observations for the wax mutant *shn3*, which exhibited higher wax amounts but a lower stomatal density than the wild type. Further measurements of the cuticular permeability and stomatal conductance could not be correlated to the determined wax/ cutin amounts or the stomatal densities and indexes. Cuticular transpiration was increased in all mutants independently from increased or decreased stomatal densities or cutin/ wax amounts.

In summary, this data indicates that the simple assumption that stomatal density correlates with wax or cutin amounts may not always be true. Further physiological

data underline those findings because the permeability of the cuticle does not seem to be integrated with the density or pattern of the stomata and likewise, the conductance of stomata is not linked to the deposition of wax or cutin amounts.

# 6 Lists and References

# Bibliography

Aharoni A, Shital D, Jetter R, Thoenes E, van Arkel G, Pereira A (2004) The SHINE Clade of AP2 Domain Trancription Factors activates wax biosynthesis, alters cuticle properties and confers drought tolerance when overexpressed in Arabidopsis. *The Plant Cell* 16:2463–2480.

Baker E (1974) The influence of environment on leaf wax development in *Brassica oleracea* biological var. gemmifera. *New Phytologist* 73:955–966.

Baker E (1982) Chemistry and morphology of plant epicuticular waxes. Linnean Society symposium series.

Ballmann C, De Oliveira S, Gutenberger A, Waßmann F, Schreiber L (2011) A radioactive assay allowing the quantitative measurement of cuticular permeability of intact *Arabidopsis thaliana* leaves. *Planta* 234:9–20.

Barthlott W (1980) Morphogenese und Mikromorphologie komplexer Cuticular-Faltungsmuster an Blüten-Trichomen von *Antirrhinum L. (Scrophulariaceae). Berichte der deutschen Botanischen Gesellschaft.* 93:379–390.

Barthlott W, Neinhuis C (1997) The purity of sacred lotus or escape from contamination in biological surfaces. *Planta* 202:1–8.

Becker M, Kerstiens G, Schönherr J (1986) Water permeability of plant cuticles: permeance, diffusion and partition coefficients. *Trees* 1:54–60.

Bergmann D, Sack FD (2007) Stomatal development. *Annual Review of Plant Biology* 58:163–181.

Bernard A, Domergue F, Pascal S, Jetter R, Renne C, Faure J-D, Haslam RP, Napier JA, Lessire R, Joubes J (2012) Reconstitution of plant alkane biosynthesis in yeast demonstrates that Arabidopsis ECERIFERUM1 and ECERIFERUM3 are core components of a very-long-chain alkane synthesis complex. *The Plant Cell* 24:3106–3118.

Bernard A, Joubès J (2013) Arabidopsis cuticular waxes: Advances in synthesis, export and regulation. *Progress in Lipid Research* 52:110–129.

Bhave NS, Veley KM, Nadeau JA, Lucas JR, Bhave SL, Sack FD (2009) TOO MANY MOUTHS promotes cell fate progression in stomatal development of Arabidopsis stems. *Planta* 229:357–367.

Bhushan B (2003) Adhesion and stiction: Mechanisms, measurement techniques, and methods for reduction. *Journal of Vacuum Science & Technology B* 21:2262–2296.

Biddulph O, Nakayama FS, Cory R (1961) Transpiration stream & ascension of calcium. *Plant Physiology* 36:429–436.

Bird D, Beisson F, Brigham A, Shin J, Greer S, Jetter R, Kunst L, Wu X, Yephremov A, Samuels L (2007) Characterization of Arabidopsis ABCG11/WBC11, an ATP binding cassette (ABC) transporter that is required for cuticular lipid secretion. *Plant Journal* 52:485–498.

Bird SM, Gray JE (2003) Signals from the cuticle affect epidermal cell differentiation.

*New Phytologist* 157:9–23.

Bonaventure G, Beisson F, Ohlrogge J, Pollard M (2004) Analysis of the aliphatic monomer composition of polyesters associated with Arabidopsis epidermis: occurrence of octadeca-cis-6, cis-9-diene-1,18-dioate as the major component. *The Plant Journal* 40:920–930.

Bourdenx B, Bernard A, Domergue F, Pascal S, Leger A, Roby D, Pervent M, Vile D, Haslam RP, Napier JA, Lessire R, Joubes J (2011) Overexpression of Arabidopsis ECERIFERUM1 promotes wax very-long-chain alkane biosynthesis and influences plant response to biotic and abiotic stresses. *Plant Physiology* 156:29–45.

Bowman JL (2000) Axial patterning in leaves and other lateral organs. *Current Opinion in Genetics and Development* 10:399–404.

Brewer CA, Smith WK, Vogelmann TC (1991) Functional interaction between leaf trichomes, leaf wettability and the optical properties of water droplets. *Plant, Cell & Environment* 14:955–962.

Bringe K, Schumacher CFA, Schmitz-Eiberger M, Steiner U, Oerke EC (2006) Ontogenetic variation in chemical and physical characteristics of adaxial apple leaf surfaces. *Phytochemistry* 67:161–170.

Burch AY, Zeisler V, Yokota K, Schreiber L, Lindow SE (2014) The hygroscopic biosurfactant Syringafactin produced by *Pseudomonas syringae* enhances fitness on leaf surfaces during fluctuating humidity. *Environmental Microbiology* 16:2086–2098.

Cape J (1983) Contact angles of water droplets on needles of Scots Pine (*Pinus sylvestris*) growing in polluted atmospheres. *New Phytologist* 93:293–299.

Chen X, Goodwin SM, Boroff VL, Liu X, Jenks MA (2003) Cloning and characterization of the WAX2 gene of Arabidopsis involved in cuticle membrane and wax production. *The Plant Cell online* 15:1170–1185.

Daszkowska-Golec A, Szarejko I (2013) Open or close the gate – Stomata action under the control of phytohormones in drought stress conditions. *Frontiers in Plant Science* 4:1–16.

Dow GJ, Berry JA, Bergmann DC (2014) The physiological importance of developmental mechanisms that enforce proper stomatal spacing in *Arabidopsis thaliana*. *New Phytologist* 201:1205–1217.

Draber VW, Kluth JE, Tietjen K, Trebst A (1991) Herbizide in der Photosyntheseforschung. *Angewandte Chemie* 103:1650–1663.

Duan H, Schuler MA (2005) Differential expression and evolution of the Arabidopsis CYP86A subfamily. *Plant Physiology* 137:1067–1081.

Edwards D, Edwards DS, Rayner R (1982) The cuticle of early vascular plants and its evolutionary significance. In: The plant cuticle (Cutler D, Alvin K, Price C, eds), 341–361. London, UK: Academic Press.

Edwards D, Kerp H, Hass H (1998) Stomata in early land plants: An anatomical and ecophysiological approach. *Journal of Experimental Botany* 49:255–278.

Ensikat HJ, Barthlott W (1993) Liquid substitution: A versatile procedure for SEM

specimen preparation of biological materials without drying or coating. *Journal of Microscopy* 172:195–203.

Espelie KE, Davis RW, Kolattukudy PE (1980) Composition, ultrastructure and function of the cutin and suberin containing layers in the leaf, fruit peel, juice-sac and inner seed coat of Grapefruit (*Citrus paradisi* Macfed.). *Planta* 149:498–511.

Franke R, Briesen I, Wojciechowski T, Faust A, Yephremov A, Nawrath C, Schreiber L (2005) Apoplastic polyesters in Arabidopsis surface tissues: A typical suberin and a particular cutin. *Phytochemistry* 66:2643–2658.

Franks PJ, Drake PL, Beerling DJ (2009) Plasticity in maximum stomatal conductance constrained by negative correlation between stomatal size and density: An analysis using *Eucalyptus globulus*. *Plant, Cell and Environment* 32:1737–1748.

Geisler M, Yang M, Sack FD (1998) Divergent regulation of stomatal initiation and patterning in organ and suborgan regions of the Arabidopsis mutants *too many mouths* and *four lips*. *Planta* 205:522–530.

Geisler M, Nadeau J, Sack FD (2000) Oriented asymmetric divisions that generate the stomatal spacing pattern in Arabidopsis are disrupted by the *too many mouths* mutation. *The Plant Cell* 12:2075–2086.

Genty B, Briantais JM, Baker NR (1989) The relationship between the quantum yield of photosynthetic electron transport and quenching of chlorophyll fluorescence. *Biochimica et Biophysica Acta* 990:87–92.

Goulas Y, Cerovic ZG, Cartelat A, Moya I (2004) Dualex: A new instrument for field measurements of epidermal ultraviolet absorbance by chlorophyll fluorescence. *Applied Optics* 43:4488–4496.

Graham LE (1993) Origin of Land Plants. New York, U.S.A.: John Wiley and Sons Inc.

Gray JE, Holroyd GH, van der Lee FM, Bahrami AR, Sijmons PC, Woodward FI, Schuch W, Hetherington AM (2000) The HIC signaling pathway links $CO_2$ perception to stomatal development. *Nature* 408:713–716.

Greer S, Wen M, Bird D, Wu X, Samuels L, Kunst L, Jetter R (2007) The cytochrome P450 enzyme CYP96A15 is the midchain alkane hydroxylase responsible for formation of secondary alcohols and ketones in stem cuticular wax of Arabidopsis. *Plant Physiology* 145:653–667.

Gregory FG, Milthorpe FL, Pearse HL, Spencer HJ (1950) Experimental studies of the factors controlling transpiration: II. The relation between transpiration rate and leaf water content. *Journal of Experimental Botany* 1:15–28.

Gülz P (1994) Epicuticular leaf waxes in the evolution of the plant kingdom. *Journal of Plant Physiology* 143:453–464.

Haworth M, Elliott-Kingston C, McElwain JC (2011) Stomatal control as a driver of plant evolution. *Journal of Experimental Botany* 62:2419–2423.

Hegebarth D, Buschhaus C, Wu M, Bird D, Jetter R (2016) The composition of surface wax on trichomes of *Arabidopsis thaliana* differs from wax on other epidermal

cells. *The Plant Journal* 88:762–774.

Hetherington AM, Woodward FI (2003) The role of stomata in sensing and driving environmental change. *Nature* 424:901–908.

Holloway P (1970) Surface factors affecting the wetting on leaves. *Pesticide Science* 1:156–163.

Holloway P (1971) The chemical and physical characteristics of leaf surfaces. In: Ecology of leaf surface microorganisms, pp.39 London: *Academic Press*.

Holloway P (1982) Structure and histochemistry of plant cuticular membranes: An overview. In: The plant cuticle. pp.1-32 London: *Linnean Society symposium series*.

Hronková M, Wiesnerová D, Šimková M, Skůpa P, Dewitte W, Vráblová M, Zažímalová E, Šantrůček J (2015) Light-induced STOMAGEN-mediated stomatal development in Arabidopsis leaves. *Journal of Experimental Botany* 66:4621–4630.

Jeffree C (1986) The cuticle, epicuticular waxes and trichomes of plants, with reference to their structure, functions and evolution. *Insects and the Plant Surface*:23–64.

Jeffree C (2006) The fine structure of the plant cuticle. In: Biology of the Plant Cuticle, pp. 11–125. Oxford, UK: *Blackwell Publishing Ltd.*

Jenks MA, Tuttle HA, Eigenbrode SD, Feldmann KA (1995) Leaf epicuticular waxes of the *eceriferum* Mutants in Arabidopsis. *Plant Physiology* 108:369–377.

Jenks MA, Eigenbrode SD, Lemieux B (2002) Cuticular Waxes of Arabidopsis. In: The Arabidopsis Book; 1-22. *American Society of Plant Biologists*

Jetter R, Kunst L, Samuels A (2006) Composition of plant cuticular waxes. In: Biology of the Plant cuticle. Oxford, UK. *Blackwell Publishing Ltd*

Jones H (2013) Plants and Microclimate, 3rd Edition. *Cambridge University Press*.

Joubès J, Domergue F (2018) Biosynthesis of the Plant Cuticle. In: *Hydrocarbons, Oils and Lipids: Diversity, Origin, Chemistry and Fate*. pp. 1–19. Heinz Wilkes (Eds.).

Kim H, Choi D, Suh MC (2017) Cuticle ultrastructure, cuticular lipid composition, and gene expression in hypoxia-stressed Arabidopsis stems and leaves. *Plant Cell Reports* 36:815–827.

Knoll D (1998) Die Beduetung der Kutikula bei der Interaktion zwischen epiphyllen Mikroorganismen und Blattoberflächen.Dissertation, Universität Bonn

Koch K, Barthlott W (2009) Superhydrophobic and superhydrophilic plant surfaces: An inspiration for biomimetic materials. *Philosophical Transactions of the Royal Society A* 367:1487–1509.

Kolattukudy PE, Walton T (1972) The biochemistry of plant cuticular lipids. *Progress in the Chemistry of Fats and Other Lipids* 13:121.

Kolattukudy PE, Agrawal VP (1974) Structure and composition of aliphatic constituents of potato tuber skin (suberin). *Lipids* 9:682–691.

Kolattukudy PE (1984) Biochemistry and function of cutin and suberin. *Canadian Journal of Botany* 62:2918–2933.

Krauss P, Markstädter C, Riederer M (1997) Attenuation of UV radiation by plant

cuticles from woody species. *Plant, Cell and Environment* 20:1079–1085.

Kunst L, Samuels A (2003) Biosynthesis and secretion of plant cuticular wax. *Progress in Lipid Research* 42:51–80.

Kurata T, Kawabata-Awai C, Sakuradani E, Shimizu S, Okada K, Wada T (2003) The YORE-YORE gene regulates multiple aspects of epidermal cell differentiation in Arabidopsis. *Plant Journal* 36:55–66.

Lee SB, Suh MC (2015) Advances in the understanding of cuticular waxes in *Arabidopsis thaliana* and crop species. *Plant Cell Reports* 34:557–572.

Lemieux B (1996) Molecular genetics of epicuticular wax biosynthesis. *Trends in Plant Science* 1:312–318.

Lendzian KJ, Kerstiens G (1991) Sorption and transport of gases and vapors in plant cuticles. *Reviews of Enivironmental Contamination and Toxicology* 121:65–128.

Lolle SJ, Berlyn GP, Engstrom EM, Krolikowski KA, Reiter WD, Pruitt RE (1997) Developmental regulation of cell interactions in the Arabidopsis *fiddlehead-1* mutant: A role for the epidermal cell wall and cuticle. *Developmental Biology* 189:311–321.

Matas A, Sanz M, Heredia A (2003) Studies on the structure of the plant wax nonacosan-10-ol, the main component of epicuticular wax conifers. *International Journal of Biological Macromolecules* 33:31–35.

McFarlane HE, Watanabe Y, Yang W, Huang Y, Ohlrogge J, Samuels AL (2014) Golgi- and Trans-Golgi network-mediated vesicle trafficking is required for wax secretion from epidermal cells. *Plant Physiology* 164:1250–1260.

Mendgen K (1996) Fungal attachment and penetration. Oxford, UK. *BIOS Scientific Publishers*.

Mitra PP, Loqué D (2014) Histochemical staining of *Arabidopsis thaliana* secondary cell wall elements. *Journal of Visualized Experiments*: 87:1–11.

Mott KA, Michaelson O (1991) Amphistomy as an adaptation to high light intensity in *Ambrosia cordifolia* (*Compositae*). *American Journal of Botany* 78:76–79.

Muir C (2015) Making pore choices: repeated regime shifts in stomatal ratio. *Proceedings of the Royal Society B* 282:1–9.

Nadeau JA, Sack FD (2002) Control of stomatal distribution on the Arabidopsis leaf surface. *Science* 296:1697–1701.

Nawrath C (2002) The biopolymers cutin and suberin. In: The Arabidopsis Book 1; 1-14. *American Society of Plant Biologists*

Nawrath C (2006) Unraveling the complex network of cuticular structure and function. *Current Opinion in Plant Biology* 9:281–287.

Nobel PS (1980) Leaf anatomy and water use efficiency. New York, U.S.A. John Wiley and Sons Inc.

Percy K, Baker E (1990) Effects of simulated acid rain on epicuticular wax production, morphology, chemical composition and on cuticular membrane thickness in two clones of Sitka spruce [*Picea sitchensis* (Bong.) Carr.]. *New Phytologist* 116:79–87.

Prats E, Gay AP, Mur LAJ, Thomas BJ, Carver TLW (2006) Stomatal lock-open, a consequence of epidermal cell death, follows transient suppression of stomatal opening in barley attacked by *Blumeria graminis*. *Journal of Experimental Botany* 57:2211–2226.

Riederer M, Schönherr J (1990) Effects of surfactants on water permeability of isolated plant cuticles and on the composition of their cuticular waxes. *Pesticide Science* 29:85–94.

Riederer M, Schreiber L (2001) Protecting against water loss: analysis of the barrier properties of plant cuticles. *Journal of Experimental Botany* 52:2023–2032.

Rowland O, Lee R, Franke R, Schreiber L, Kunst L (2007) The CER3 wax biosynthetic gene from *Arabidopsis thaliana* is allelic to WAX2/YRE/FLP1. *FEBS Letters* 581:3538–3544.

Sachs T (1991) Pattern formation in plant tissues. Cambridge University Press. Cambridge, UK:

Sadler C, Schroll B, Zeisler V, Waßmann F, Franke R, Schreiber L (2016) Wax and cutin mutants of Arabidopsis: Quantitative characterization of the cuticular transport barrier in relation to chemical composition. *Biochimica et Biophysica Acta* 1861:1336–1344.

Salisbury E.J. (1927) On the causes and ecological significance of stomatal frequency, with special reference to the woodland flora. *Philosophical Transactions of the Royal Society B* 216:1–65.

Schlegel TK, Schönherr J, Schreiber L (2005) Size selectivity of aqueous pores in stomatous cuticles of *Vicia faba* leaves. *Planta* 221:648–655.

Schnurr JA, Shockey JM, de Boer G-J, Browse JA (2002) Fatty acid export from the chloroplast. Molecular characterization of a major plastidial acyl-coenzyme. A synthetase from Arabidopsis. *Plant Physiology* 129:1700–1709.

Schönherr J (1982) Resistance of plant surfaces to water loss: Transport properties of cutin, suberin and associated lipids. In: *Encyclopedia of Plant Physiology*, 153–179. Berlin: Springer.

Schönherr J (2006) Characterization of aqueous pores in plant cuticles and permeation of ionic solutes. *Journal of Experimental Botany* 57:2471–2491.

Schönherr J, Bukovac M (1972) Penetration of Stomata by Liquids. *Plant Physiology* 1:813–819.

Schönherr J, Riederer M (1989) Foliar penetration and accumulation of organic chemicals in plant cuticles.*Reviews of Environmental Contamination and Toxicology*. 108:1-70

Schreiber L (2001) Effect of temperature on cuticular transpiration of isolated cuticular membranes and leaf discs. *Journal of Experimental Botany* 52:1893–1900.

Schreiber L (2005) Polar paths of diffusion across plant cuticles: New evidence for an old hypothesis. *Annals of Botany* 95:1069–1073.

Schreiber L (2010) Transport barriers made of cutin, suberin and associated waxes. *Trends*

*in Plant Science* 15:546–553.

Schreiber L, Schönherr J (1990) Phase transitions and thermal expansion coefficients of plant cuticles: The effects of temperature on structure and function. *Planta* 182:186–193.

Schreiber L, Riederer M (1996) Ecophysiology of cuticular transpiration: Comparative investigation of cuticular water permeability of plant species from different habitats. *Oecologia* 107:426–432.

Schreiber L, Schorn K, Heimburg T (1997) $^{2}$H NMR study of cuticular wax isolated from *Hordeum vulgare* L. leaves: Identification of amorphous and crystalline wax phases. *European Biophysics Journal* 26:317–380.

Schreiber L, Skrabs M, Hartmann K, Diamantopoulos P, Simanova E, Šantrůček J (2001) Effect of humidity on cuticular water permeability of isolated cuticular membranes and leaf disks. *Planta* 214:274–282.

Schreiber L, Schönherr J (2009) Water and solute permeability of plant cuticles. Berlin Heidelberg, Germany: *Springer.*

Seo PJ, Lee SB, Suh MC, Park M-J, Go YS, Park C-M (2011) The MYB96 Transcription Factor Regulates Cuticular Wax Biosynthesis under Drought Conditions in Arabidopsis. *The Plant Cell* 23:1138–1152.

Sieber P, Schorderet M, Ryser U, Buchala A, Kolattukudy PE, Métraux JP, Nawrath C (2000) Transgenic Arabidopsis plants expressing a fungal cutinase show alterations in the structure and properties of the cuticle and postgenital organ fusions. *The Plant cell* 12:721–737.

Sugano SS, Shimada T, Imai Y, Okawa K, Tamai A, Mori M, Hara-Nishimura I (2010) Stomagen positively regulates stomatal density in Arabidopsis. *Nature* 463:241–246.

Suh MC, Samuels AL, Jetter R, Kunst L, Pollard M, Ohlrogge J, Beisson F (2005) Cuticular lipid composition, surface structure, and gene expression in Arabidopsis stem epidermis. *Plant Physiology* 139:1649–1665.

Tanaka T, Tanaka H, Machida C, Watanabe M, Machida Y (2004) A new method for rapid visualization of defects in leaf cuticle reveals five intrinsic patterns of surface defects in Arabidopsis. *Plant Journal* 37:139–146.

Tanaka Y, Sugano SS, Shimada T, Hara-Nishimura I (2013) Enhancement of leaf photosynthetic capacity through increased stomatal density in Arabidopsis. *New Phytologist* 198:757–764.

Vráblová M, Vrábl D, Hronková M, Kubásek J, Šantrůček J (2017) Stomatal function, density and pattern, and $CO_2$ assimilation in *Arabidopsis thaliana tmm1* and *sdd1-1* mutants. *Plant Biology* 19:689–701.

Wang C, Chin CK, Gianfagna T (2000) Relationship between cutin monomers and tomato resistance to powdery mildew infection. *Physiological and Molecular Plant Pathology* 57:55–61.

Xiao F, Goodwin SM, Xiao Y, Sun Z, Baker D, Tang X, Jenks MA, Zhou JM (2004) Arabidopsis CYP86A2 represses *Pseudomonas syringae* type III genes and is required for cuticle development. *The EMBO Journal* 23:2903–2913.

Yang J, Isabel Ordiz M, Jaworski JG, Beachy RN (2011) Induced accumulation of cuticular waxes enhances drought tolerance in Arabidopsis by changes in development of stomata. *Plant Physiology and Biochemistry* 49:1448–1455.

Yang M, Sack FD (1995) The *too many mouths* and *four lips* mutations affect stomatal production in Arabidopsis. *The Plant Cell* 7:2227–2239.

Yeats T, Rose J (2013) The formation and function of plant cuticles. *Journal of Applied Sciences Research* 163:5–20.

Zeiger E, Farquhar GD, Cowan IR (1987) Stomatal function. Stanford, U.S.A.: *Stanford University Press.*

Zeisler-Diehl V, Müller Y, Schreiber L (2018) Epicuticular wax on leaf cuticles does not establish the transpiration barrier, which is essentially formed by intracuticular wax. *Journal of Plant Physiology* 227:66–74.

# List of Figures

# List of Tables

# List of Equations

# 7 Supplemental

## 7.1 Leaf surface morphology of Arabidopsis cutin and stomatal mutant (FE-SEM)

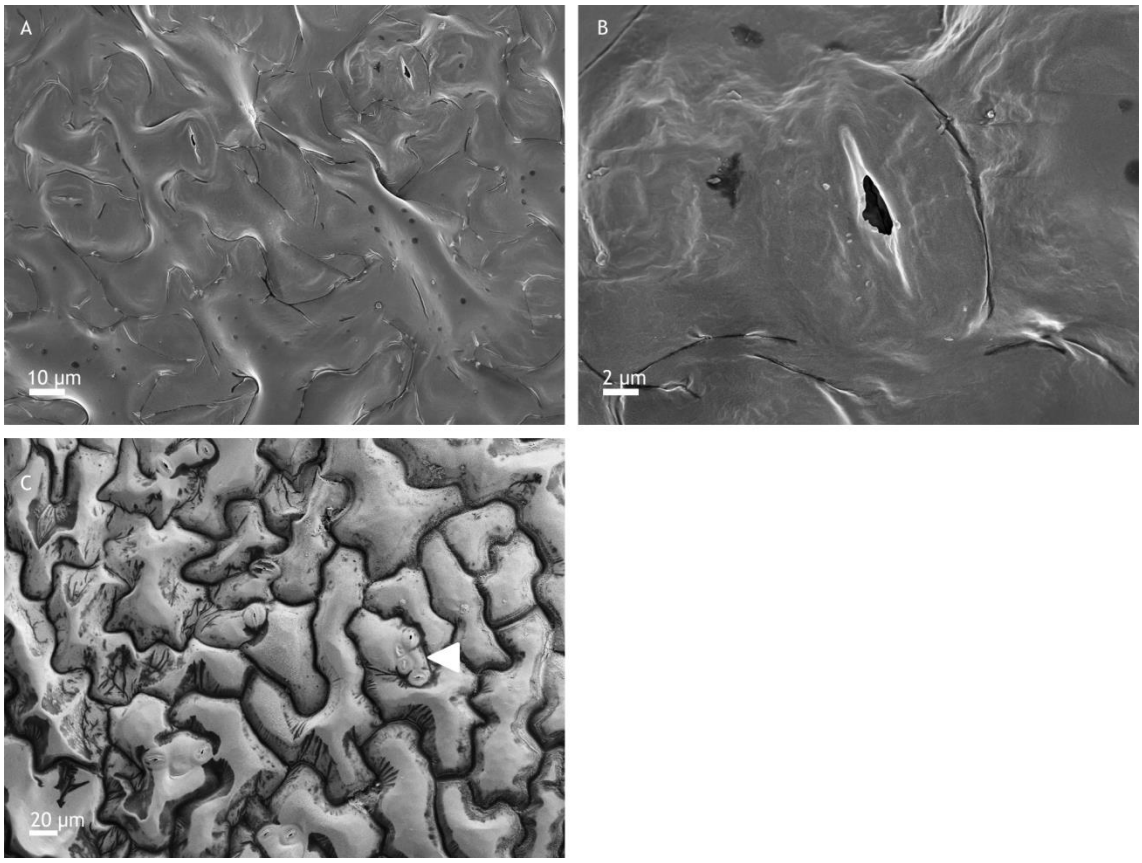


Figure 30: FE-SEM micrograph of the leaf surface morphology

Overview (A+C) and detailed view (B) of Arabidopsis mutants

A, B: *att1*, abaxial leaf side. C: *tmm*, adaxial leaf side (arrow: small stomatal cluster, remaining stomata without clustering)

## 7.2 Chlorophyll-Fluorescence measurements

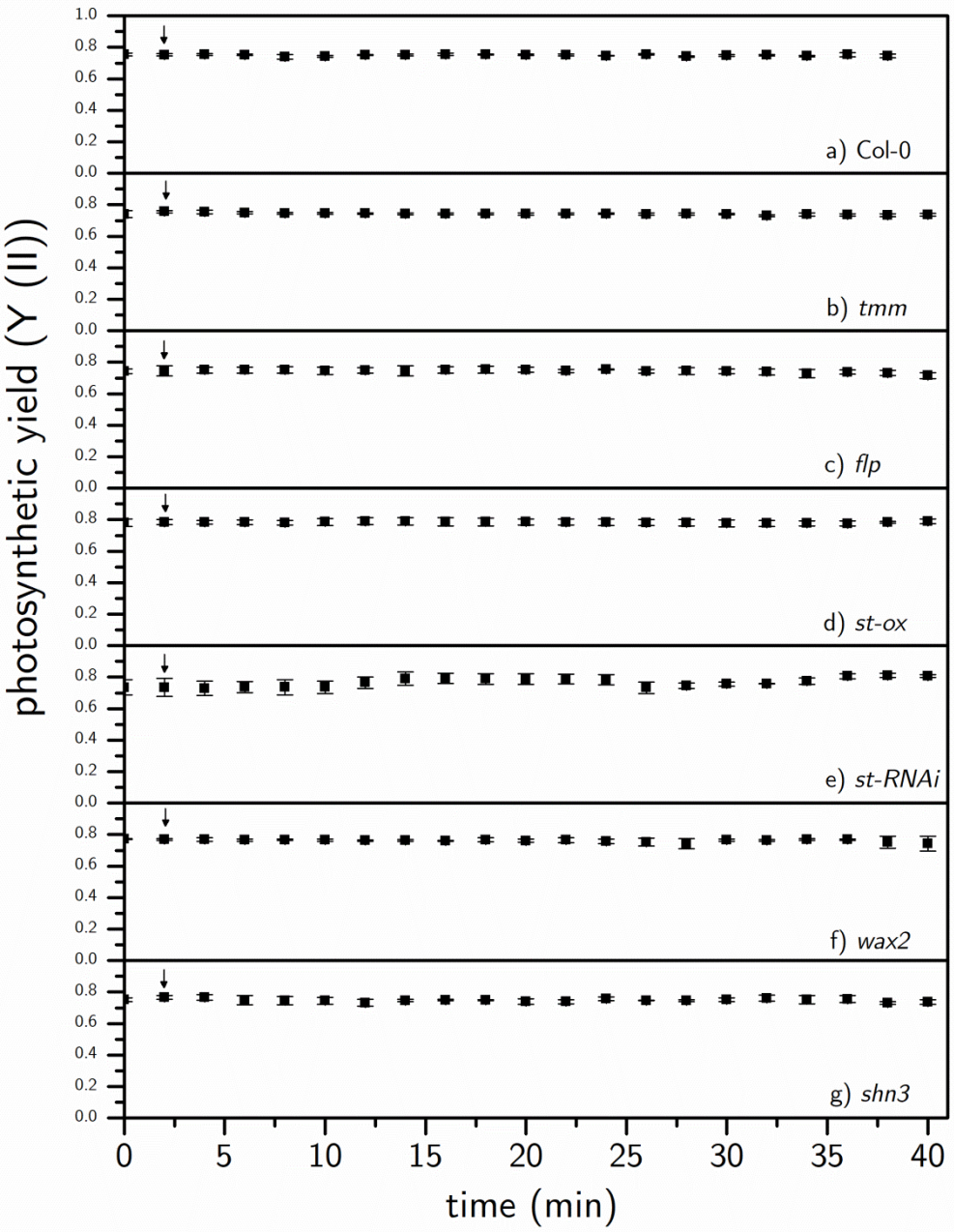


Figure 31: Photosynthetic yield in Arabidopsis genotypes

Control kinetics shown for the Arabidopsis wild type (a) Col-0 and corresponding mutants (b) *tmm*, (c) *flp*, (d) *st-ox*, (e) *st-RNAi*, (f) *wax2*, (g) *att1*. Arrows indicate the application of a 50µl water droplet on the adaxial leaf surface. Kinetics represent the means calculated from single values of individual leaves used (n= at least 3 biological replicates).

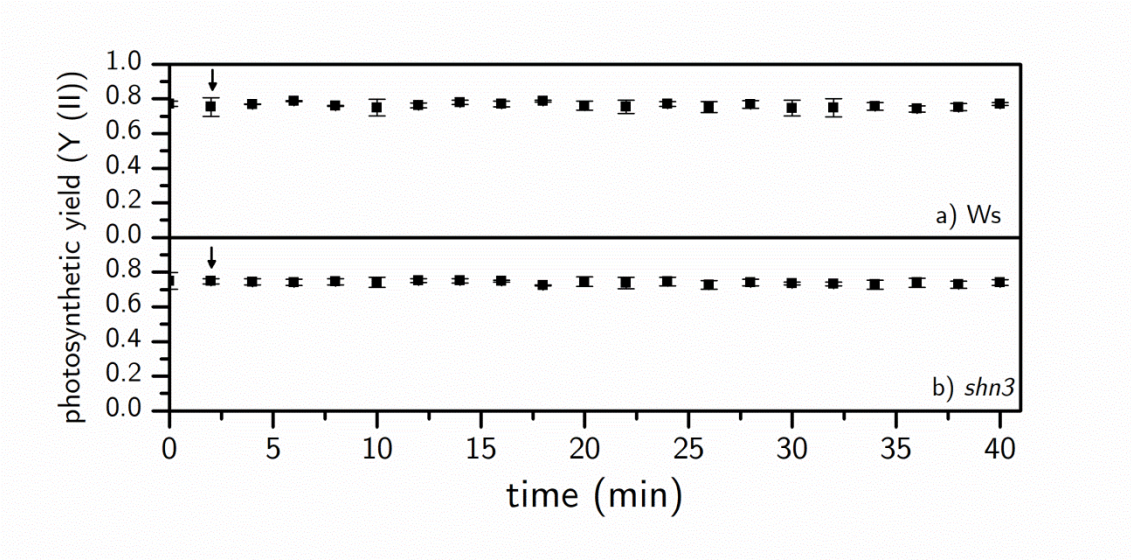


Figure 32: Photosynthetic yield in Arabidopsis genotypes

Control kinetics shown for the Arabidopsis wild type (a) Ws and corresponding mutant (b) *shn3*. Arrows indicate the application of a 50µl water droplet on the adaxial leaf surface. Kinetics represent the means calculated from single values of individual leaves used (n= at least 3 biological replicates).

# Acknowledgment

I would like to thank all people who contributed through their personal support or with fruitful discussions to the completion of this work.

My special thanks go to:

- My supervisor Prof. Dr. Lukas Schreiber for giving me the opportunity to work on this topic. I am thankful for his scientific advice and his always open door for questions and discussions. It was a great pleasure for me to work in your lab and in this project!
- My second advisor Prof. Kerstin Koch for her time and effort to discuss my topic and occurring questions. Also, I am thankful for suggestions concerning my project and the opportunity to let me work on the FE- SEM in your lab at the Hochschule Rhein- Waal.
- Miriam and Axel Huth, for spending a lot of their time with me, preparing for and actually helping me with the FE- SEM at the Hochschule Rhein Waal.
- Dr. Christian Kleusch, Dr. Viktoria Zeisler- Diehl, Dr. Tino Krezies, Vera Göser, Dr. Tatjana Hoppe, and Filip Fuchs for countless hints and help on scientific or computer (software) related questions and tasks. Also, of course, for proofreading this work!
- The entire group of Ecophysiology (current and former members) and especially my B.Sc. / M.Sc. students.